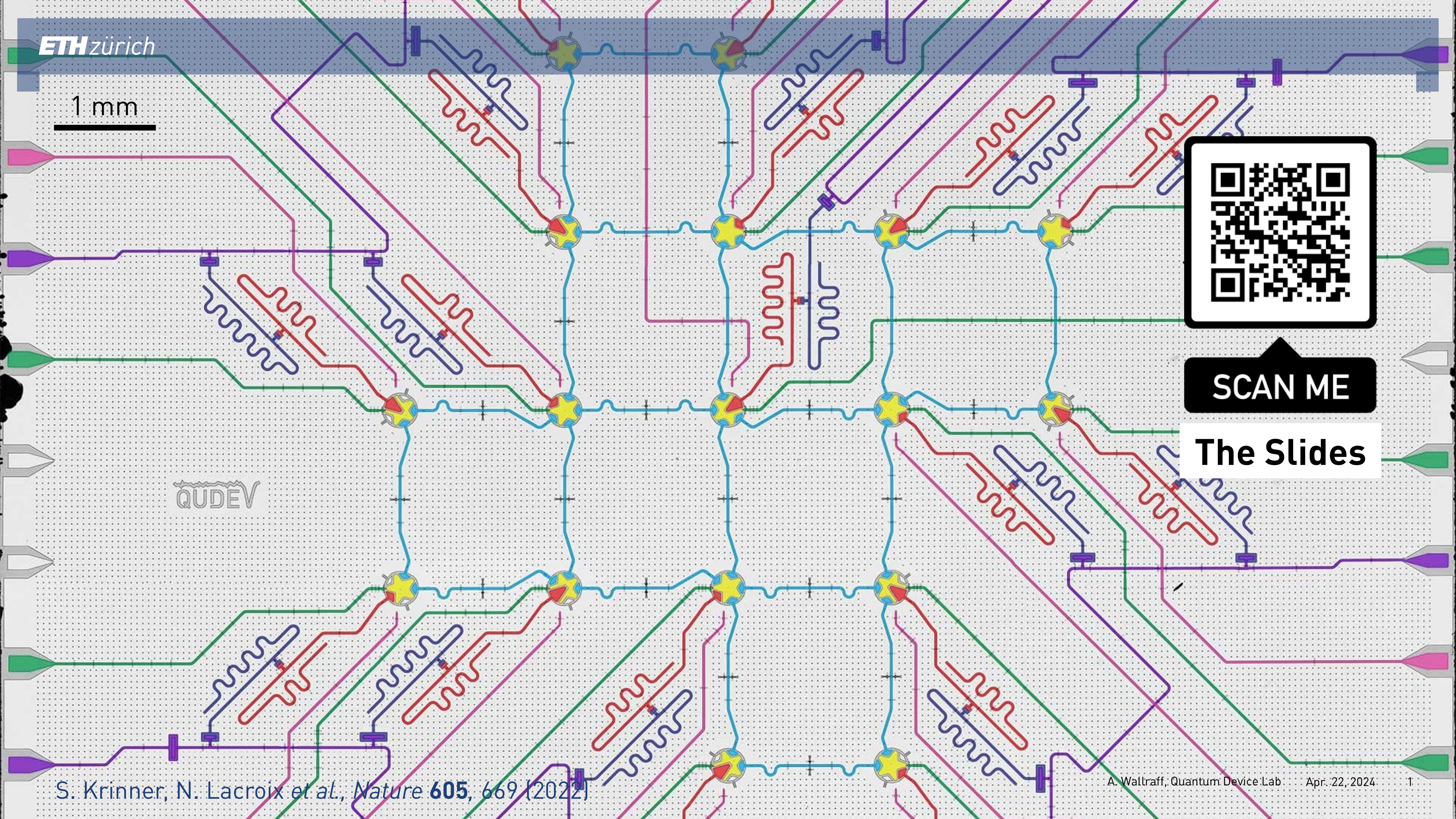

SCAN ME

The Slides

S. Krinner, N. Lacroix *et al.*, *Nature* **605**, 669 (2022)

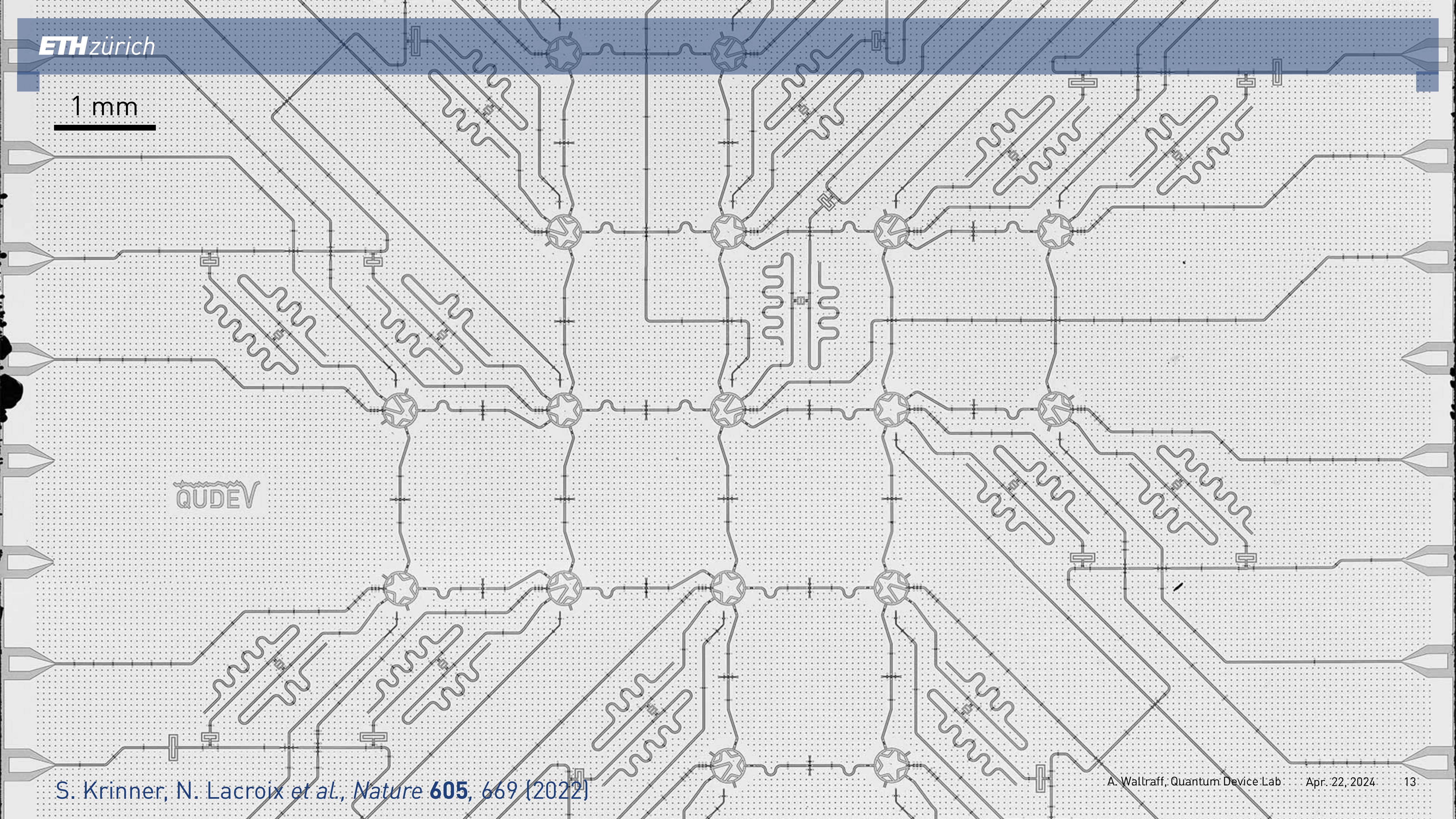

S. Krinner, N. Lacroix *et al.*, *Nature* **605**, 669 (2022)

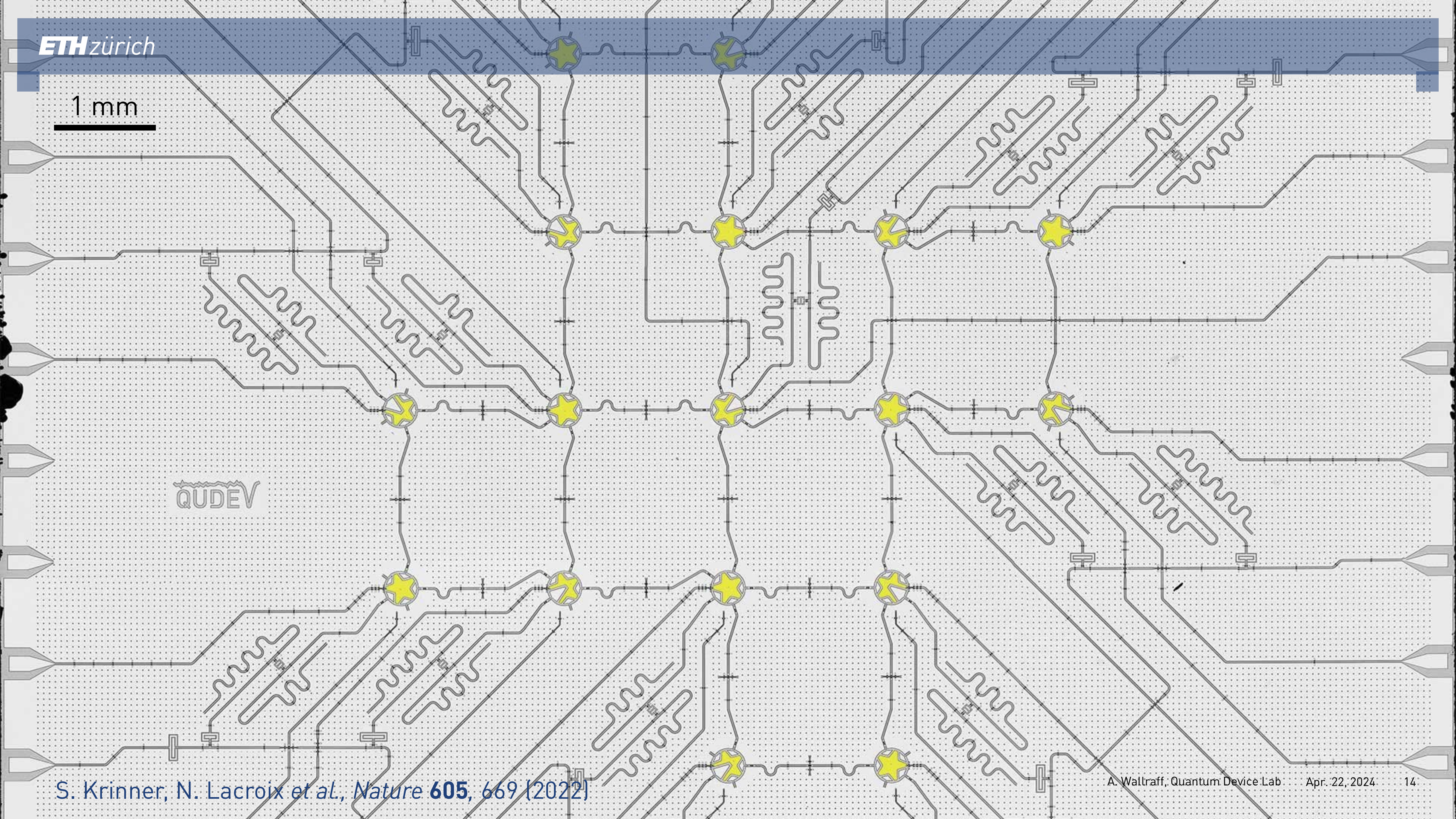

S. Krinner, N. Lacroix *et al.*, *Nature* **605**, 669 (2022)

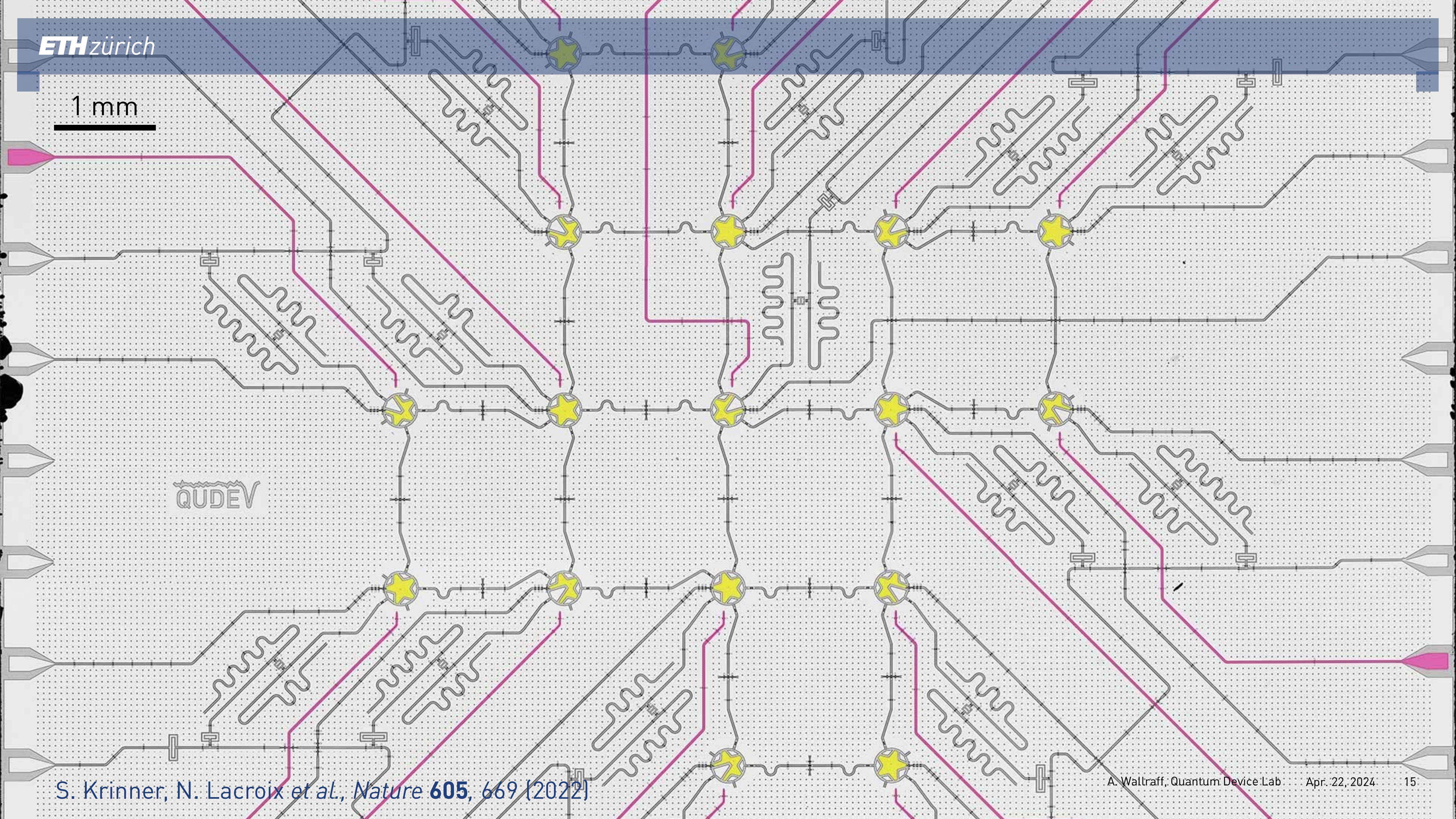

S. Krinner, N. Lacroix *et al.*, *Nature* **605**, 669 (2022)

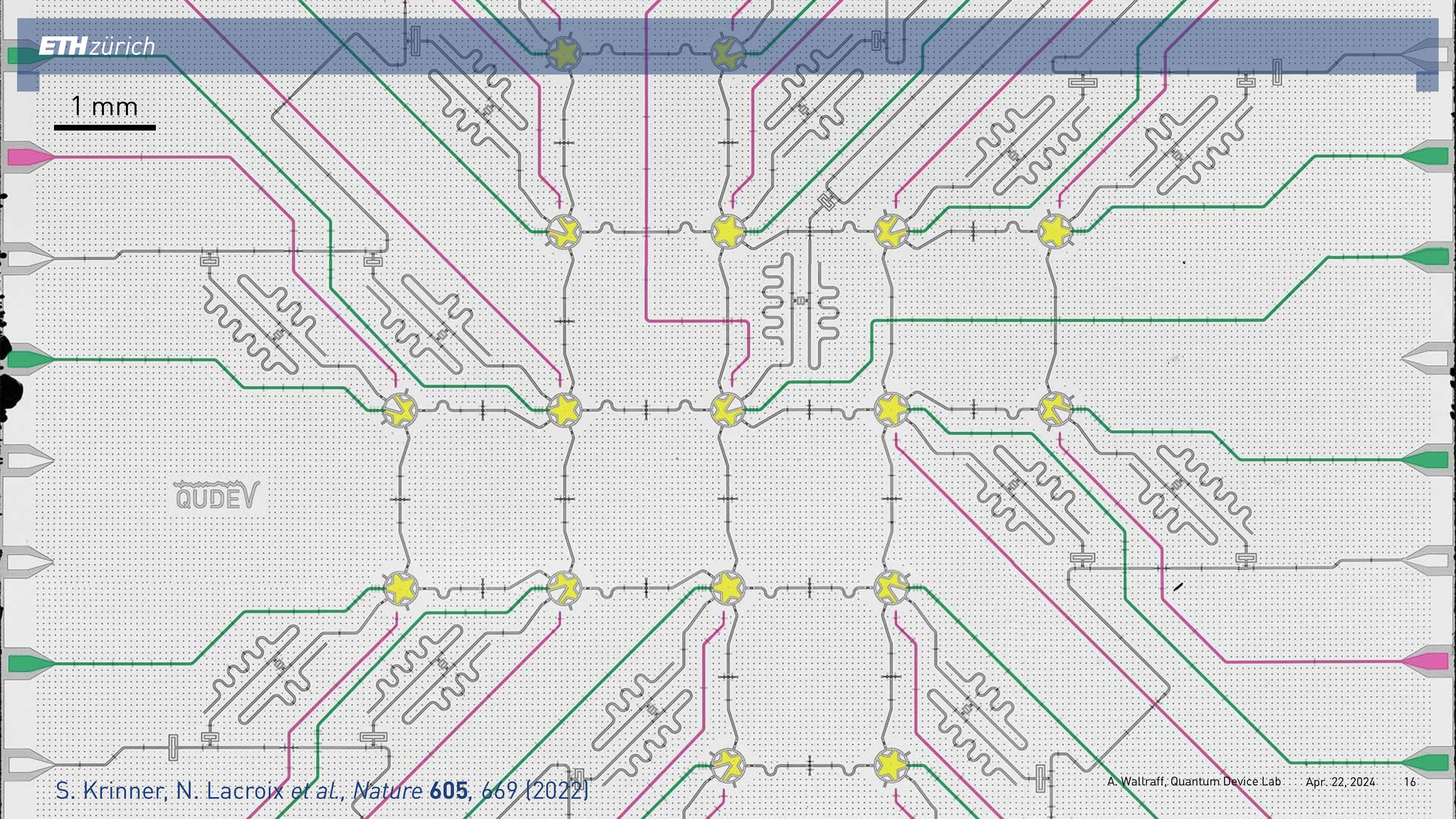

S. Krinner, N. Lacroix *et al.*, *Nature* **605**, 669 (2022)

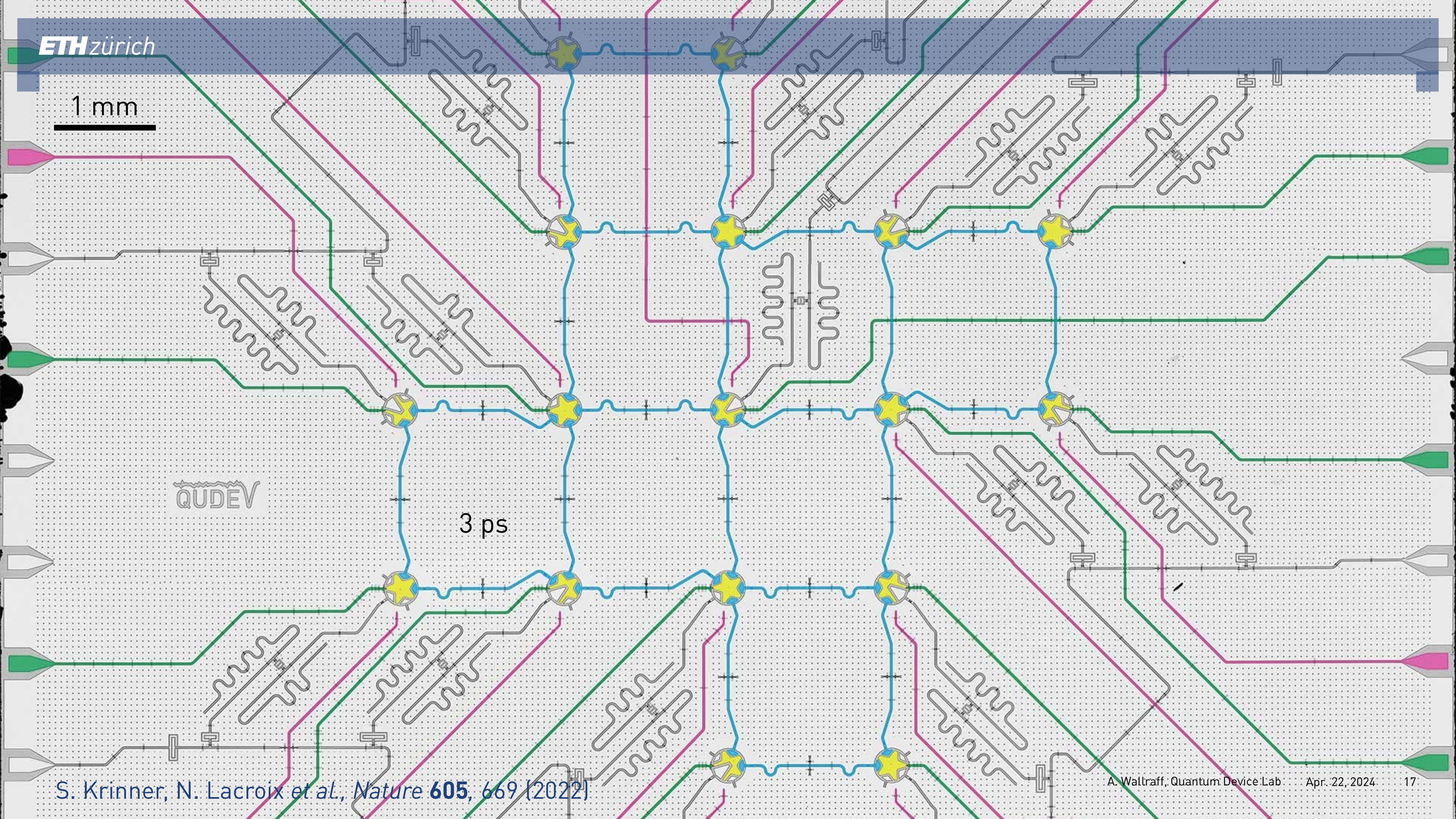

S. Krinner, N. Lacroix *et al.*, *Nature* **605**, 669 (2022)

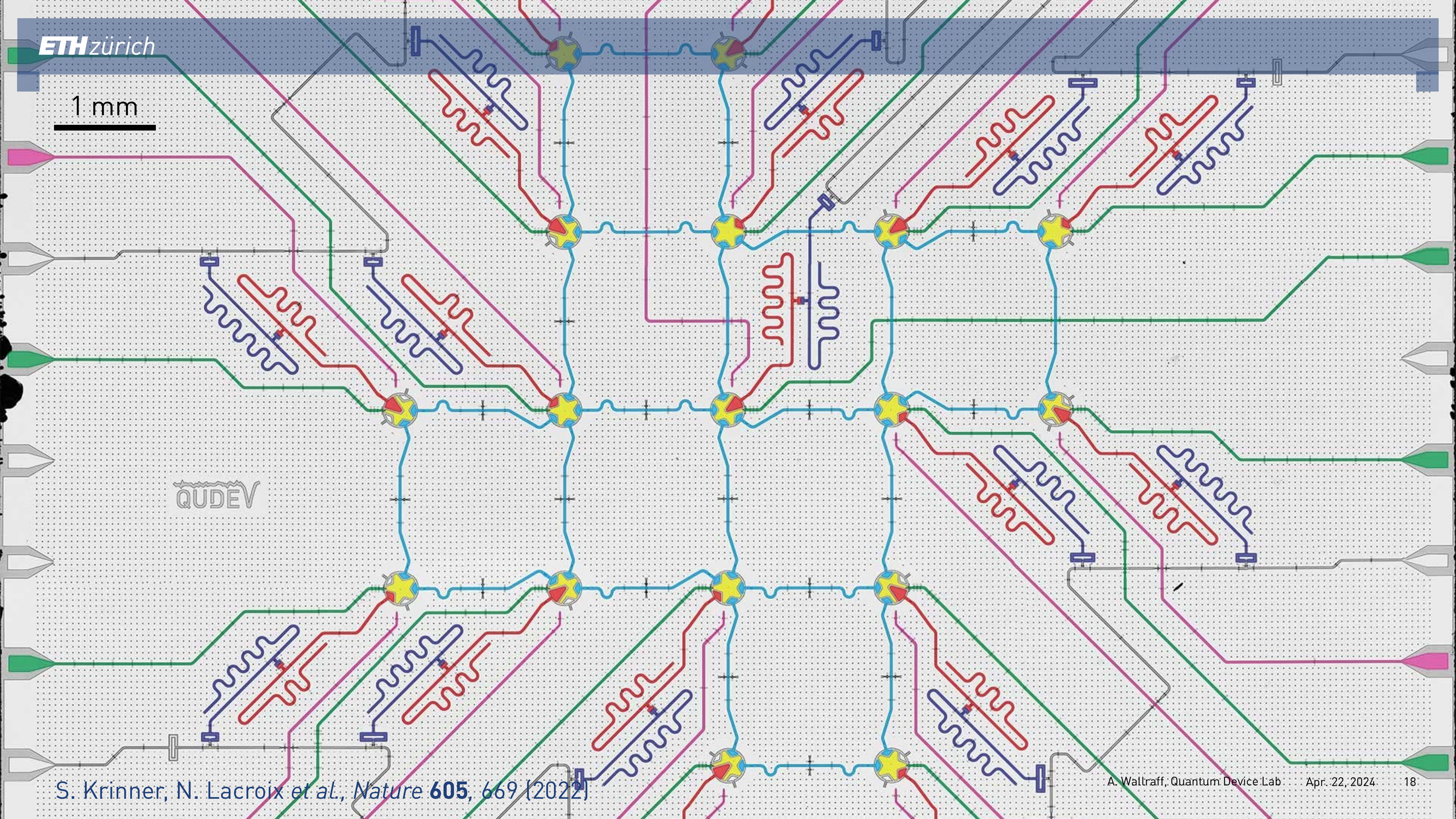

S. Krinner, N. Lacroix *et al.*, *Nature* **605**, 669 (2022)

Close-up of a Superconducting Qubit (Transmon-Style)

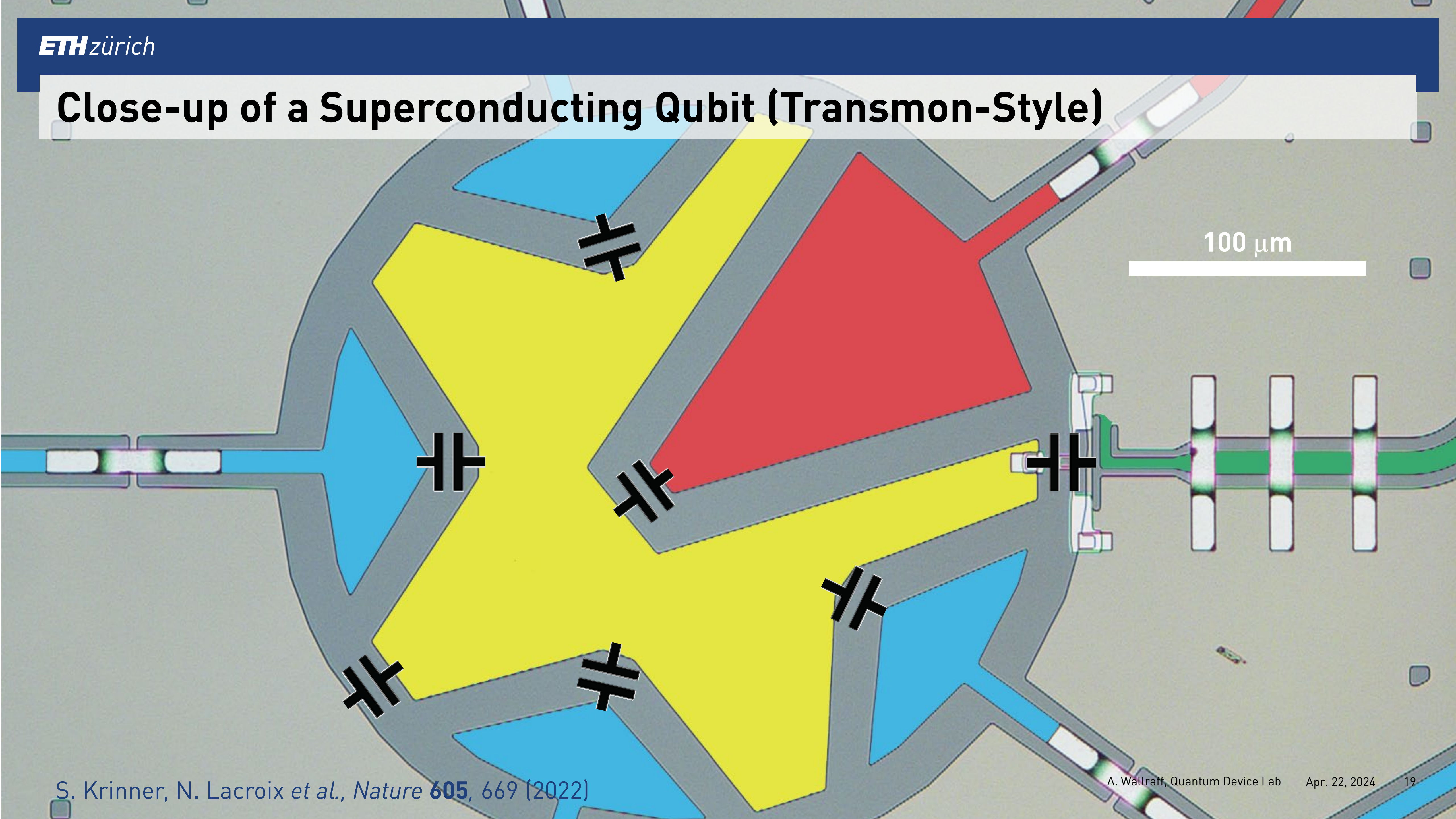

S. Krinner, N. Lacroix *et al.*, *Nature* **605**, 669 (2022)

Tunnel Junctions, SQUID, and Fluxline

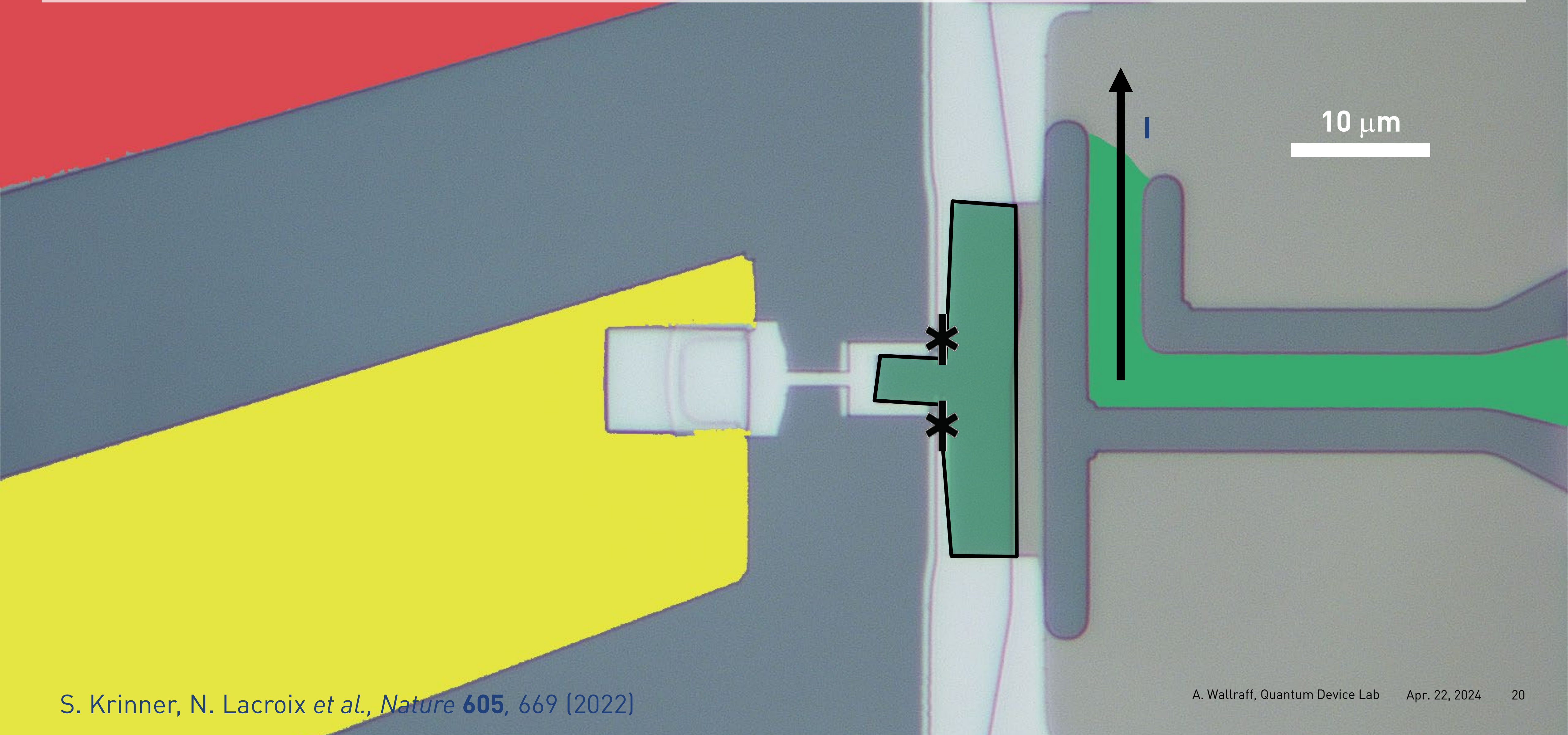

S. Krinner, N. Lacroix *et al.*, *Nature* **605**, 669 (2022)

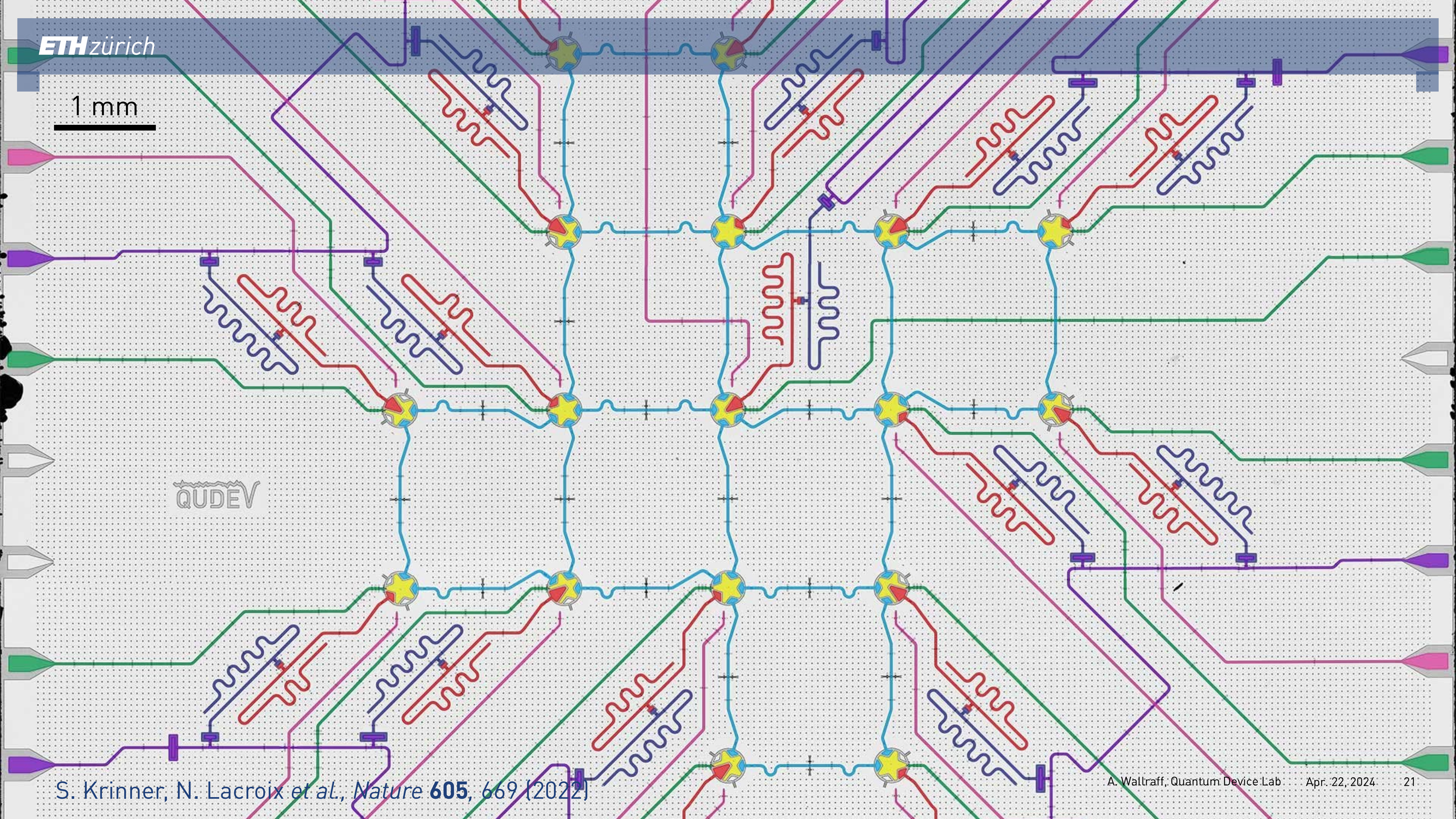

S. Krinner, N. Lacroix *et al.*, *Nature* **605**, 669 (2022)

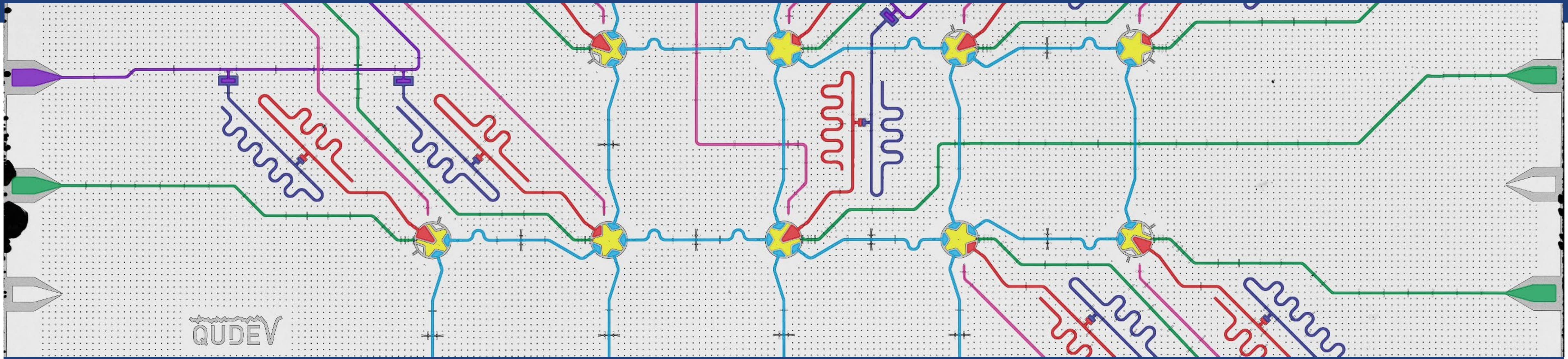

Quantum Information Processing with Superconducting Circuits

Sci. Team: E. Al-Tavil, L. Beltran, I. Besedin, J.-C. Besse, D. Colao Zanuz, Xi Dai, K. Dalton, J. Ekert, S. Frasca, A. Grigorev, D. Hagmann, C. Hellings,, A. Hernandez-Anon, I. Hesner, L. Hofele, M. Kerschbaum, S. Krinner, A. Kulikov, N. Lacroix, G. Norris, M. Pechal, K. Reuer, A. Rosario, C. Scarato, J. Schaer, Y. Song, F. Swiadek, F. Wagner, A. Wallraff *(ETH Zurich)*

Eng. & Tech. Team: A. Akin, M. Bahrani, A. Flasby, A. Fauquex, R. Keller, N. Kohli, R. Siegbert, M. Werner *(ETH Zurich)*

IARPA
BE THE FUTURE

Schweizerischer Nationalfonds

Innovation project supported by

Schweizerische Eidgenossenschaft
Confédération suisse
Confederazione Svizzera
Confederaziun svizra

Swiss Confederation

Innosuisse – Swiss Innovation Agency

Past Group Members & Current Collaboration Partners

www.qudev.ethz.ch

Former group members now
Faculty/PostDoc/PhD/Industry

A. Abdumalikov (Gorba AG)
M. Allan (Leiden)
C. K. Andersen (TU Delft)
M. Baur (ABB)
J. Basset (U. Paris Sud)
S. Berger (AWK Group)
R. Bianchetti (ABB)
D. Bozyigit (Scandit)
R. D. Buijs (ASML)
M. Collodo (Zurich Instruments)
A. Copetudo (NU Singapore)
C. Eichler (FAU Erlangen)
A. Fedorov (UQ Brisbane)
Q. Ficheux (CNRS Grenoble)
S. Filipp (WMI & TU Munich)
J. Fink (IST Austria)
A. Fragner (Kappa)
T. Frey (Bosch)
M. Gabureac (Scrona)
S. Garcia (College de France)
S. Gasparinetti (Chalmers)
M. Goppl (Sensirion)
J. Govenius (VTT)
J. Heinsoo (IQM)
L. Huthmacher (Stellbrink & Prtnr)
D.-D. Jarausch (Leica)
K. Juliusson (IQM)
P. Kurpiers (Rohde & Schwarz)
J. Krause (U. Of Cologne)
C. Lang (Radionor)
S. Lazar (Zurich Instruments)
P. Leek (Oxford)
S. M. Llima (BSC-CNS)
J. Luetolf (D-PHYS, ETH Zurich)
P. Magnard (Alice and Bob)
P. Maurer (Chicago)
J. Mlynek (Siemens)
M. Mondal (IACS Kolkata)
M. Oppliger
J. O'Sullivan (CEA Saclay)
A. Potocnik (imec)
G. Puebla (QZabre)
A. Remm (Atlantic Quantum)
A. Safavi-Naeini (Stanford)
Y. Salathe (Zurich Instruments)
P. Scarlino (EPF Lausanne)
M. Stammeier (Huba Control)
L. Steffen (AWK Group)
A. Stockklauser (Rigetti)
T. Thiele (Zurich Instruments)
I. Tsitsilin (TUM)
J. Ungerer (Harvard)
A. van Loo (RIKEN)
D. van Woerkom (Microsoft)
J. Waissman (HUJI)
T. Walter (deceased)
L. Wernli (Sensirion)
A. Wulff
S. Zeytinoğlu (Harvard)

Collaborations (last 5 years) with groups of

C. Abellan (Quside)
P. Bertet (CEA Saclay)
A. Blais (Sherbrooke)
J. Bylander (Chalmers)
H. J. Carmichael (Auckland)
A. Chin (Cambridge)
I. Cirac (MPQ)
K. Ensslin (ETH Zurich)
M. Hartmann (FAU Erlangen)
T. Ihn (ETH Zurich)
A. Imamoğlu (ETH Zurich)
F. Marquardt (MPL Erlangen)
F. Merkt (ETH Zurich)
A. Messmer (Zurich Instruments)
M. W. Mitchell (ICFO)
M. Müller (RWTH Aachen, FZJ)
M. A. Martin-Delgado (Madrid)
M. Poggio (Basel)
B. Royer (Sherbrooke)
N. Sangouard (CEA Saclay)
H. Tureci (Princeton)
W. Wegscheider (ETH Zurich)

QuSurf
SOLID
aqute
scaleQIT
GEOMDISS
ETH
Eidgenössische Technische Hochschule Zürich
Swiss Federal Institute of Technology Zurich
FNSNF
Swiss National Science Foundation
QSIT Quantum Science and Technology
National Centre of Competence in Research
QED
CIRCUIT AND CAVITY
QUANTUM ELECTRODYNAMICS
erc
SEVENTH FRAMEWORK PROGRAMME

A Representative Quantum Computational Advantage Experiment

Main message

- A complex quantum computing experiments with 53 superconducting qubits
- Milestone: Demonstrated advantage over conventional computers for one task

Challenges

- Economically viable noisy intermediate scale quantum (NISQ) applications need more and much better qubits
- Universal fault-tolerant quantum computation requires quantum error correction
- Major advances are required

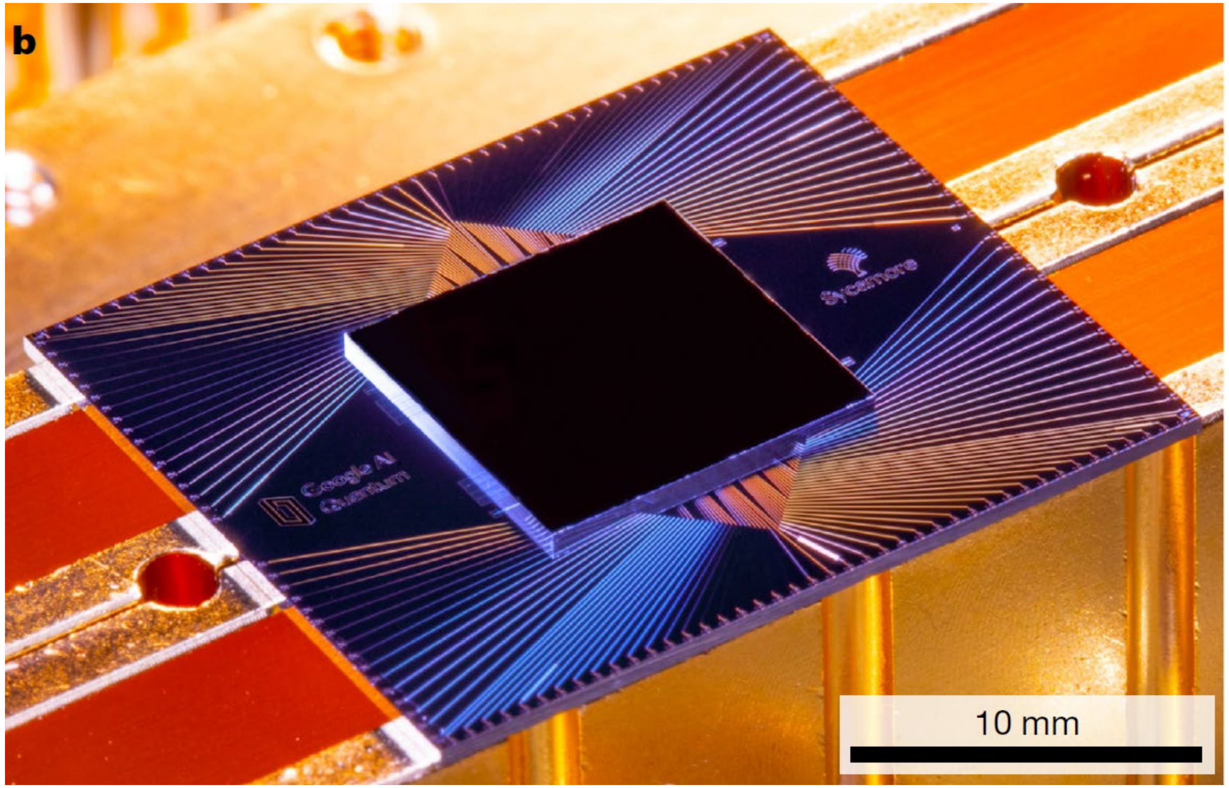

F. Arute, …, J. M. Martinis *et al.*, *Nature* **574**, 505 (2019)

Quantum Computational Advantage Experiment by Google

Features

- 53 qubits on a 54 qubit chip
- Excellent single and two-qubit operations (< 1% error)
- Good single-shot qubit readout (<4% error)
- Randomly chosen long (m = 20) gate sequences on large number of qubits (n = 53)
- Hard to simulate outcome even on the largest supercomputers
- Final state (cross-entropy) fidelity $F_{XEB} \sim 10^{-3} << 1$
- Limited by coherence (< 100 μs) and gate fidelity

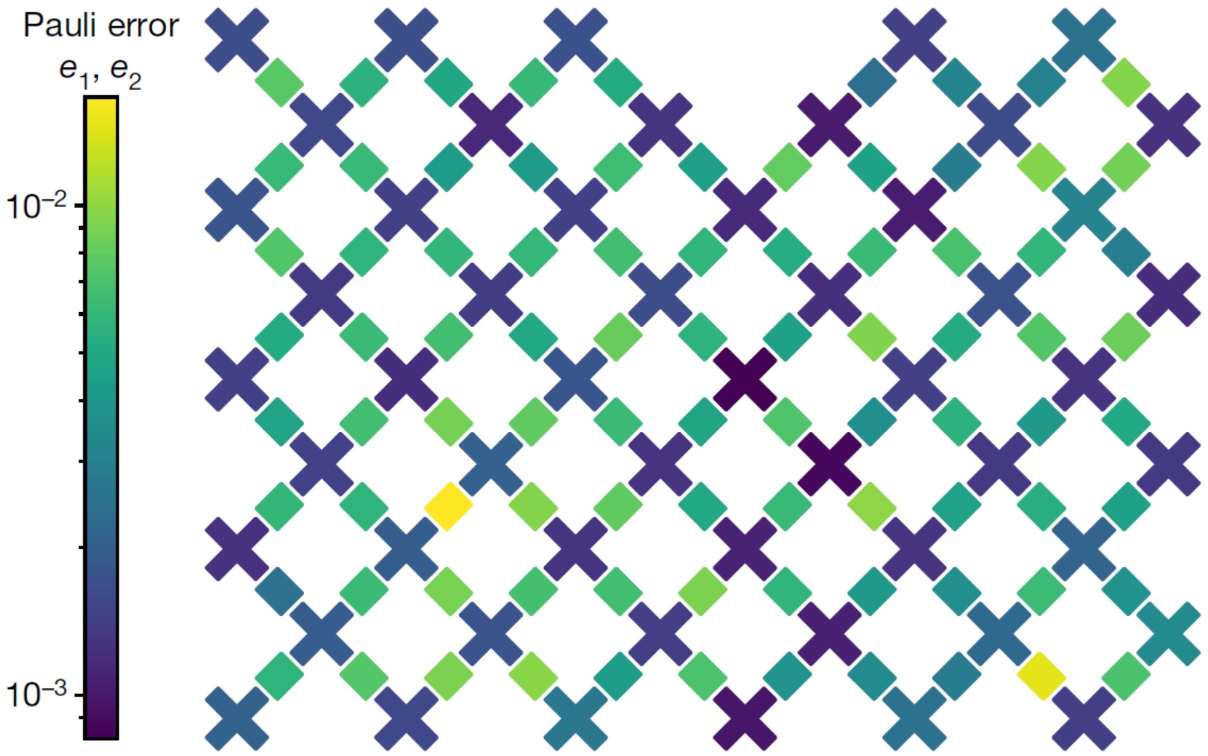

Universal fault-tolerant quantum computation requires **quantum error correction**

F. Arute, …, J. M. Martinis *et al.*, *Nature* **574**, 505 (2019)

Two of the Major Goals in Quantum Information Processing …

… with superconducting circuits

Noisy Intermediate Scale Quantum (NISQ) algorithms displaying a quantum advantage

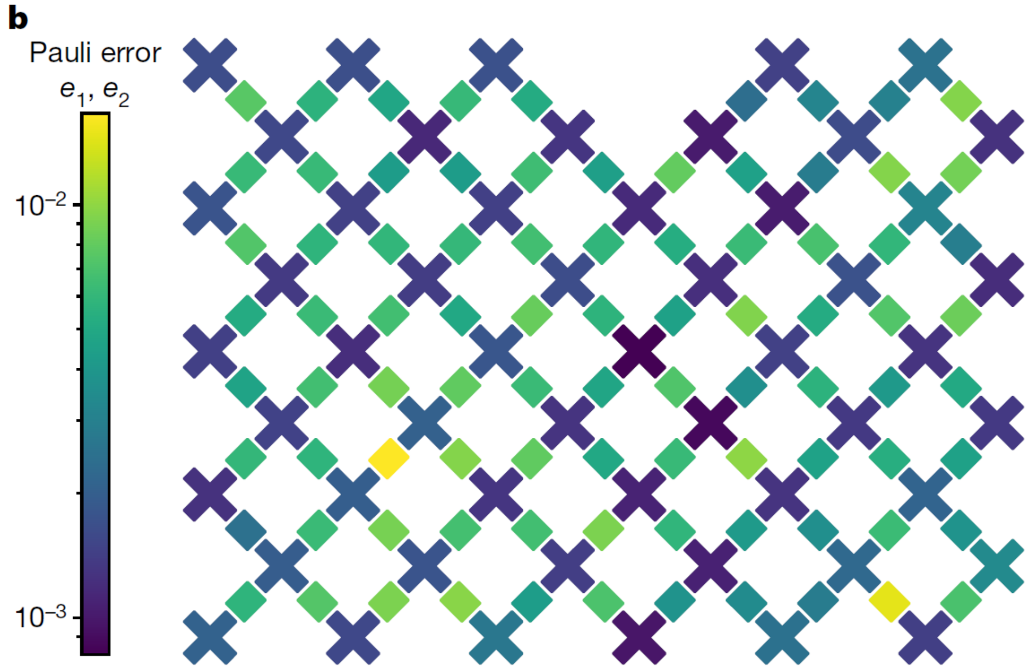

F. Arute, …, J. M. Martinis *et al.*, *Nature* **574**, 505 (2019)

Fault-tolerant, error-corrected, universal quantum information processor

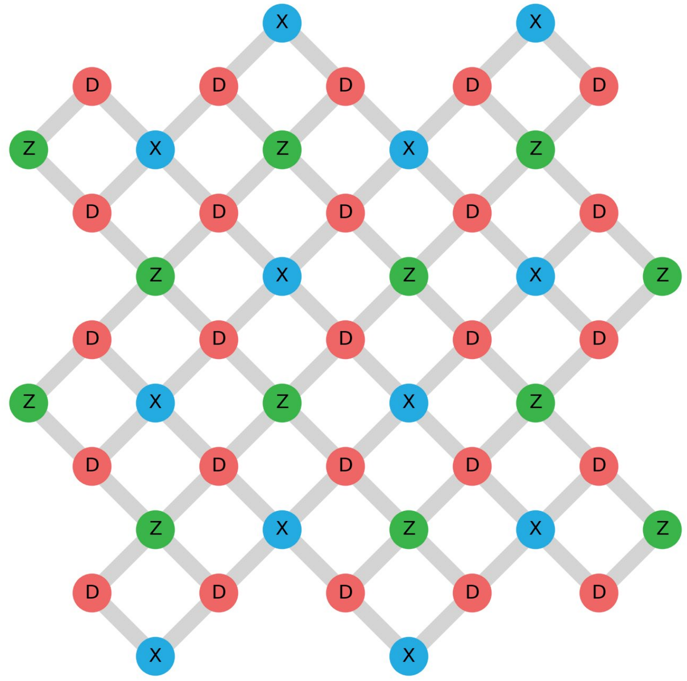

Fowler *et al., Phys. Rev. A* **86**, 032324 (2012)

Lectures, April 22 - 24, 2024

Part 1:
An Introduction to Superconducting Circuits

- Quantum physics of electronic circuits
- Circuit QED

Part 2:
Controlling and Reading Out Qubits

- Single and two-qubit gates
- Qubit readout

Reading Material:
Circuit QED Review:
A. Blais *et al.*,
Rev. Mod. Phys. **93**, 025005 (2021)

SCAN ME

The slides:

Part 3:
Quantum Error Correction

- Quantum error correction, why and how?
- The concept
- The device
- Stabilizer measurements
- Distance-Three surface code

Reading Material:

S. Krinner, N. Lacroix et al., Nature 605, 669 (2022)
C. K. Andersen et al., Nat. Phys. 16, 875 (2020)

Conventional Electronic Circuits

basic circuit elements:

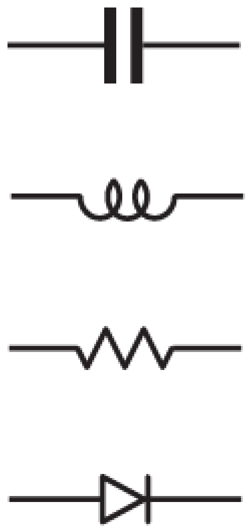

basis of modern information and communication technology

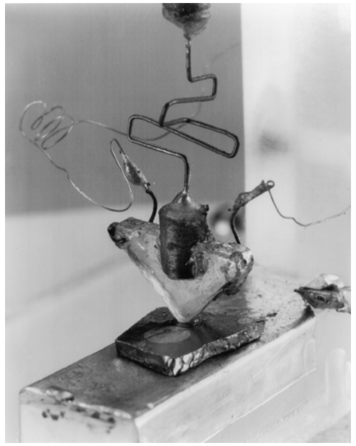

first transistor at Bell Labs (1947)

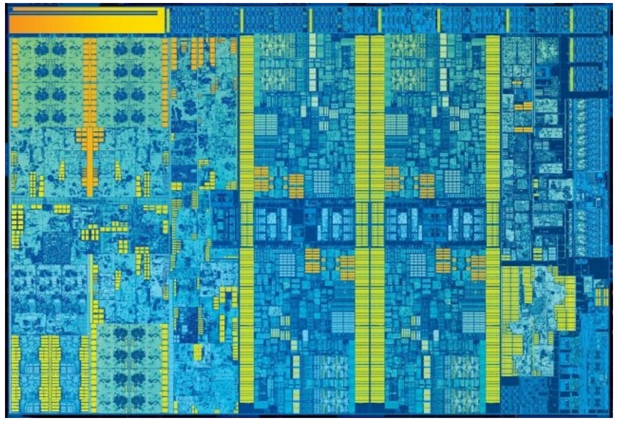

Intel Core i7-6700K Processor

smallest feature size 14 nm
clock speed ~ 4.2 GHz
> 3. 10^9 transistors
power consumption > 10 W

properties :

- classical physics
- no quantum mechanics
- no superposition principle
- no quantization of fields

Quantum Electronic Circuits

basic circuit elements:

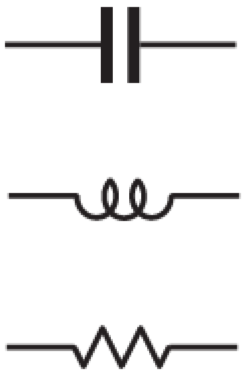

charge on a capacitor:

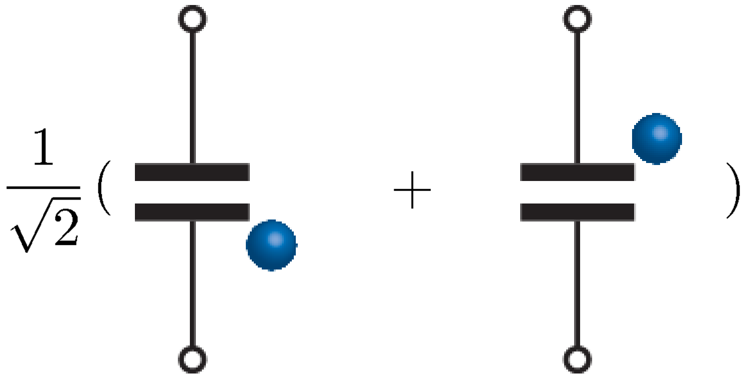

quantum superposition states of:

- charge Q
- flux ϕ

current or magnetic flux in an inductor:

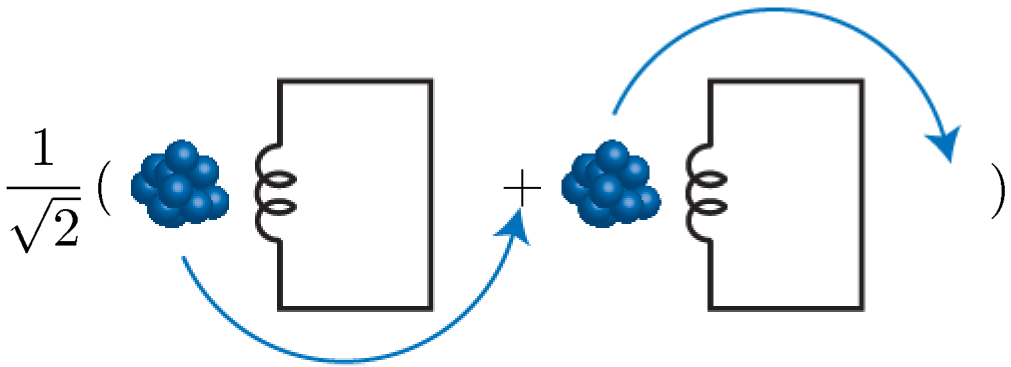

Q, ϕ are conjugate variables

uncertainty relation $\Delta\phi\Delta Q > h$

Linear vs. Nonlinear Superconducting Electronic Oscillators

LC resonator:

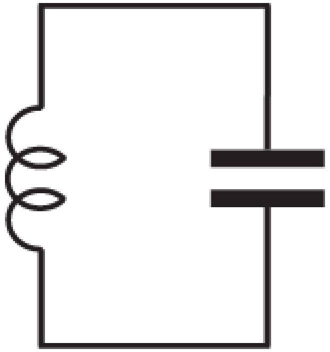

Josephson junction resonator:

Josephson junction = nonlinear inductor

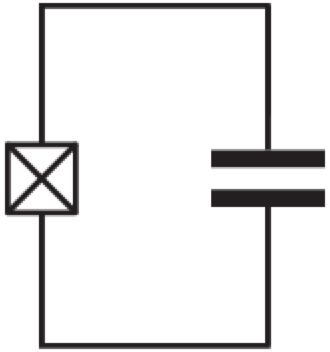

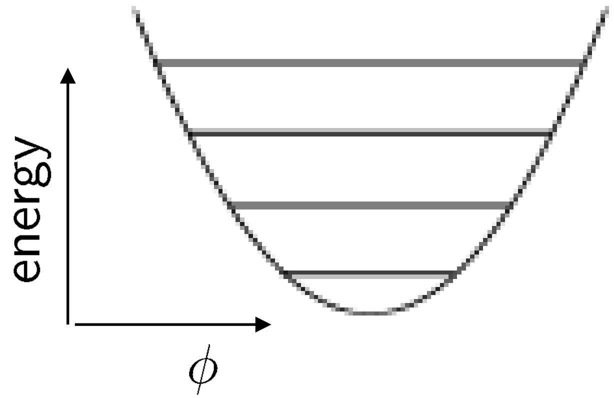

anharmonicity defines effective two-level system

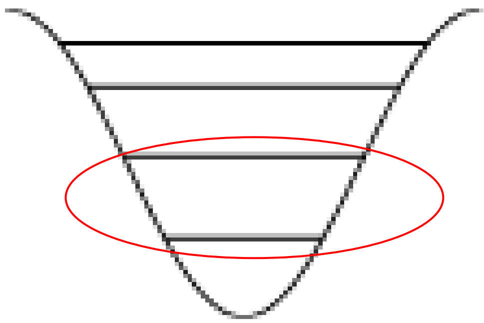

Circuit QED Review: A. Blais *et al.*, *Rev. Mod. Phys.* **93**, 025005 (2021)

Constructing Linear Quantum Electronic Circuits

basic circuit elements:

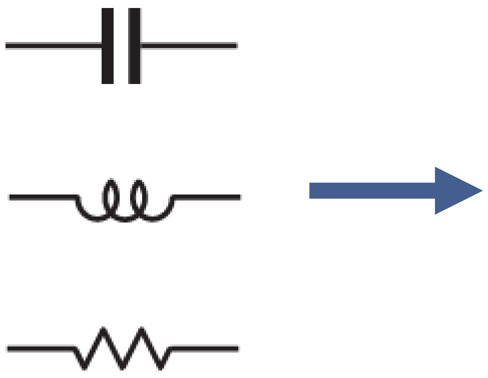

harmonic LC oscillator:

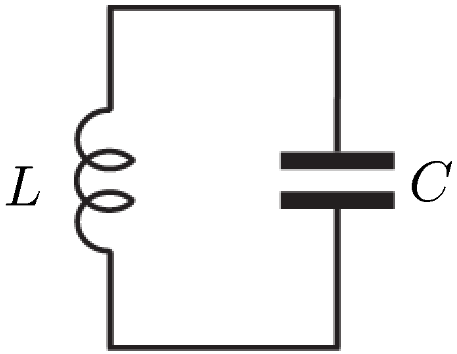

$$\omega = \frac{1}{\sqrt{LC}} \sim 5\,\mathrm{GHz}$$

typical inductor: L = 1 nH
wire in vacuum L ~ 1 nH/mm

typical capacitor: C = 1 pF
size 10 x 10 μm^2 and
dielectric AlOx (ε = 10) of
10 nm thickness: C ~ 1 pF

energy:

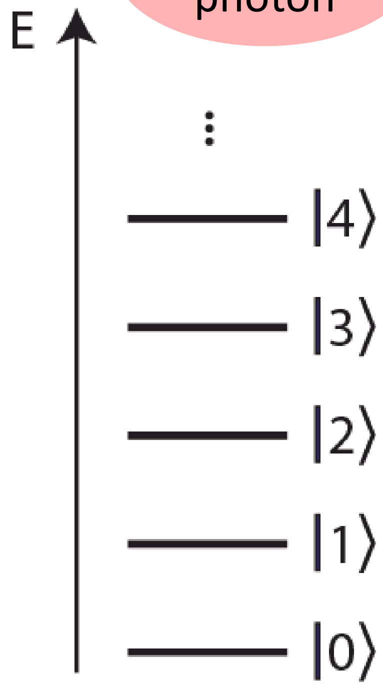

electronic photon

classical physics:

$$H = \frac{\phi^2}{2L} + \frac{Q^2}{2C}$$

quantum mechanics:

$$\hat{H} = \frac{\hat{\phi}^2}{2L} + \frac{\hat{Q}^2}{2C} = \hbar\omega(\hat{a}^\dagger\hat{a} + \frac{1}{2}) \qquad \left[\hat{\phi}, \hat{Q}\right] = i\hbar$$

Review: A. Blais *et al.*, *Rev. Mod. Phys.* **93**, 025005 (2021)
U. Vool and M. Devoret, *Int. J. Circ. Theor. Appl.* 45, 897 (2017)

Quantization of an Electronic Harmonic LC Oscillator

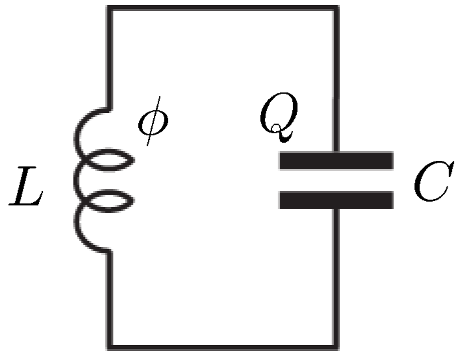

$$\begin{aligned} Q &= CV \\ \phi &= LI \\ V &= -L\dot{I} = -\dot{\phi} \end{aligned}$$

Charge on capacitor

Flux in inductor

Voltage across inductor

Hamiltonian function:

$$H = \frac{CV^2}{2} + \frac{LI^2}{2} = \frac{Q^2}{2C} + \frac{\phi^2}{2L}$$

Conjugate variables:

$$\frac{\partial H}{\partial \phi} = \frac{\phi}{L} = I = \dot{Q}\,, \quad \frac{\partial H}{\partial Q} = \frac{Q}{C} = V = -L\dot{I} = -\dot{\phi}$$

Hamilton operator:

$$\hat{H} = \frac{\hat{\phi}^2}{2L} + \frac{\hat{Q}^2}{2C}$$

Flux and charge operator (flux basis):

$$\begin{aligned} \hat{\phi} &= \phi \\ \hat{Q} &= -i\hbar\frac{\partial}{\partial \phi} \end{aligned}$$

Commutation relation:

$$\left[\hat{\phi}, \hat{Q}\right] = i\hbar$$

Voltages and Currents as Creation and Annihilation Operators

Hamilton operator of harmonic oscillator in second quantization:

$$\hat{H} = \frac{\hat{\phi}^2}{2L} + \frac{\hat{Q}^2}{2C} = \hbar\omega(\hat{a}^\dagger\hat{a} + 1/2)$$

Compare with mechanical harmonic oscillator

$$\hat{a}^\dagger |n\rangle = \sqrt{n+1}\,|n+1\rangle$$ Creation operator

$$\hat{a}\,|n\rangle = \sqrt{n}\,|n-1\rangle$$ Annihilation operator

$$\hat{a}^\dagger\hat{a}\,|n\rangle = n\,|n\rangle$$ Number operator

$$\hat{Q} = \sqrt{\frac{\hbar}{2Z_C}}(\hat{a}^\dagger + \hat{a})$$ Charge/voltage operator $$\hat{V} = \frac{\hat{Q}}{C}$$

$$\hat{\phi} = i\sqrt{\frac{\hbar Z_C}{2}}(\hat{a}^\dagger - \hat{a})$$ Flux/current operator $$\hat{I} = \frac{\hat{\phi}}{L}$$

With characteristic impedance:

$$Z_C = \sqrt{\frac{L}{C}}$$

Flavors of Superconducting Resonators

lumped element resonator:

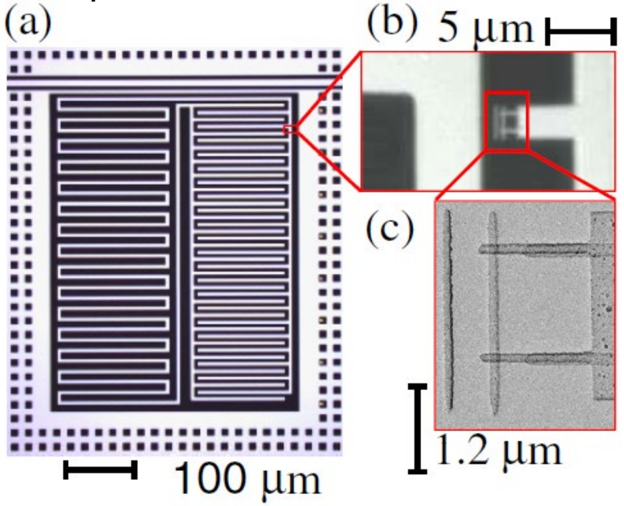

Kim *et al.*, *PRL* **106**, 120501 (2011)

3D cavity:

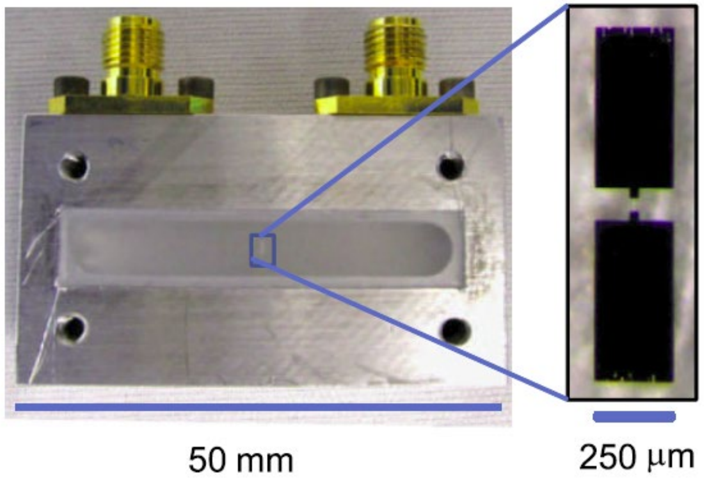

Paik *et al.*, *PRL* **107**, 240501 (2011)

planar transmission line:

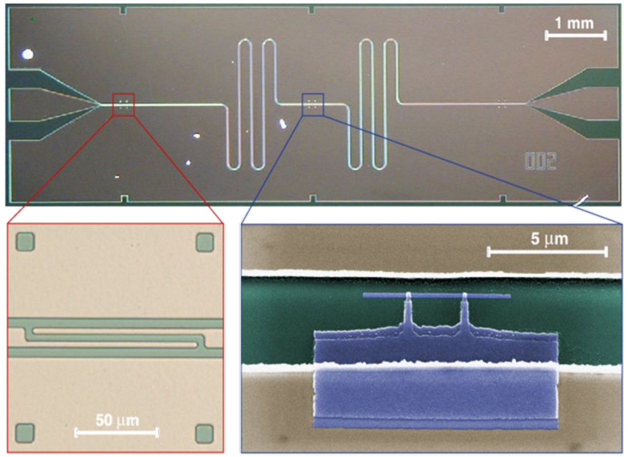

Wallraff *et al.*, *Nature* **431**, 162 (2004)

weakly nonlinear junction:

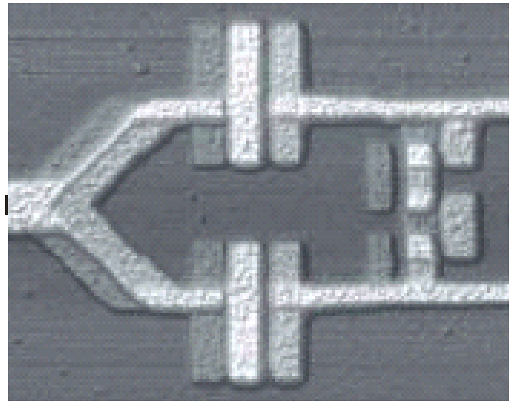

Chiorescu *et al.*, *Nature* **431**, 159 (2004)

Linear vs. Nonlinear Superconducting Electronic Oscillators

LC resonator:

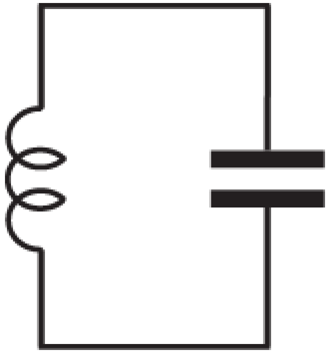

Josephson junction resonator:
Josephson junction = nonlinear inductor

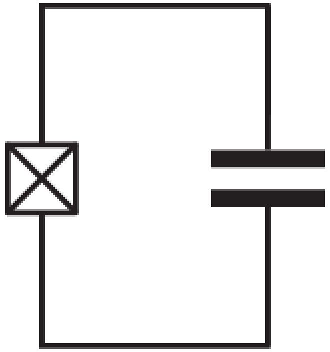

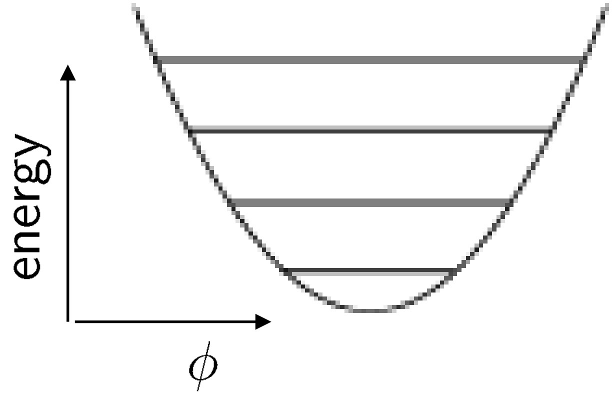

anharmonicity defines effective two-level system

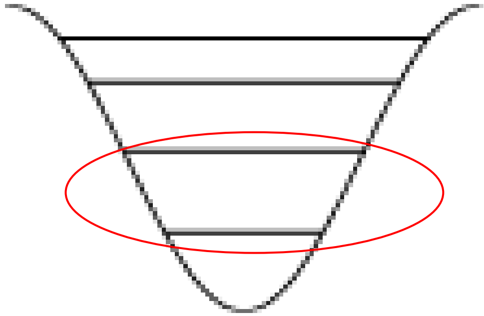

A Low-Loss Nonlinear Element: The Josephson Tunnel Junction

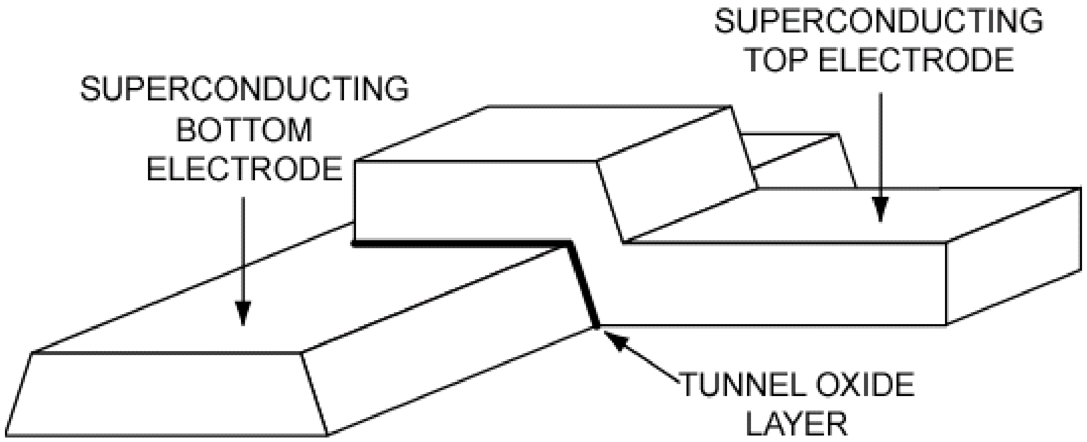

superconductors: Nb, Al
tunnel barrier: AlO_x

Josephson junction fabricated by shadow evaporation:

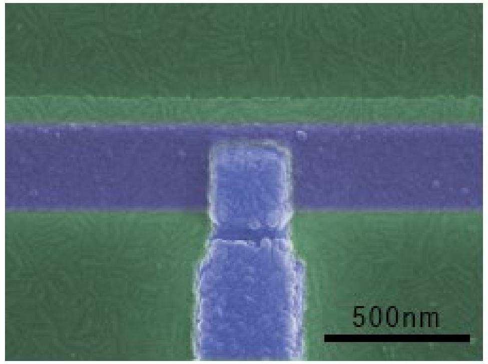

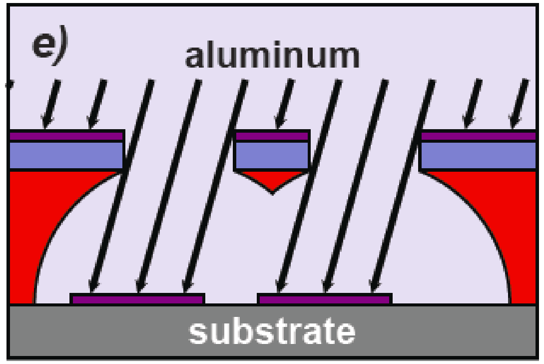

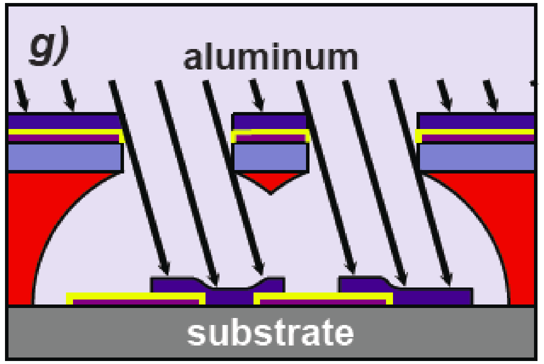

M. Tinkham, Introduction to Superconductivity, McGraw-Hill

Josephson Tunnel Junctions

The only non-linear resonator with (ideally) no dissipation (BCS, $k_B T < \Delta$)

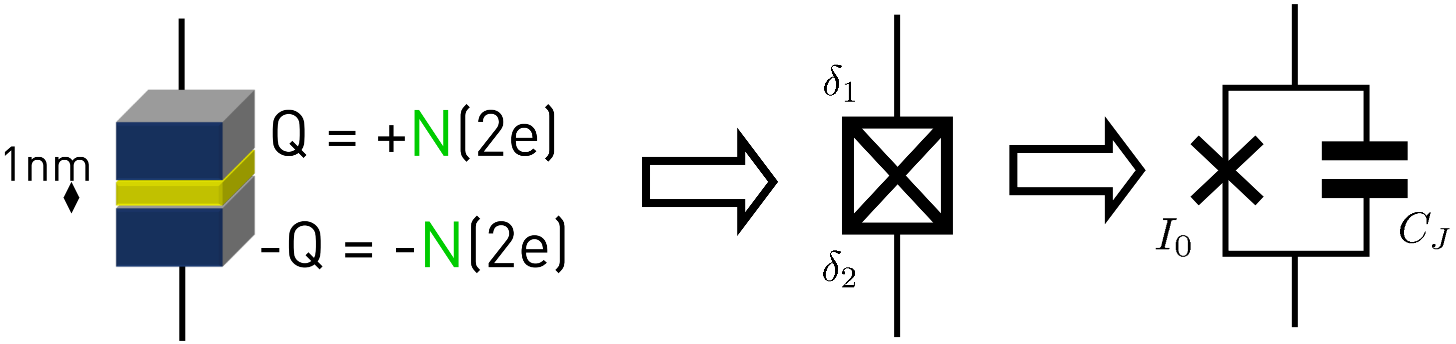

Tunnel junction parameters:

- Critical current I_0
- Junction capacitance C_J
- Tunnel junction resistance R_J

interpretation as tunable nonlinear lossless inductor

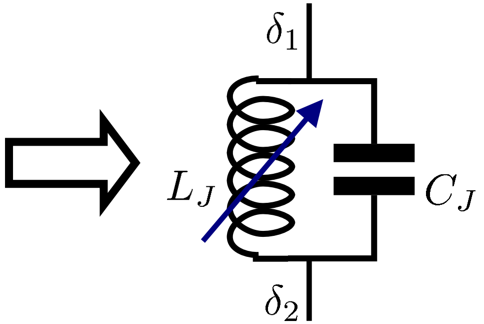

Josephson relations:

$$I = I_0 \sin \delta$$

$$V = \frac{\phi_0}{2\pi} \dot{\delta}$$

Flux quantum: $\phi_0 = \frac{h}{2e}$

Phase difference: $\delta = \delta_2 - \delta_1$

derivation of Josephson effect, see e.g.
chap. 21 in R. A. Feynman: Quantum mechanics, The Feynman Lectures on Physics. Vol. 3 (Addison-Wesley, 1965)

The Josephson Junction as an Ideal Non-Linear Inductor

a nonlinear inductor without dissipation

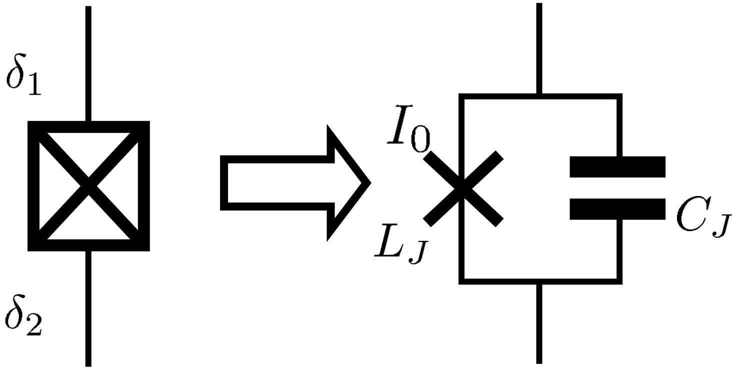

DC/AC Josephson relations: $I = I_0 \sin\delta = I_0 \sin\left[2\pi\phi(t)/\phi_0\right]$ $\quad V = \dfrac{\phi_0}{2\pi}\dot{\delta} = \dot{\phi}$

nonlinear current/phase relation

gauge inv. phase difference: $\delta = \delta_2 - \delta_1 = 2\pi\phi(t)/\phi_0$

Josephson inductance: $V = -L_J \dot{I} = \dfrac{\phi_0}{2\pi I_0}\dfrac{1}{\cos\delta}\dot{I}$

specific Josephson inductance: $L_{J0} = \dfrac{\phi_0}{2\pi I_0}$

I_0 = 100 nA corresponds to L_{J0} ~ 3 nH

Josephson energy:

$$E_J = \int V I dt = \frac{I_0\phi_0}{2\pi}\cos\delta$$

specific Josephson energy: $E_{J0} = \dfrac{I_0\phi_0}{2\pi} = \dfrac{h\Delta}{8e^2R_J}$

M. Tinkham, Introduction to Superconductivity, McGraw-Hill

I_0 = 100 nA corresponds to E_{J0}/h ~ 50 GHz

The Charge Qubit, a.k.a. the Cooper Pair Box Qubit, the Transmon ...

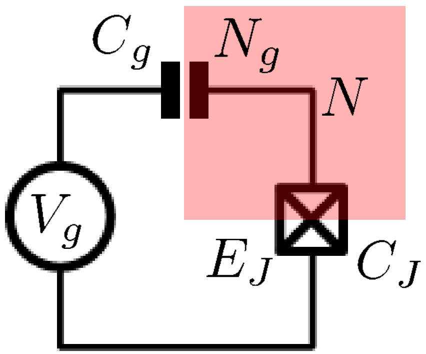

discrete charge on island: $N = \dfrac{Q}{2e}$

continuous gate charge: $N_g = \dfrac{C_g V_g}{2e}$

total box capacitance $C_\Sigma = C_g + C_J$

C_Σ = 1 pF corresponds to E_C/h ~ 77 MHz

Hamiltonian: $H = H_{\text{el}} + H_{\text{mag}}$

charging energy E_C

electrostatic part:

$$H_{\text{el}} = \frac{Q^2}{2C} = \frac{(2e)^2}{2C_\Sigma}(N - N_g)^2$$

magnetic part:

$$H_{\text{mag}} = -E_J \cos\delta \approx \frac{\phi^2}{2L_{J0}}$$

Josephson energy

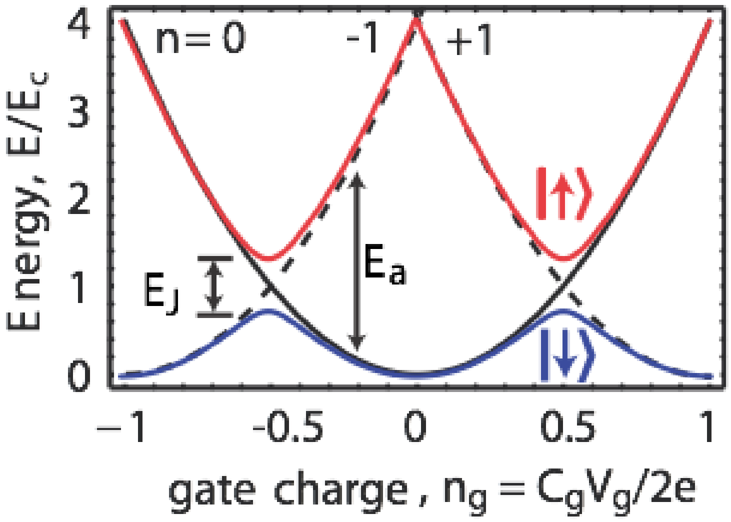

V. Bouchiat, D. Vion, P. Joyez, D. Esteve, and M. H. Devoret, *Physica Scripta* **T76**, 165 (1998).

Hamilton Operator of the Cooper Pair Box Qubit

Hamiltonian: $$\hat{H} = \hat{H}_{\mathrm{el}} + \hat{H}_{\mathrm{mag}} = E_C(\hat{N} - N_g)^2 + E_J \cos\hat{\delta}$$ with $\cos\hat{\delta} = \frac{1}{2}(e^{i\hat{\delta}} + e^{-i\hat{\delta}})$

commutation relation: $$[\hat{\delta}, \hat{N}] = i$$

charge number operator:
$$\hat{N}|N\rangle = N|N\rangle$$ eigenvalues, eigenfunctions
$$\sum_N |N\rangle\langle N| = 1$$ completeness
$$\langle N|M\rangle = \delta_{NM}$$ orthogonality

phase basis:
$$|\delta\rangle = \frac{1}{\sqrt{2\pi}}\sum_N e^{iN\delta}|N\rangle$$ basis transformation
$$e^{\pm i\hat{\delta}}|N\rangle = |N \pm 1\rangle$$

J. Koch *et al.*, *Phys. Rev. A* **76**, 042319 (2007)
U. Vool and M. Devoret, *Int. J. Circ. Theor. Appl.* 45, 897 (2017), arXiv:1610.03438

Lectures, April 22 - 24, 2024

Part 1:
An Introduction to Superconducting Circuits
- Quantum physics of electronic circuits
- Circuit QED

Part 2:
Controlling and Reading Out Qubits
- Single and two-qubit gates
- Qubit readout

Reading Material:
Circuit QED Review:
A. Blais *et al.*,
Rev. Mod. Phys. **93**, 025005 (2021)

SCAN ME

The slides:

Part 3:
Quantum Error Correction
- Quantum error correction, why and how?
- The concept
- The device
- Stabilizer measurements
- Distance-Three surface code

Reading Material:
S. Krinner, N. Lacroix et al., Nature 605, 669 (2022)
C. K. Andersen et al., Nat. Phys. 16, 875 (2020)

Solving the Cooper Pair Box Qubit Hamiltonian

Hamilton operator in the **charge basis** N:

$$\hat{H} = \sum_N \left[E_C (N - N_g)^2 |N\rangle\langle N| - \frac{E_J}{2} (|N\rangle\langle N+1| + |N+1\rangle\langle N|) \right]$$

solutions in the charge basis: $\hat{H}|\psi_n(N)\rangle = E_n|\psi_n(N)\rangle$

Hamilton operator in the **phase basis** δ: (see e.g. J. Koch *et al.*, PRA **76**, 042319 (2007))

$$\hat{H} = E_C(\hat{N} - N_g)^2 + E_J \cos\hat{\delta} = E_C\left(-i\frac{\partial}{\partial\delta} - N_g\right)^2 + E_J \cos\hat{\delta}$$

transformation of the number operator:

$$\hat{N} = \frac{\hat{Q}}{2e} = -i\hbar\frac{1}{2e}\frac{\partial}{\partial\phi} = -i\frac{\partial}{\partial\delta}$$

solutions in the phase basis: $\hat{H}|\psi_n(\delta)\rangle = E_n|\psi_n(\delta)\rangle$

J. Koch *et al., Phys. Rev. A* **76**, 042319 (2007)

U. Vool and M. Devoret, *Int. J. Circ. Theor. Appl.* 45, 897 (2017), arXiv:1610.03438

Charge and Phase Wave Functions ($E_J << E_C$)

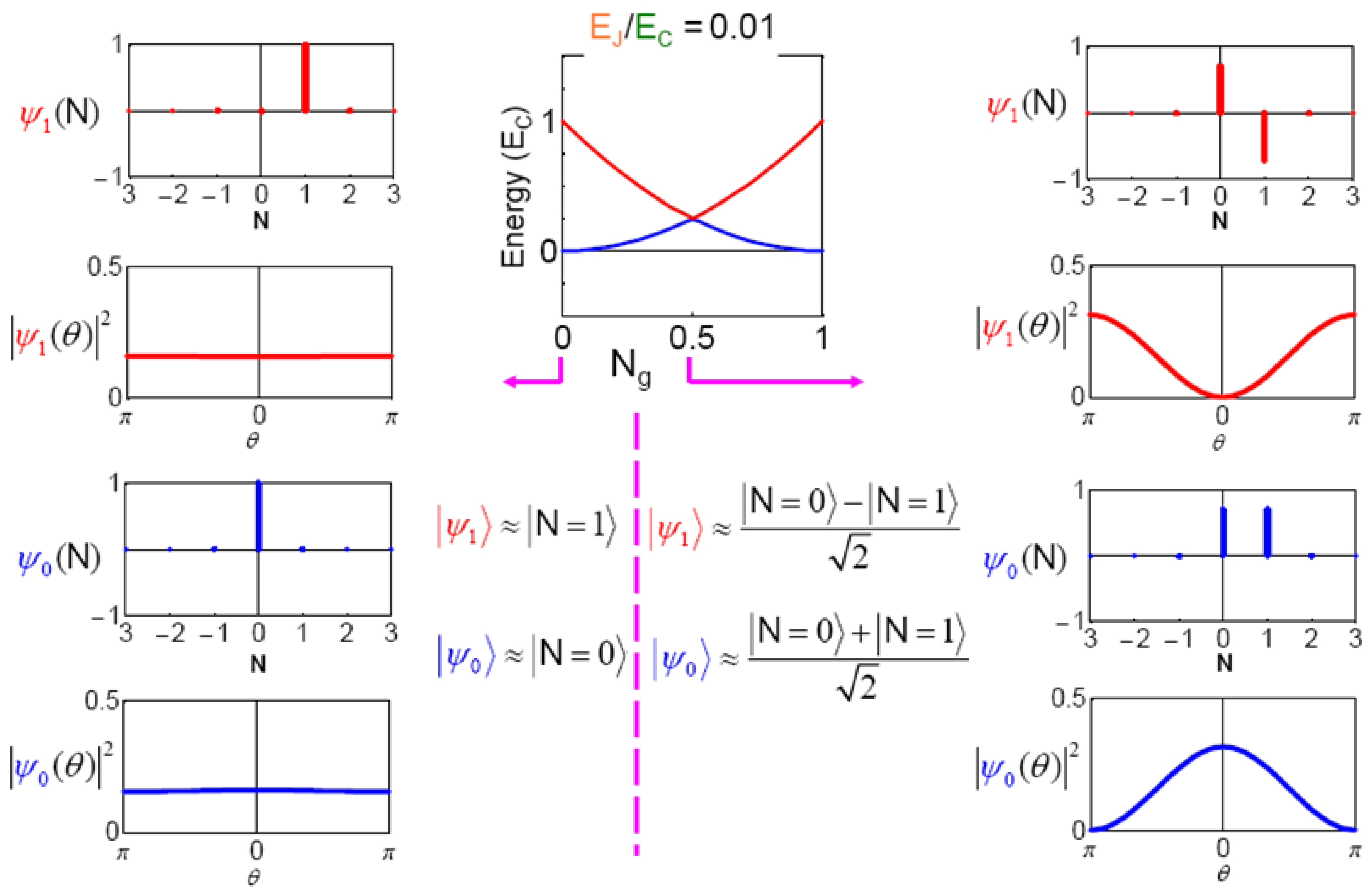

courtesy CEA Saclay

Charge and Phase Wave Functions ($E_J \sim E_C$)

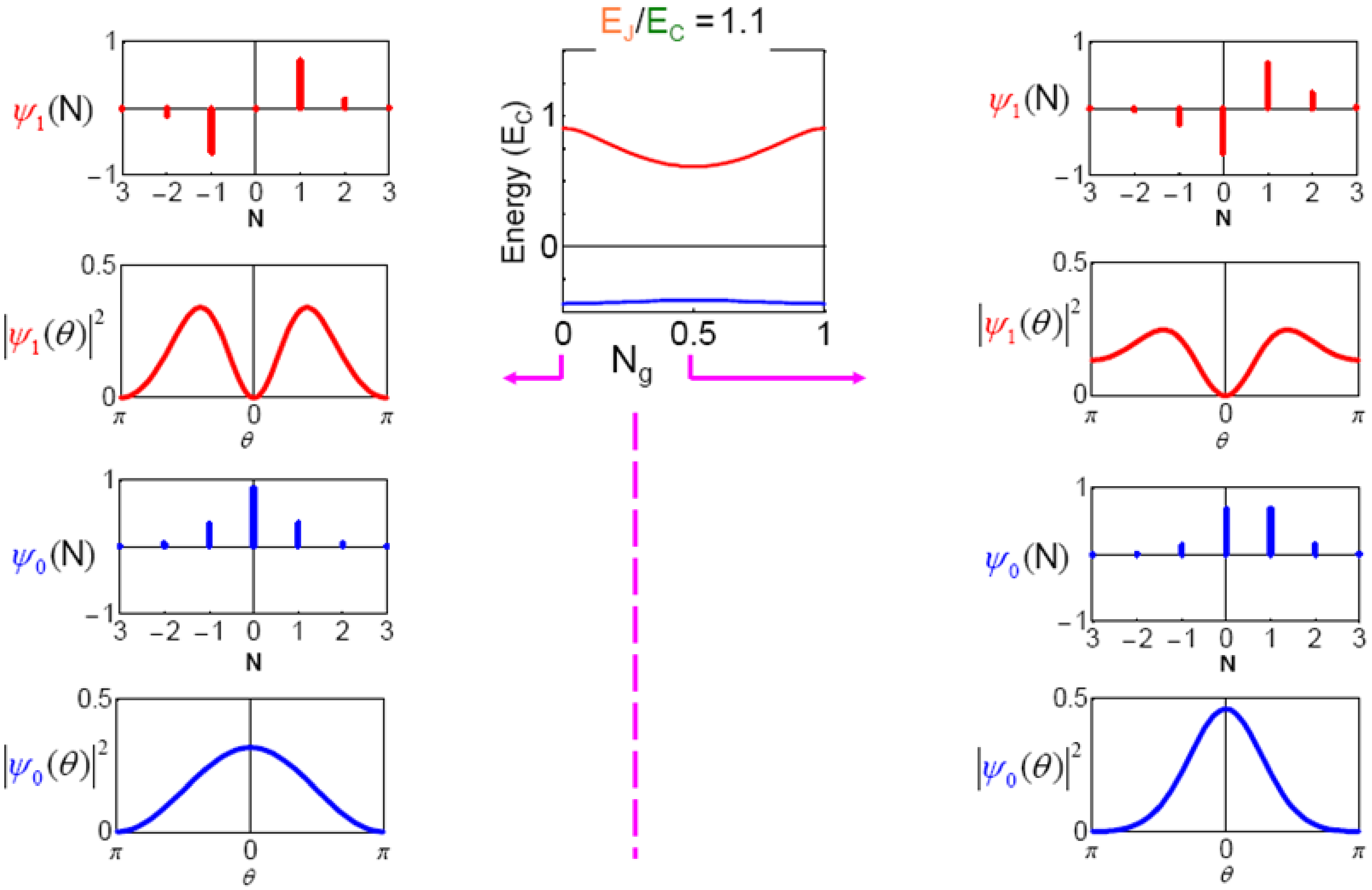

courtesy CEA Saclay

From Cooper Pair Box to Transmon: A Charge Noise Insensitive Qubit

Cooper pair box energy levels:

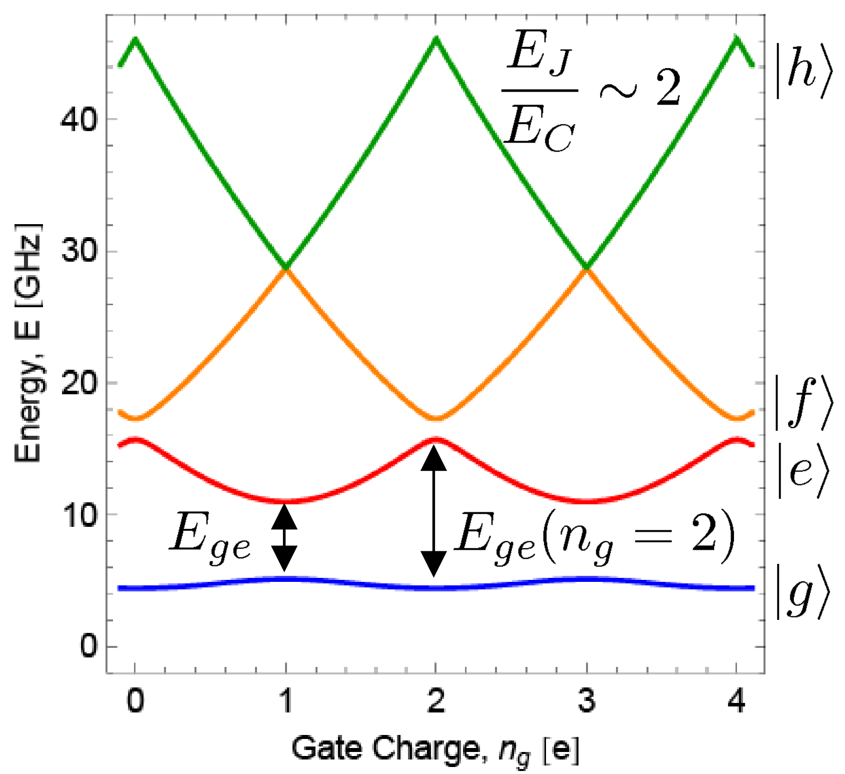

Transmon energy levels:

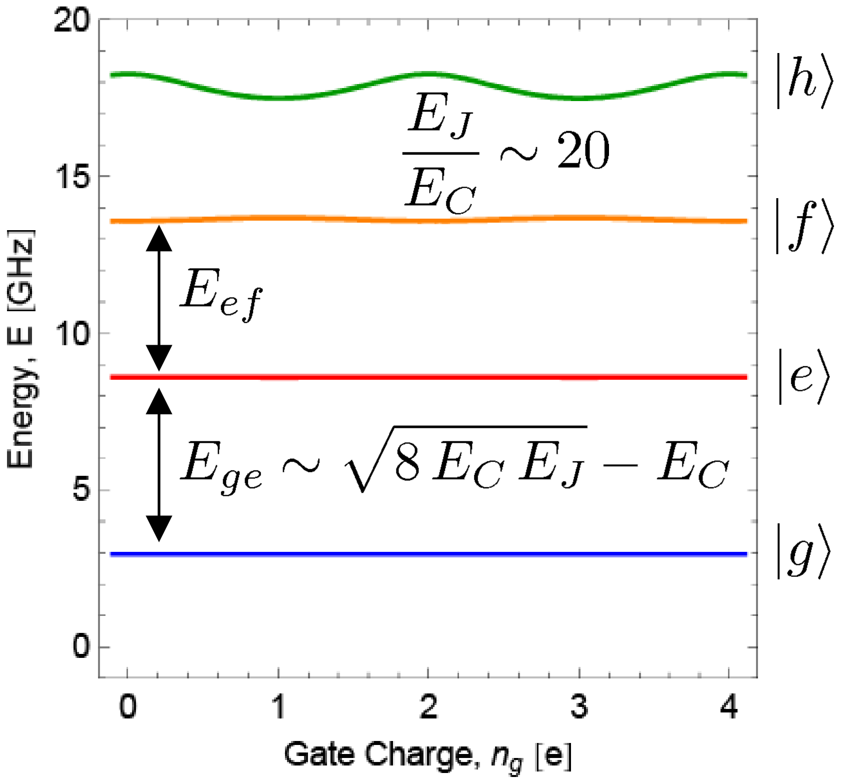

Reduced sensitivity to gate charge:

- Disables tuning by gate charge
- Reduces sensitivity to charge noise
- Use magnetic flux for tuning instead

Reduced anharmonicity

- Creates channel for leakage
- Limits shortest possible single qubit gate times
- Use optimized pulse shapes

dispersion:

$$\epsilon = E_{ge}(n_g = 1) - E_{ge}(n_g = 2)$$

relative anharmonicity:

$$\alpha_r = \frac{E_{ef} - E_{ge}}{E_{ge}}$$

J. Koch *et al.*, *Phys. Rev. A* **76**, 042319 (2007)

Dispersion and Anharmonicity of the Transmon Qubit

Charge dispersion:

$$\epsilon = E_{ge}(n_g = 1) - E_{ge}(n_g = 2)$$

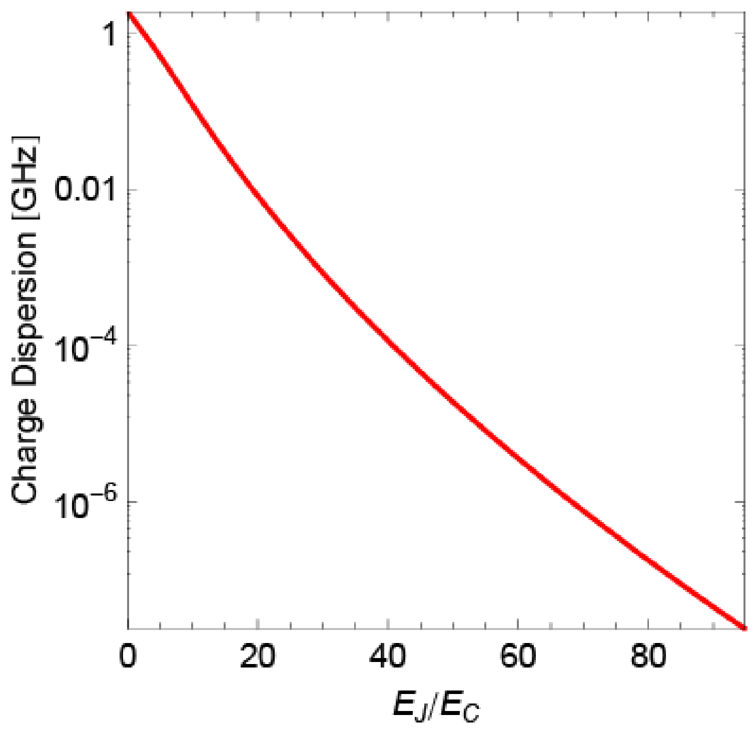

Anharmonicity:

$$\alpha_r = \frac{E_{ef} - E_{ge}}{E_{ge}}$$

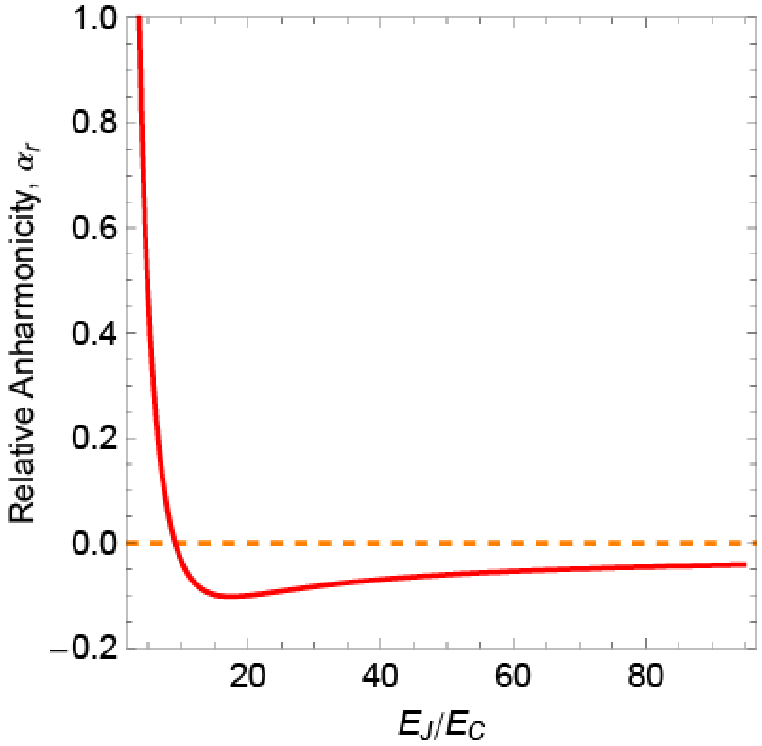

J. Koch *et al.*, *Phys. Rev. A* **76**, 042319 (2007)

The Transmon: A Cooper Pair Box with an Extra Capacitor

Cooper Pair Box

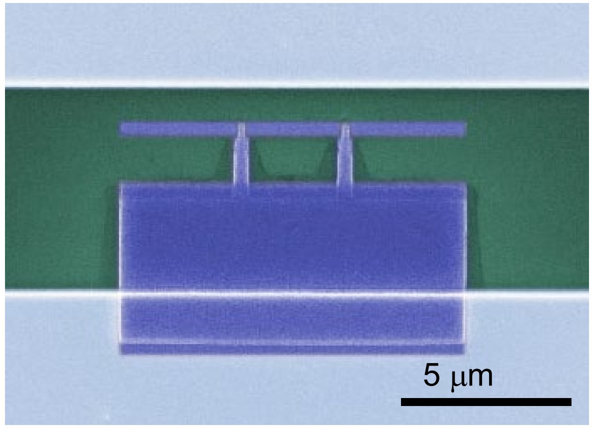

Transmon qubit

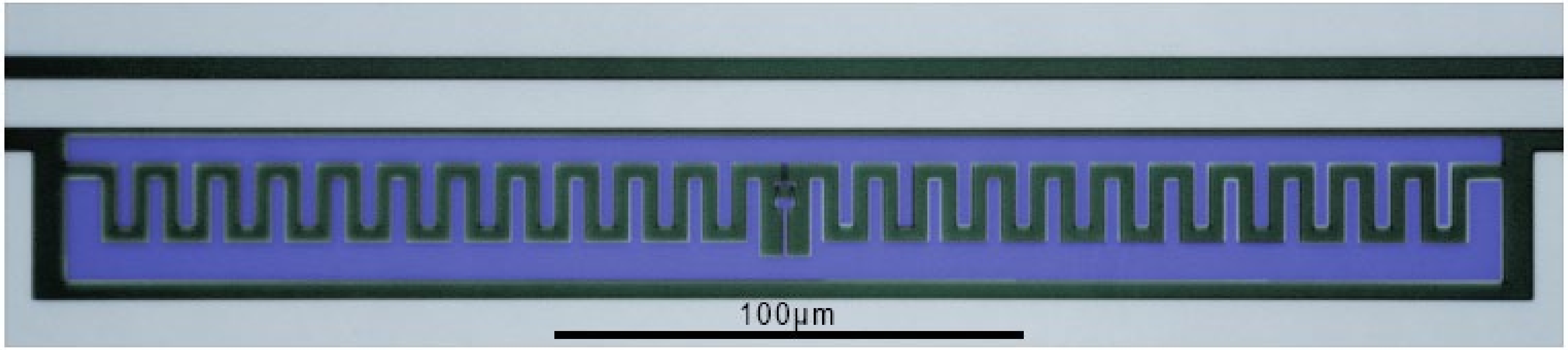

circuit diagram:

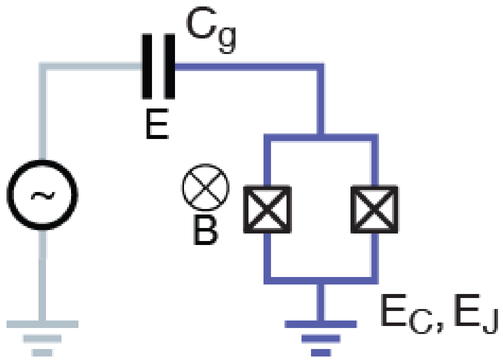

- Large shunt capacitance
- Large physical size
- Large dipole coupling to microwave resonator
- Split Jospehson junction (SQUID) for magnetic flux tuning

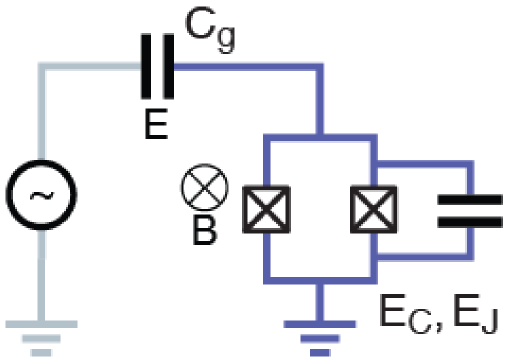

J. Koch *et al.*, *Phys. Rev. A* **76**, 042319 (2007)
J. Schreier *et al.*, *Phys. Rev. B* **77**, 180502 (2008)

Tuning Transmon Qubits with Applied Magnetic Flux

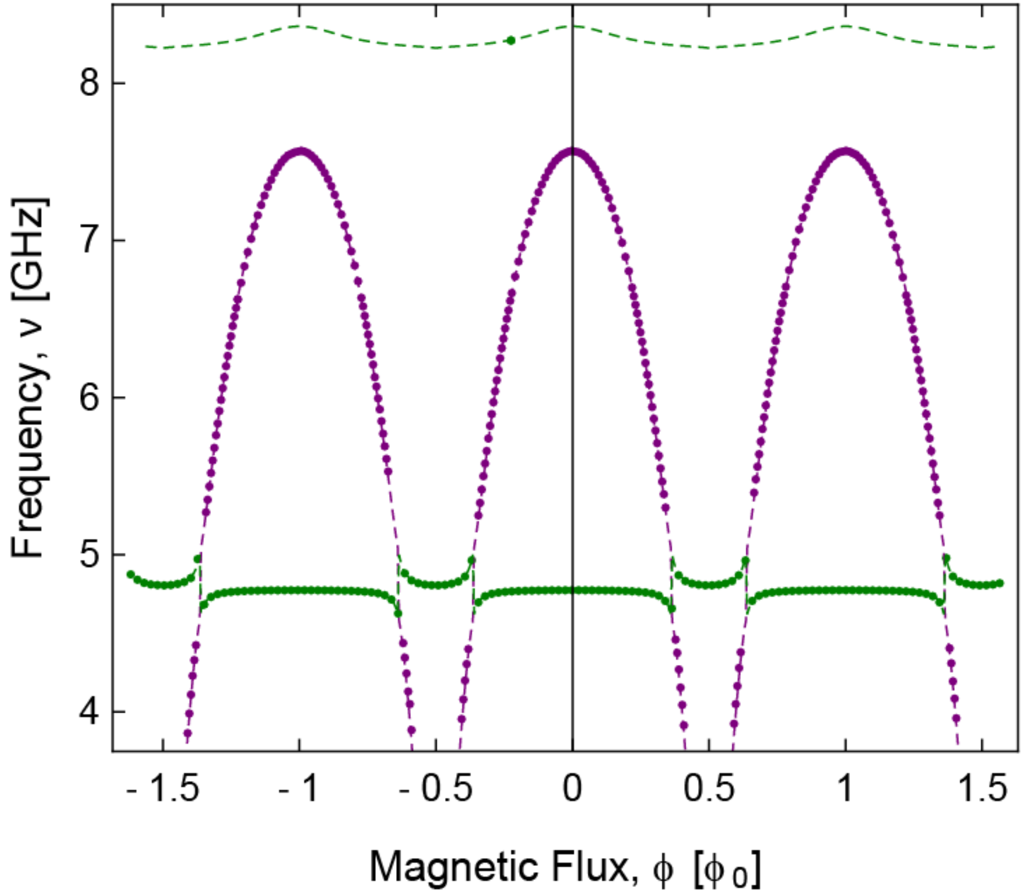

Measured qubit/resonator freq. (*,*)
Fit to full Hamiltonian (-,-)

Changing Qubit Transition Frequency:

- Make qubits with superconducting quantum interference device (SQUID) loop
  M. Tinkham, Introduction to Superconductivity, McGraw-Hill

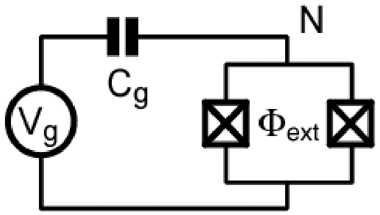

$$E_J = E_{J,\max} \cos\left(\pi \frac{\phi_{\text{ext}}}{\phi_0}\right)$$

- Apply global magnetic field using off-chip coil
- Apply “local” magnetic field using on-chip flux line

Reminder: Resonator and Qubit Spectroscopy:

- Probe resonator
- Drive qubit
- When drive matches the qubit transition, change in transmission of resonator probe observed.

Superconducting Circuits as Components for a Quantum Computer

constructing quantum electronic circuits from basic circuit elements:

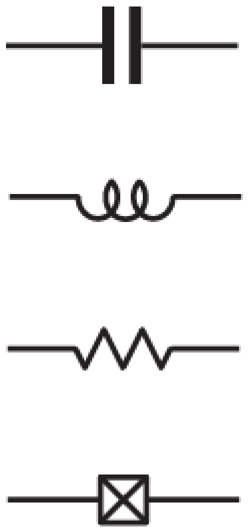

Josephson junction: a non-dissipative nonlinear element (inductor)

harmonic LC oscillator:

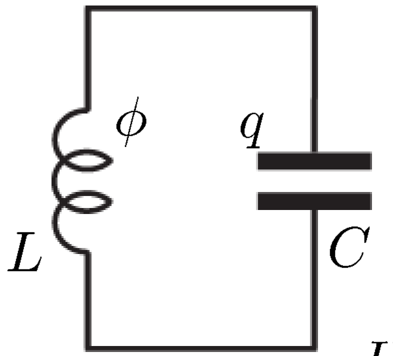

$$H = \hbar\omega(\hat{a}^\dagger \hat{a} + \frac{1}{2})$$

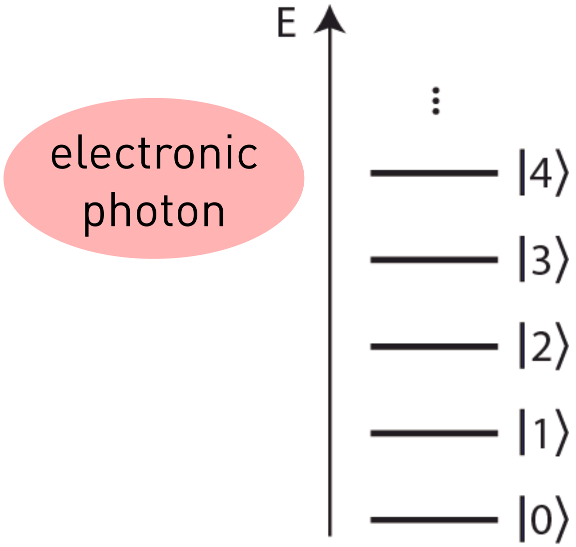

anharmonic oscillator:

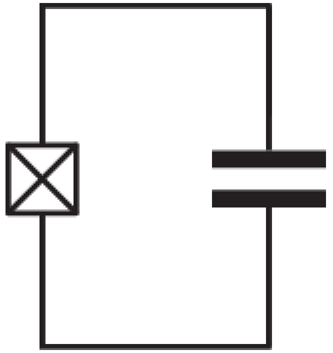

$$H \approx \hbar(\omega_{ge}\,\hat{b}^\dagger \hat{b} - \frac{\alpha}{2}\,\hat{b}^{\dagger 2}\hat{b}^2)$$

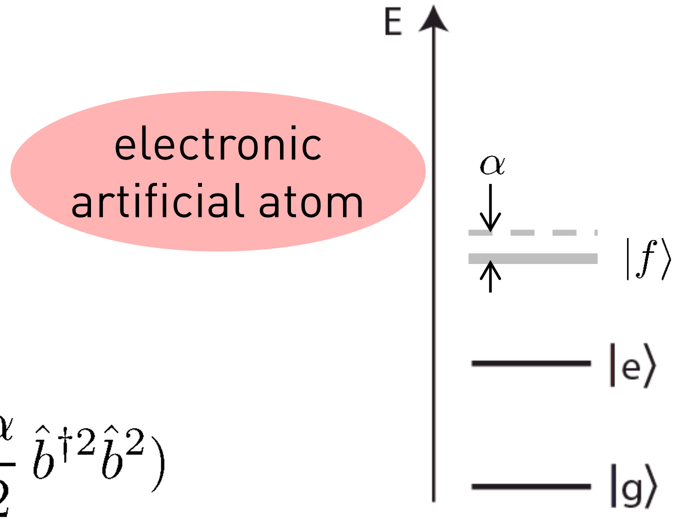

Review: M. H. Devoret, A. Wallraff and J. M. Martinis, *condmat/0411172* (2004)

Cavity Quantum Electrodynamics (QED) with Superconducting Circuits

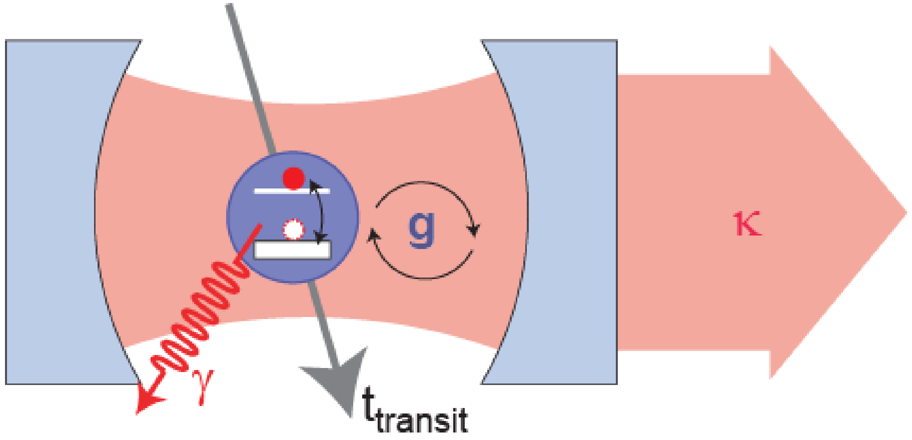

Controllable coherent interaction
of **single photons** with **individual two level systems** ...

With atoms:
J. M. Raimond *et al., Rev. Mod. Phys.* **73**, 565 (2001)
S. Haroche & J. Raimond, *OUP Oxford* (2006)
J. Ye., H. J. Kimble, H. Katori, *Science* **320**, 1734 (2008)

With superconducting circuits:

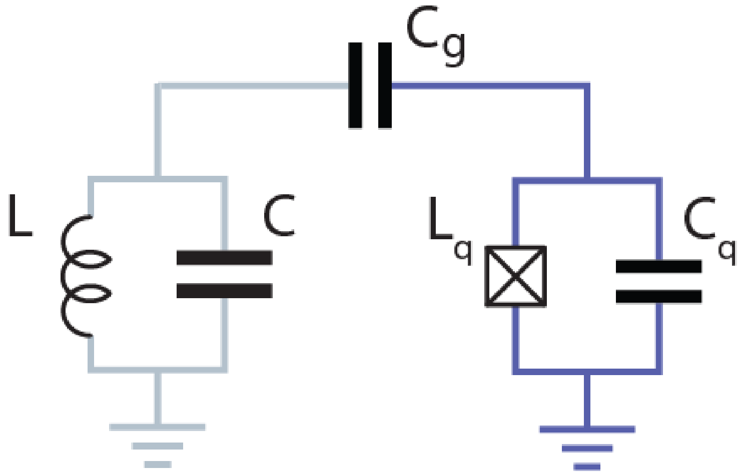

How is circuit QED useful for quantum information processing?

- Isolating qubits from their electromagnetic environment
- Maintaining addressability of qubits
- Reading out the state of qubits
- Coupling qubits to each other
- Converting stationary qubits to flying qubits

Circuit QED Review: A. Blais *et al., Rev. Mod. Phys.* **93**, 025005 (2021)
Concept: A. Blais *et al.*, *PRA* **69**, 062320 (2004), Exp.: A. Wallraff et al., *Nature* **431**, 162 (2004)

First Cavity QED Experiments with Superconducting Circuits

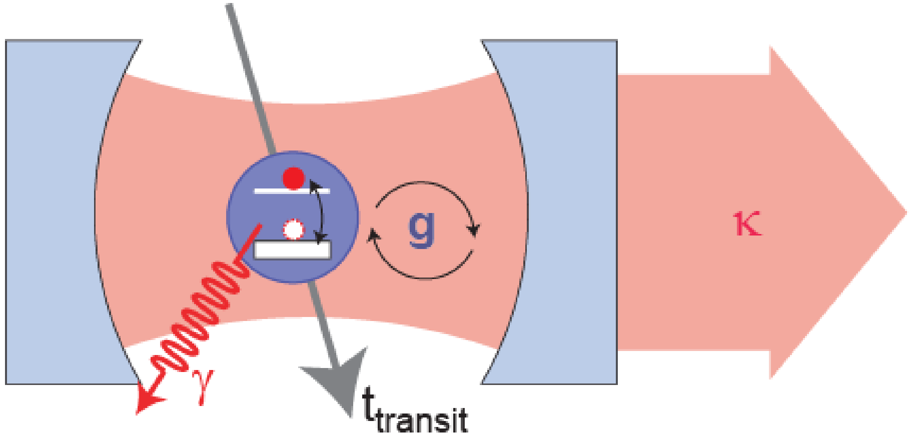

Controllable coherent interaction of **single photons** with **individual two-level systems** (qubits)

Elements:

- the cavity: a superconducting 1D transmission line resonator with large vacuum field E_0 and long photon lifetime $1/\kappa$
- the artificial atom: a superconducting qubit with large dipole moment d and long coherence time $1/\gamma$

… in superconducing circuits:

circuit quantum electrodynamics

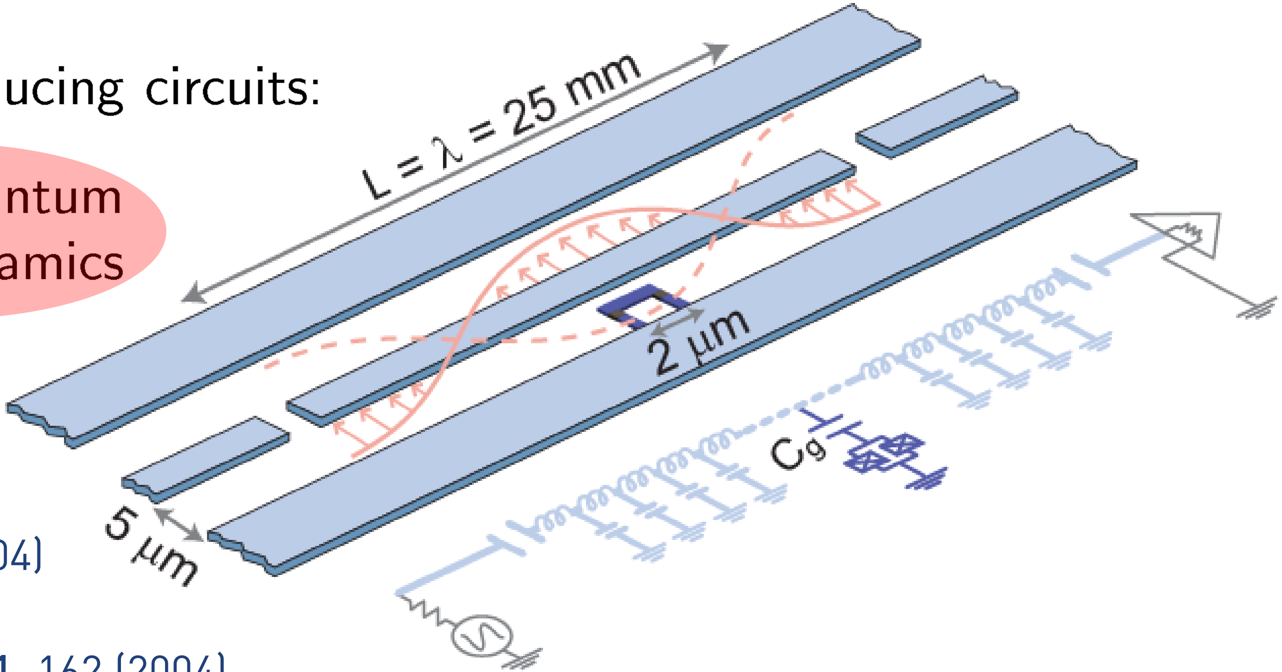

A. Blais, et al. , *PRA* **69**, 062320 (2004)

A. Wallraff et al., *Nature (London)* **431**, 162 (2004)

Qubit/Photon Coupling

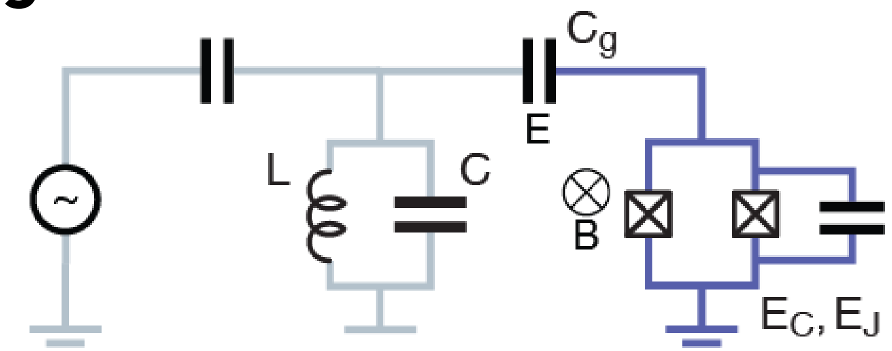

Hamilton operator of qubit (2-level approx.) coupled to resonator:

$$\hat{H} = \frac{\hat{Q}^2}{2C} + \frac{\hat{\phi}^2}{2L} + \frac{E_C}{2}(1 - 2(N_g + \hat{N}_g))\hat{\sigma}_z - \frac{E_J}{2}\hat{\sigma}_x$$

Here, 2-level approx. valid for EJ/EC ~ 1.

Similar derivation for EJ/EC >> 1 possible, see e.g.: J. Koch *et al.*, PRA **76**, 042319 (2007)

Quantum part of gate voltage due to resonator

$$\hat{N}_g = \frac{C_g}{2e}\hat{V}_g = \frac{C_g}{2e}\sqrt{\frac{\hbar\omega_r}{2C}}(\hat{a}^\dagger + \hat{a})$$

Consider bias at charge degeneracy N_g = 1/2 and change of qubit basis (*z* to *x*, *x* to -*z*).

A. Blais, et al. , *PRA* **69**, 062320 (2004)

Jaynes-Cummings Hamiltonian

Consider bias at charge degeneracy N_g = 1/2 and change of qubit basis (*z* to *x*, *x* to -*z*)

$$\hat{H} \quad = \quad \hbar\omega_r(\hat{a}^\dagger\hat{a} + 1/2) + \frac{E_J}{2}\hat{\sigma}_z + \frac{E_C}{2}\frac{C_g}{2e}\sqrt{\frac{\hbar\omega_r}{2C}}(\hat{a}^\dagger + \hat{a})\hat{\sigma}_x$$

Quantum Rabi Hamiltonian

Use qubit raising and lowering operators $\hat{\sigma}_x = \hat{\sigma}^+ + \hat{\sigma}^-$

Coupling term in the rotating wave approximation (RWA)

$$\hat{H}_g \quad = \quad \frac{E_C}{2}\frac{C_g}{2e}\sqrt{\frac{\hbar\omega_r}{2C}}(\hat{a}^\dagger\hat{\sigma}^- + \cancel{\hat{a}\hat{\sigma}^-} + \cancel{\hat{a}^\dagger\hat{\sigma}^+} + \hat{a}\hat{\sigma}^+) \approx \hbar g(\hat{a}^\dagger\hat{\sigma}^- + \hat{a}\hat{\sigma}^+)$$

Jaynes Cummings Hamiltonian

Coupling strength $\hbar g = \frac{C_g}{C_\Sigma}2e\sqrt{\frac{\hbar\omega_r}{2C}}$

Vacuum-Rabi frequency $\nu_R = \frac{2g}{2\pi} \approx 1\ldots 300\,\mathrm{MHz}$ $\quad g \gg [\kappa, \gamma]$ possible!

A. Blais, et al. , *PRA* **69**, 062320 (2004)

Cavity Quantum Electrodynamics

interaction of atom and photon in a cavity

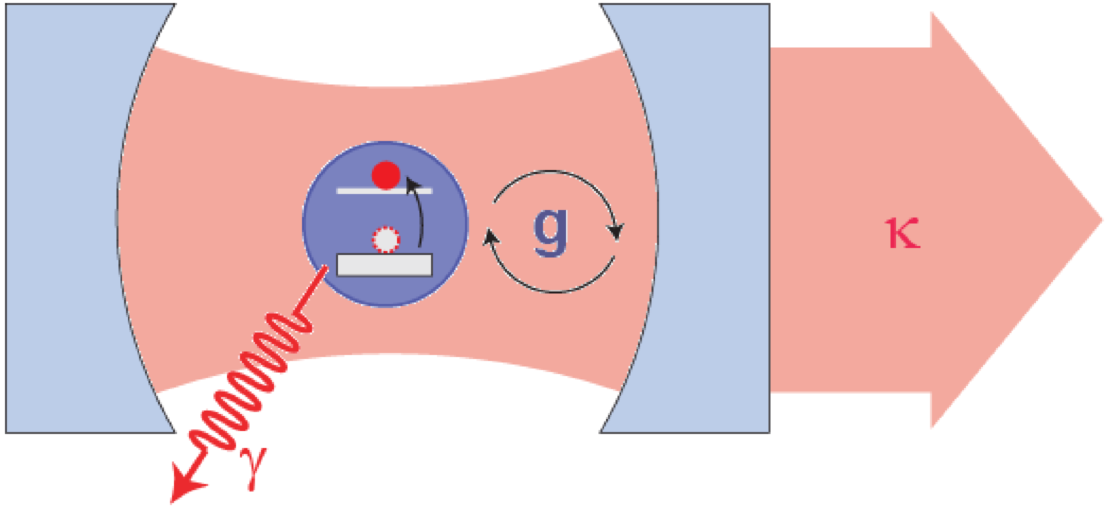

Jaynes-Cummings Hamiltonian

$$H = \hbar\omega_r \left(a^\dagger a + \frac{1}{2} \right) + \frac{\hbar\omega_a}{2}\sigma^z + \hbar g (a^\dagger \sigma^- + a\sigma^+) + H_\kappa + H_\gamma$$

strong coupling limit:

$$g = dE_0/\hbar > \gamma,\, \kappa\,,1/t_{\text{transit}}$$

D. Walls, G. Milburn, Quantum Optics, Spinger-Verlag, Berlin (1994)
S. Haroche & J. Raimond, Exploring the Quantum, OUP Oxford (2006)

Jaynes-Cummings Hamiltonian & Dressed State Energy Levels

$$H = \hbar\omega_r \left(a^\dagger a + \frac{1}{2}\right) + \frac{\hbar\omega_a}{2}\sigma^z + \hbar g(a^\dagger\sigma^- + a\sigma^+)$$

on resonance: $\omega_a - \omega_r = \Delta = 0$

strong coupling limit: $g = \dfrac{dE_0}{\hbar} > \gamma,\, \kappa$

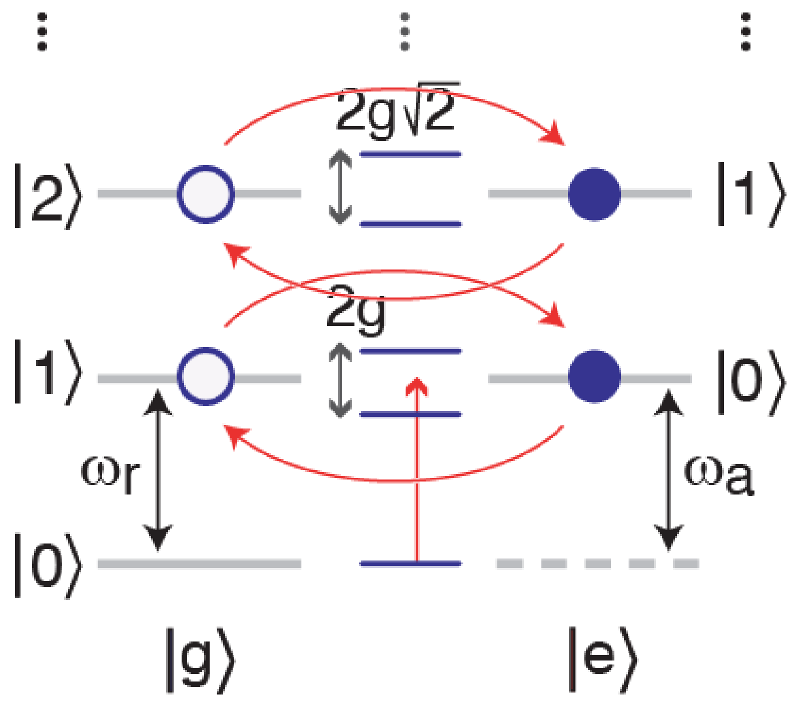

Jaynes-Cummings Ladder

atomic cavity QED reviews:

J. Ye., H. J. Kimble, H. Katori, *Science* **320**, 1734-1738 (2008)

S. Haroche & J. Raimond, Exploring the Quantum, *OUP Oxford* (2006)

Dispersive Approximation of the J-C Hamiltonian

Jaynes-Cummings Hamiltonian

$$H = \hbar\omega_r\left(a^\dagger a + \frac{1}{2}\right) + \frac{\hbar\omega_a}{2}\sigma^z + \hbar g(a^\dagger\sigma^- + a\sigma^+)$$

Unitary transformation

$$\tilde{H} = UHU^\dagger \quad \text{with} \quad U = \exp\frac{g}{\Delta}(a\sigma^+ - a^\dagger\sigma^-)$$

$$\text{and} \quad \Delta = \omega_a - \omega_r$$

Results in dispersive approximation up to 2nd order in g

$$\tilde{H} \approx \hbar\left(\omega_r + \frac{g^2}{\Delta}\sigma_z\right)a^\dagger a + \frac{1}{2}\hbar\left(\omega_a + \frac{g^2}{\Delta}\right)\sigma_z$$

A. Blais *et al., PRA* **69**, 062320 (2004)

Non-Resonant (Dispersive) Interaction

approximate diagonalization for $|\Delta| = |\omega_a - \omega_r| \gg g$

$$H \approx \hbar\left(\omega_r + \frac{g^2}{\Delta}\sigma_z\right) a^\dagger a + \frac{1}{2}\hbar\left(\omega_a + \frac{g^2}{\Delta}\right)\sigma_z$$

//

cavity frequency shift

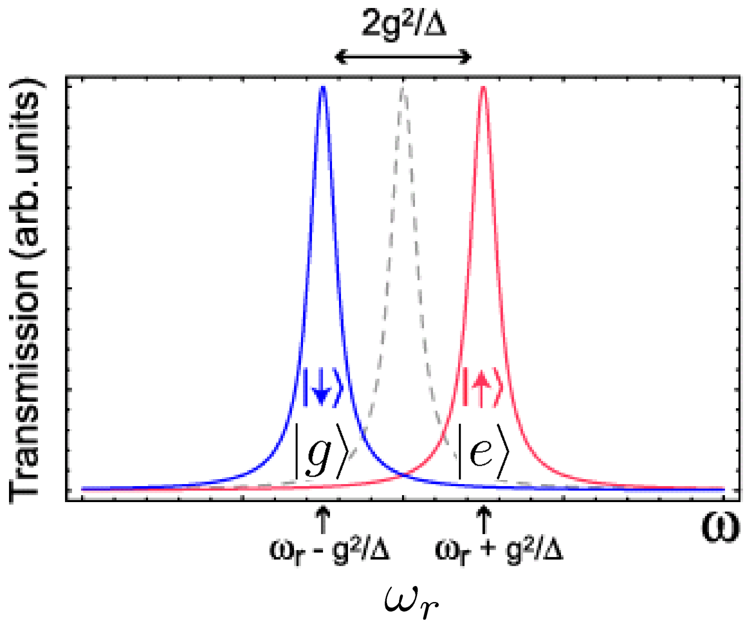

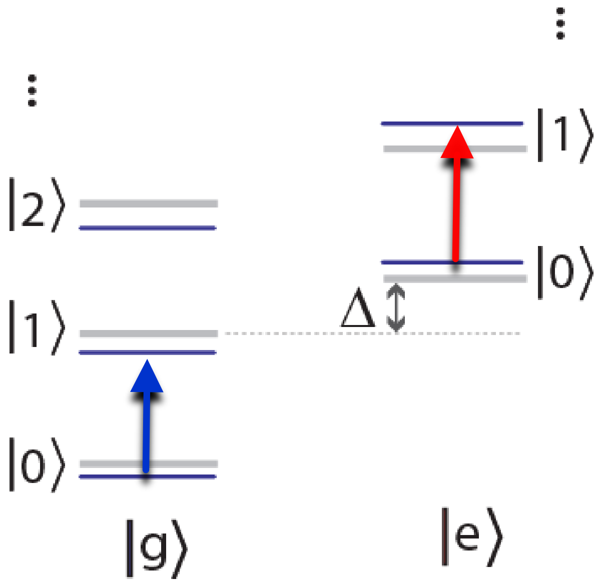

qubit detuned by Δ
from resontaor

A. Blais *et al.*, *PRA* 69, 062320 (2004)
A. Wallraff *et al.*, *Nature (London)* 431, 162 (2004)
D. I. Schuster *et al.*, *Phys. Rev. Lett.* 94, 123062 (2005)
A. Fragner *et al.*, *Science* 322, 1357 (2008)

Controlling Single Qubits (Y Rotation)

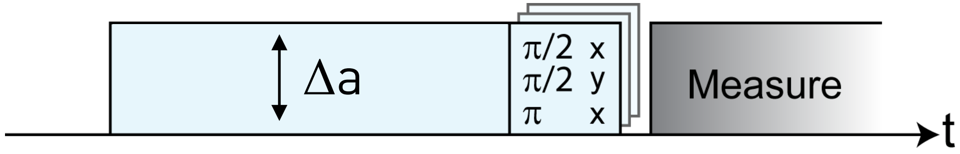

- apply microwave pulse
- followed by read-out pulse
- both with controlled length, amplitude and phase
- Characterize gates by randomized benchmarking
- F > 99 %

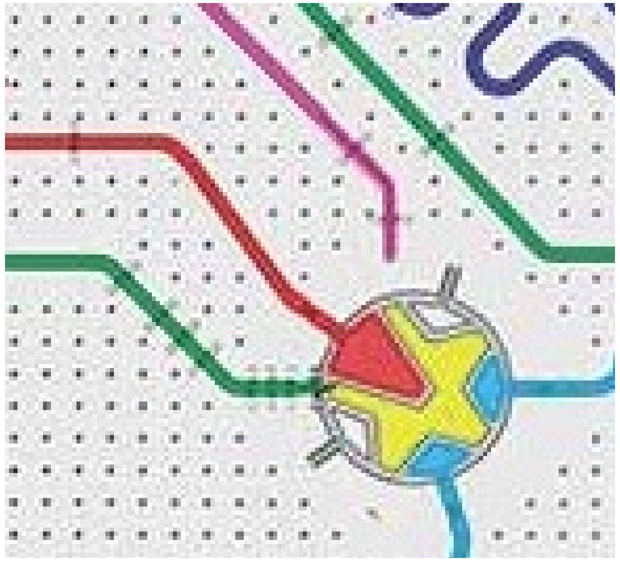

experimental density matrix and Pauli set:

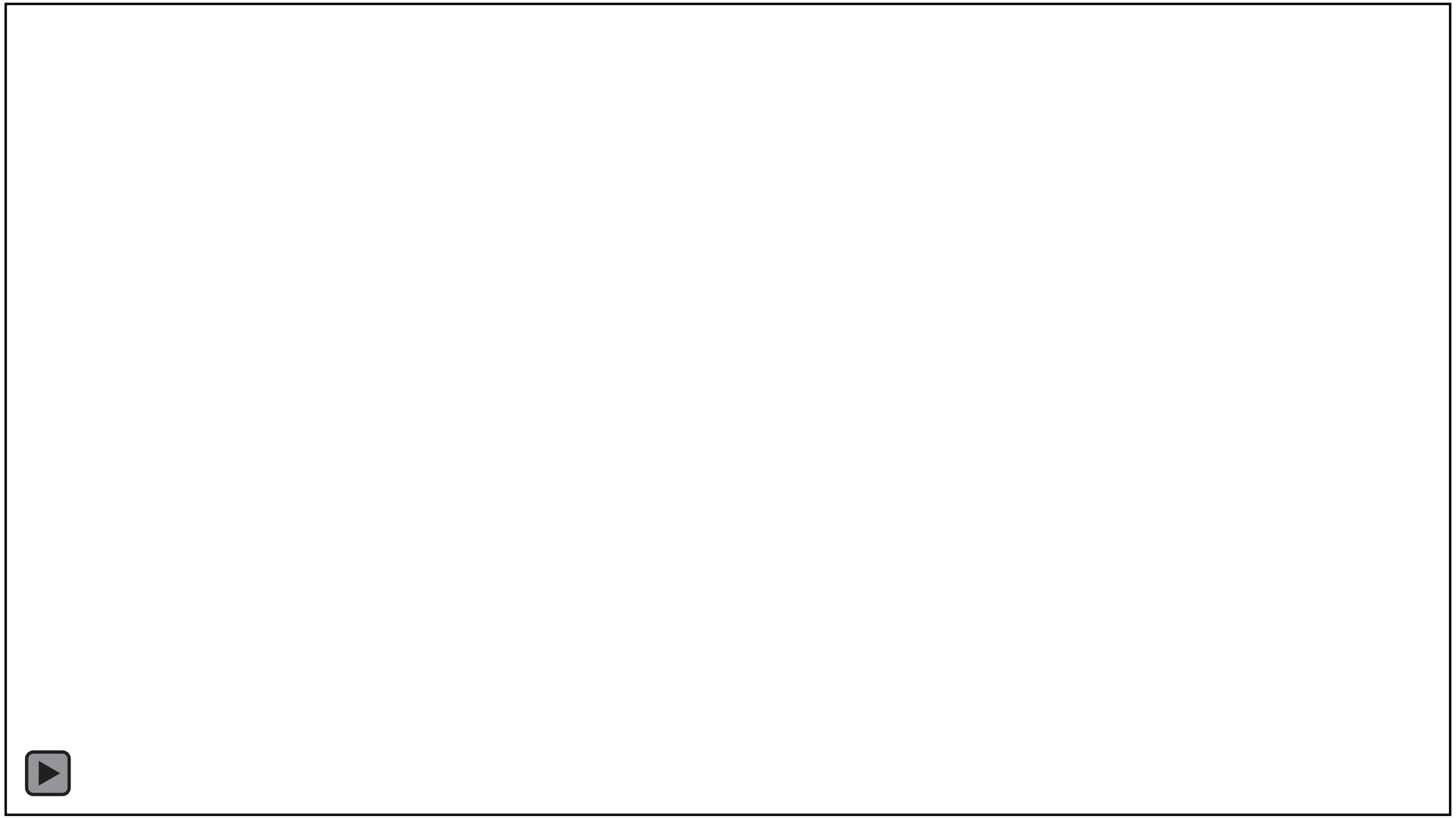

Controlling Single Qubits (X Rotation)

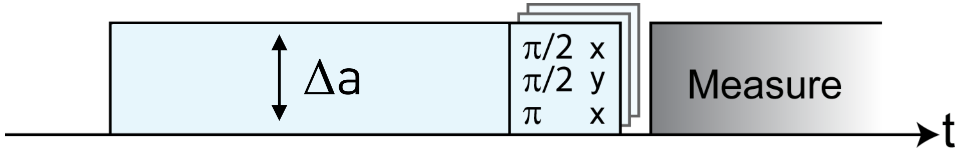

- apply microwave pulse
- followed by read-out pulse
- both with controlled length, amplitude and phase
- Characterize gates by randomized benchmarking
- F > 99 %

experimental density matrix and Pauli set:

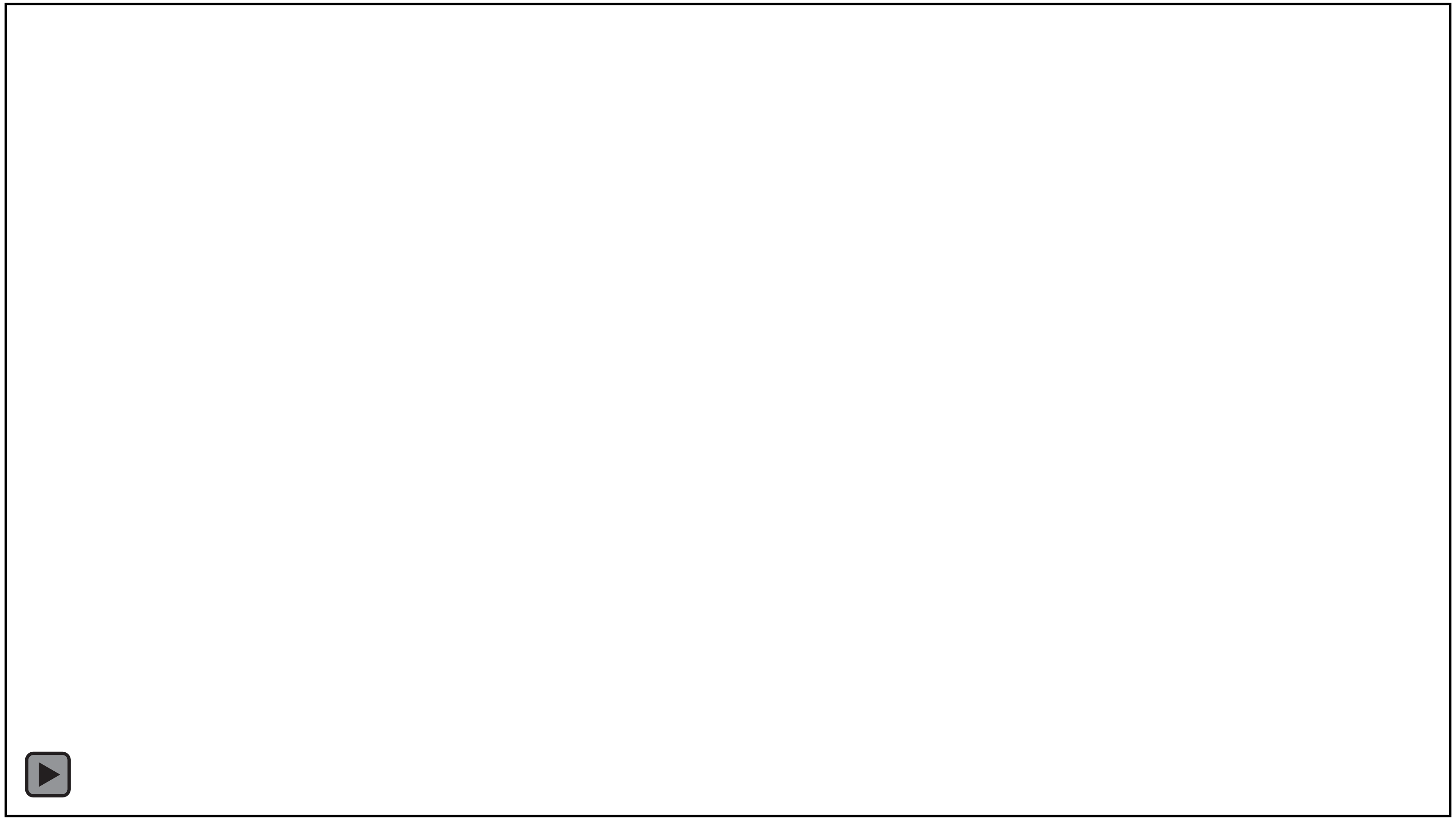

Universal Two-Qubit Controlled Phase Gate

Make use of qubit states beyond 0, 1

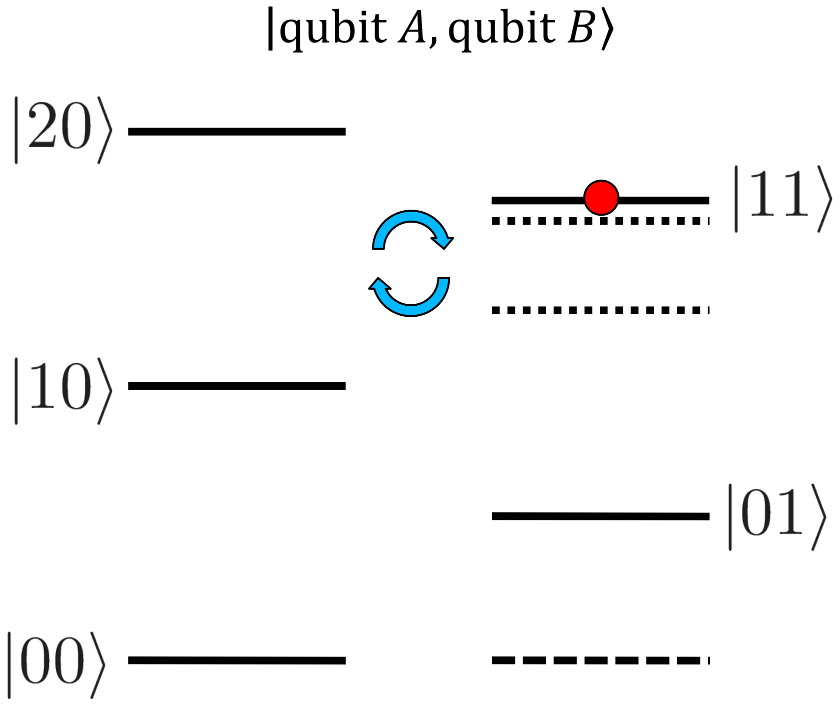

Interaction mediated by virtual photon exchange through resonator

$$|11\rangle \longrightarrow i|20\rangle \longrightarrow -|11\rangle$$

Full 2π rotation induces phase factor -1

Tune levels into resonance using magnetic field

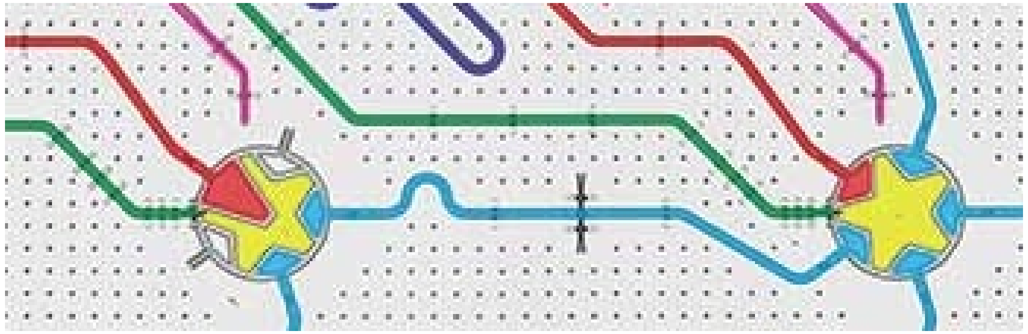

proposal: F. W. Strauch *et al., Phys. Rev. Lett.* **91**, 167005 (2003).

first implementation: L. DiCarlo *et al., Nature* **460**, 240 (2010).

Universal Two-Qubit Controlled Phase Gate

Make use of qubit states beyond 0, 1

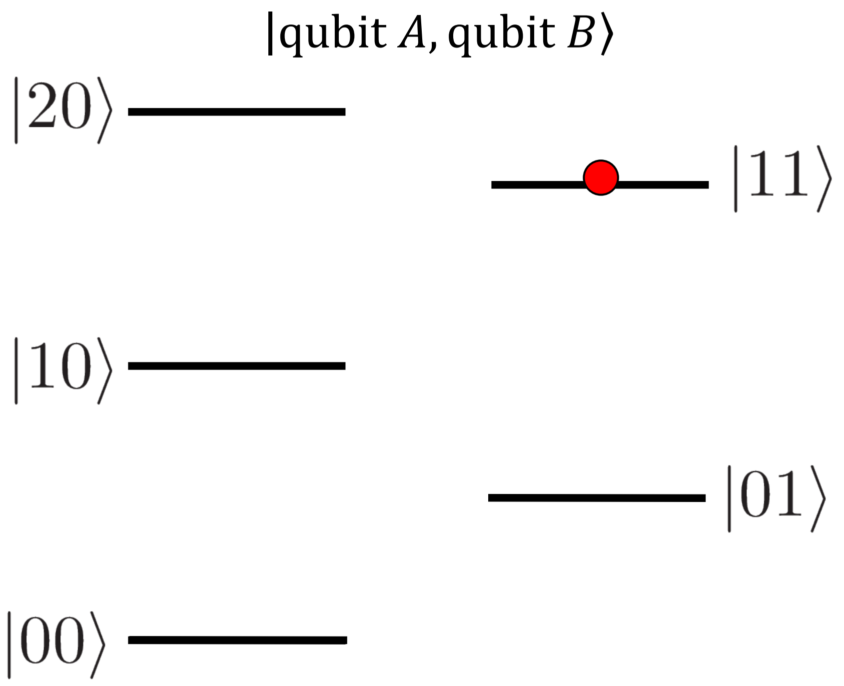

Qubits in states 01, 10 and 00 do not interact and thus acquire no phase shift

$$|11\rangle \longrightarrow i|20\rangle \longrightarrow -|11\rangle$$
$$|01\rangle \longrightarrow |01\rangle$$
$$|10\rangle \longrightarrow |10\rangle$$
$$|00\rangle \longrightarrow |00\rangle$$

C-Phase gate:

$$\begin{pmatrix} 1 & 0 & 0 & 0 \\ 0 & 1 & 0 & 0 \\ 0 & 0 & 1 & 0 \\ 0 & 0 & 0 & -1 \end{pmatrix}$$

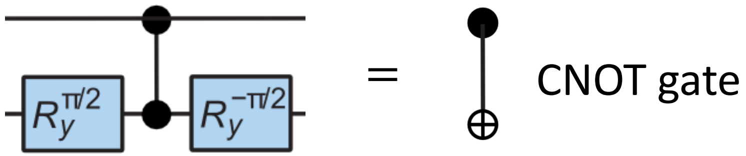

Universal two-qubit gate.

Test performance with process tomography or randomized benchmarking.

proposal: F. W. Strauch *et al., Phys. Rev. Lett.* **91**, 167005 (2003).

first implementation: L. DiCarlo *et al., Nature* **460**, 240 (2010).

Fast, High-Fidelity Single Shot Readout

Ingredient for

- Fast **qubit initialization**
  - at start of computation
    Riste *et al., PRL* **109**, 050507 (2012)
  - for **resetting auxiliary qubits**
- For **feedback** or **feed forward**
  - in **error correction**
    Reed *et al., Nature* **482**, 382 (2012)
    Kelly *et al., Nature* **519**, 66 (2015)
    Corcoles *et al., Nat. Com.* **6**, 6979 (2015)
    Ristè *et al., Nat. Com.* **6**, 6983 (2015)
  - in measurement-based **entanglement generation**
    Riste *et al., Nature* **502**, 350 (2013)
  - in **teleportation** protocols
    Steffen *et al., Nature* **500**, 319 (2013)
  - and more …

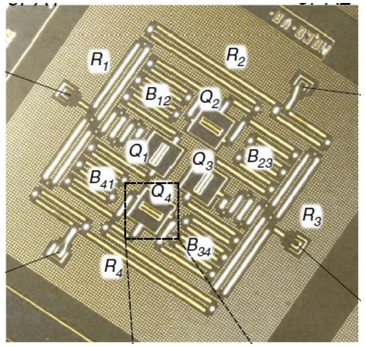

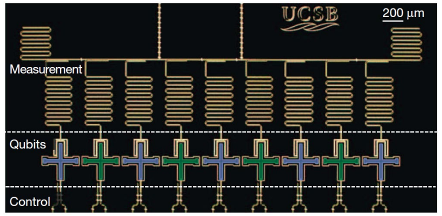

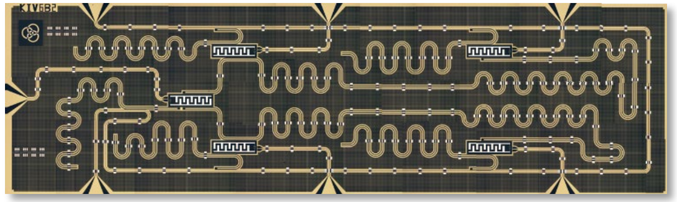

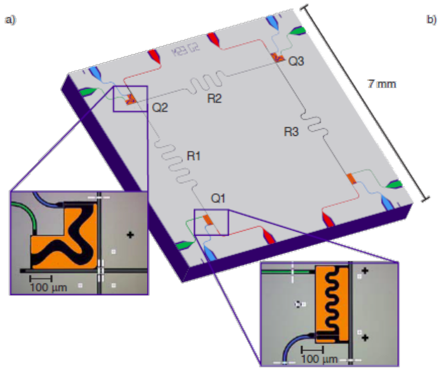

How to achieve fast, high-fidelity single shot readout?

Dispersive Interaction for Qubit Read-Out

approximate diagonalization in the dispersive limit $|\Delta| = |\omega_a - \omega_r| \gg g$

$|g\rangle : \epsilon > 1$

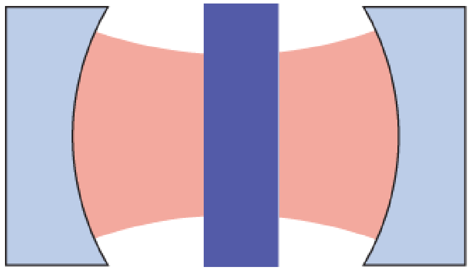

$|e\rangle : \epsilon < 1$

$$H \approx \hbar \left(\omega_r + \frac{g^2}{\Delta}\sigma_z \right) a^\dagger a + \frac{1}{2}\hbar \left(\omega_a + \frac{g^2}{\Delta} \right) \sigma_z$$

//

cavity frequency shift

Two-level approximation for qubit.

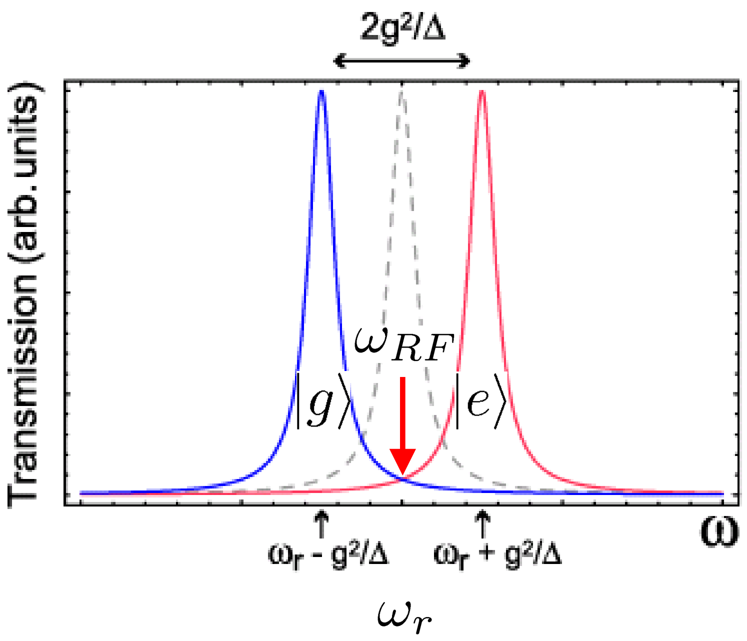

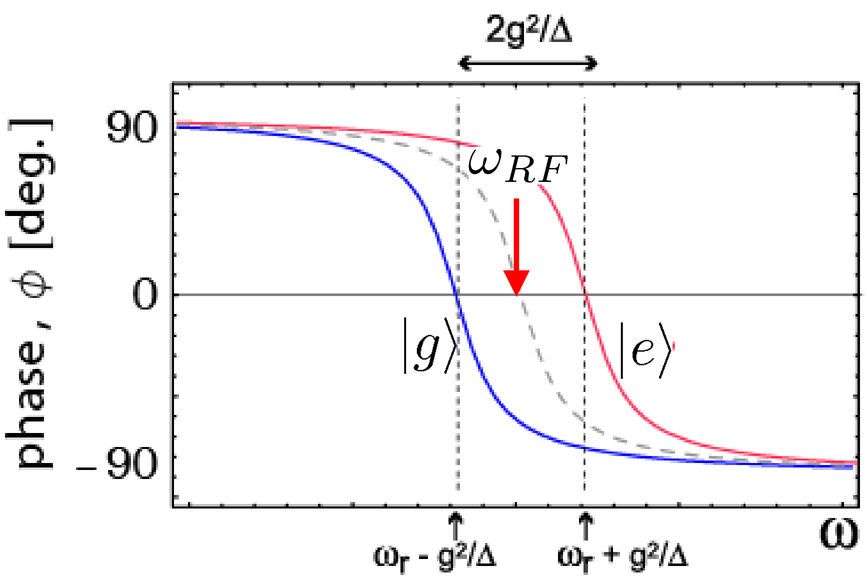

A. Blais *et al.*, *PRA* 69, 062320 (2004)

Advances in Dispersive Readout

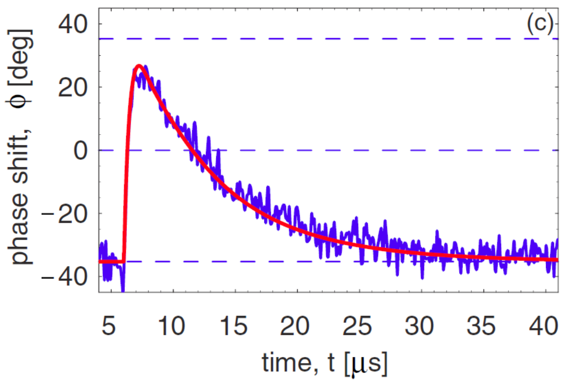

- Dispersive readout using HEMT amplifiers
  A. Wallraff *et al., PRL* **95**, 060501 (2005)
  B. Johnson *et al., Nat. Phys.* **6**, 663 (2010)
- Heralded preparation using **parametric amplifiers**
  J. E. Johnson *et al., PRL* **109**, 050506 (2012)
  D. Riste *et al., PRL* **109**, 050507 (2012)
- Purcell filters and **multiplexing** for high fidelity
  E. Jeffrey *et al., PRL* **112**, 190504 (2014)
- **Resonator depletion**
  C. C. Bultink *et al., Phys. Rev. Applied* **6**, 034008 (2016)
- and more …

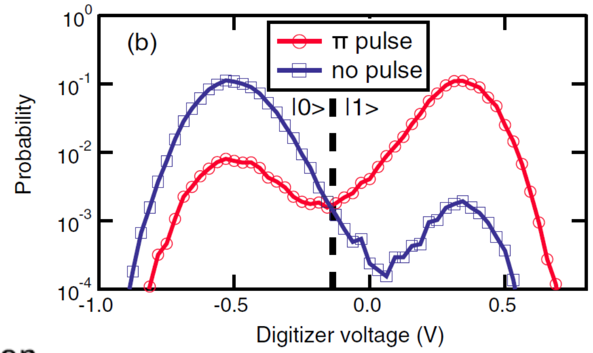

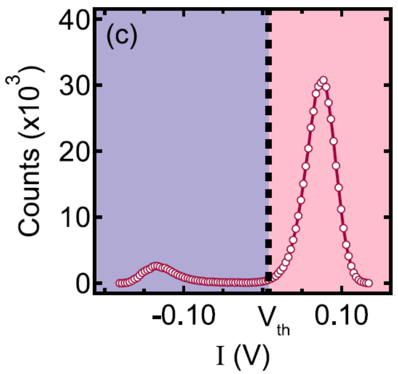

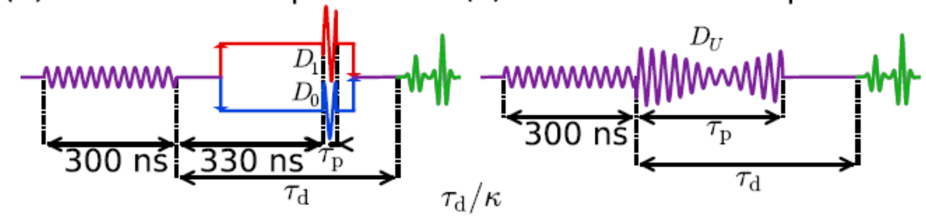

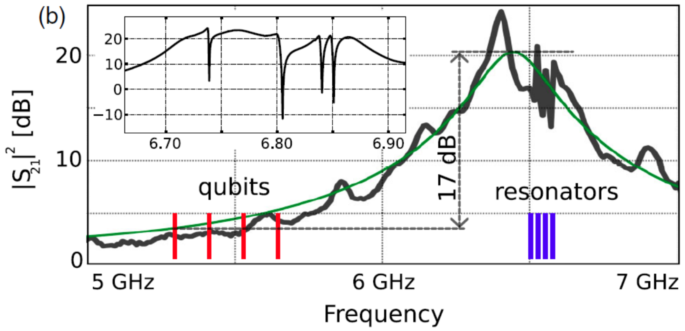

Improvements in speed and fidelity:
T. Walter, P. Kurpiers *et al., Phys. Rev. Applied* **7**, 054020 (2017)

Individual Qubit Readout Resonators with Individual Purcell Filters

Quantum bit:
- Transmon
- Drive line

Readout (bottom):
- $\lambda/4$ readout resonator
- $\lambda/4$ Purcell filter

Transfer (top):
- $\lambda/4$ Transfer resonator
- $\lambda/4$ Purcell filter

Features:
- large dispersive shift χ
- large resonator BW κ
- Purcell protection
- 2 channels

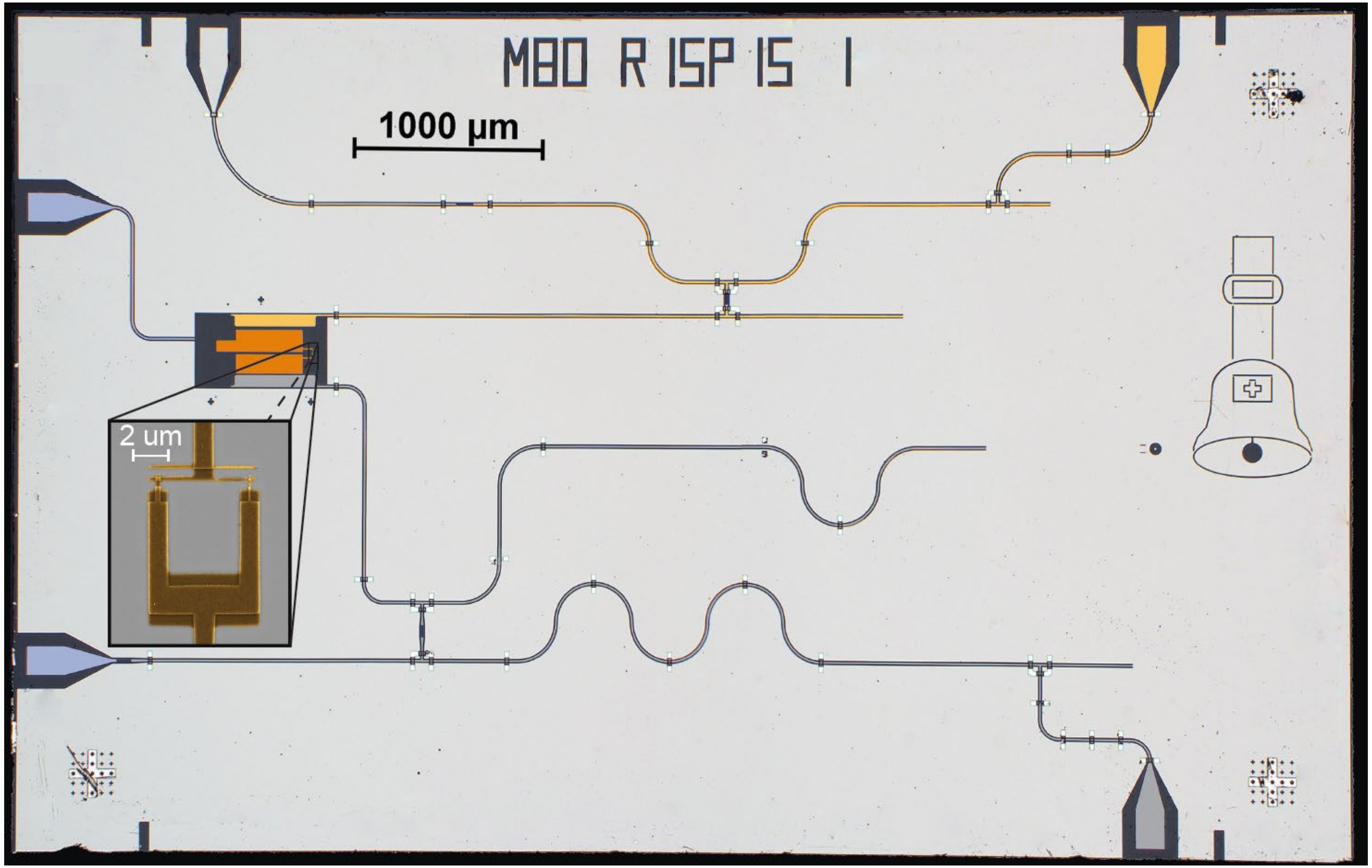

T. Walter, P. Kurpiers *et al., Phys. Rev. Applied* **7**, 054020 (2017)
P. Kurpiers , P. Magnard *et al., Nature* **558**, 264 (2018)

Readout Resonator Response

Transmission amplitude of readout resonator extracted through Purcell filter for qubit prepared in ground (g) or excited (e) state :

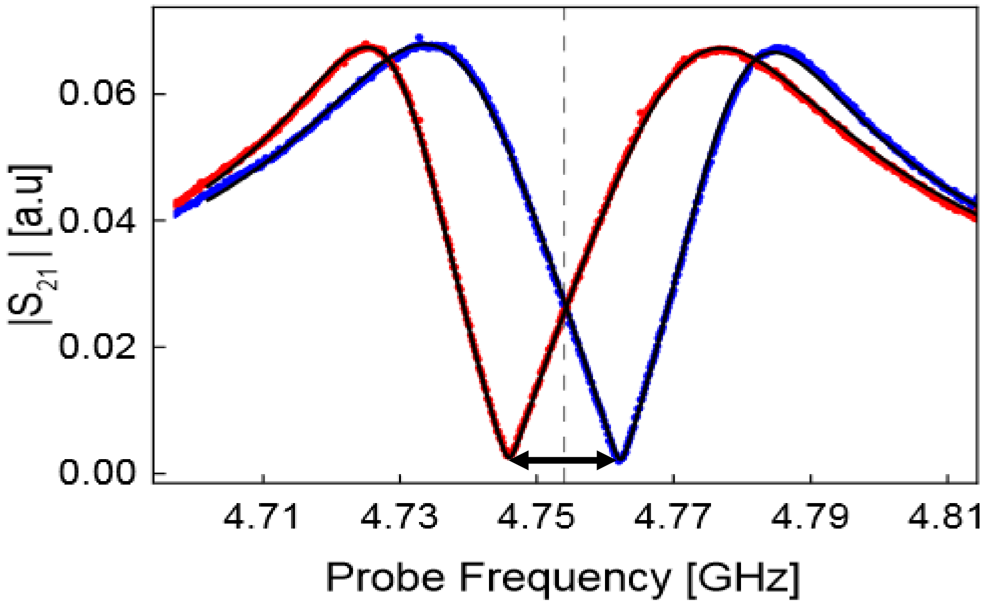

Parameter fit (model):

- Purcell filter $\kappa_p/2\pi$ = 64 MHz
- Readout resonator $\kappa_r/2\pi$ = 37.5 MHz
- State dependent resonator shift $2\chi/2\pi \backsimeq$ -16 MHz

In ground/excited state:

- Data measured after state prep. (*,*)
- Fit to resonator response model (-)

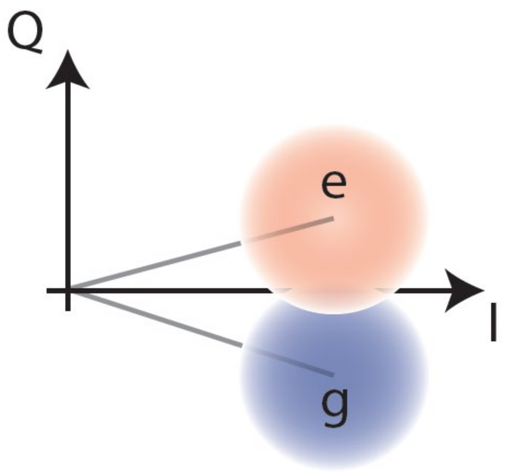

$$\chi = \frac{g^2}{\Delta}\frac{\alpha}{(\Delta + \alpha)}$$

Dispersive shift for transmon with anharmonicity α

T. Walter, P. Kurpiers *et al.*, *Phys. Rev. Applied* **7**, 054020 (2017)

Time Dependence of Measured Quadrature

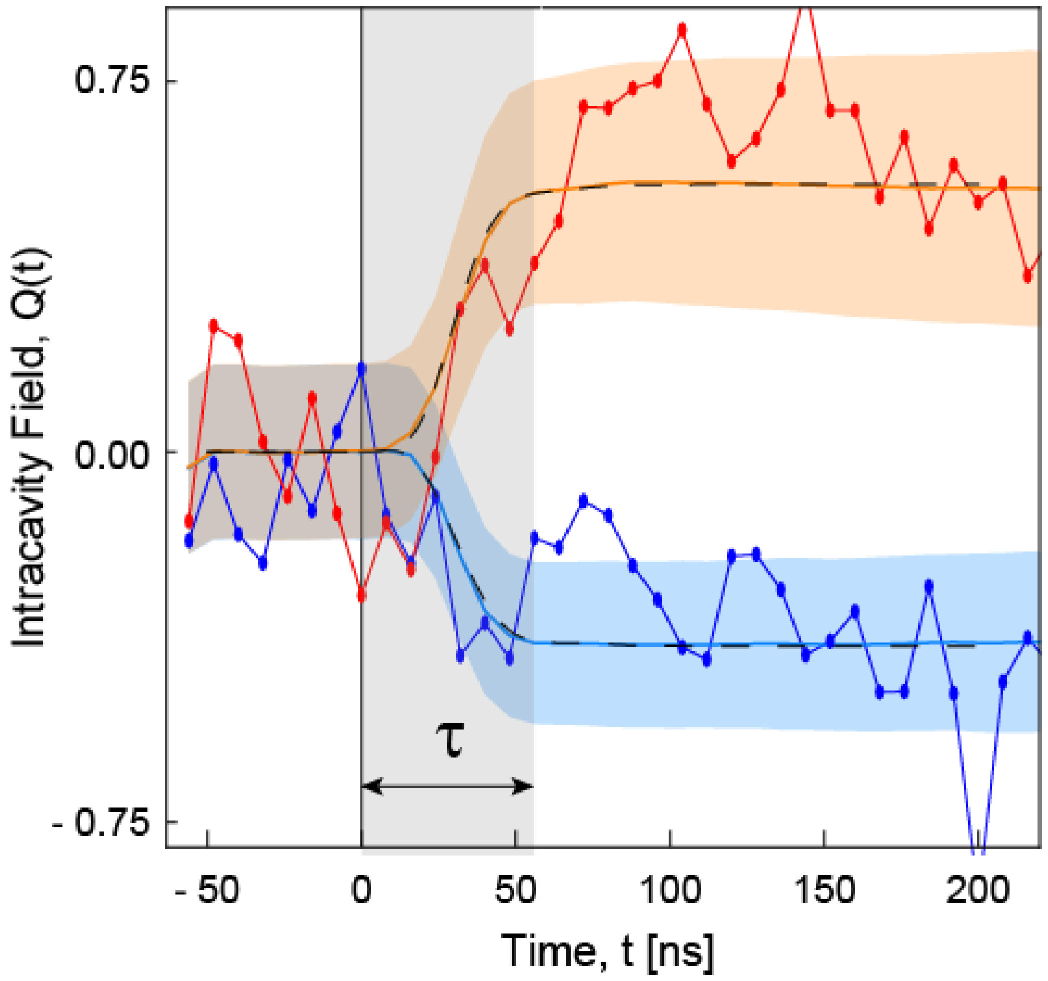

Quantities:

- Single ground state (g) trace
- Average and Stdv of g traces
- Simulated dynamics (-)
- Single excited state (e) trace
- Average and Stdv of e traces
- Simulated dynamics (-)
- Integration time τ

Observations:

- Fast rise of measurement signal (< 50 ns) due large χ (and κ)
- Small decay of average excited state trace due to Purcell protected T_1
- Little increase of average ground state trace due to measurement induced mixing

T. Walter, P. Kurpiers *et al.*, *Phys. Rev. Applied* **7**, 054020 (2017)

Histograms of Integrated Quadrature Signals

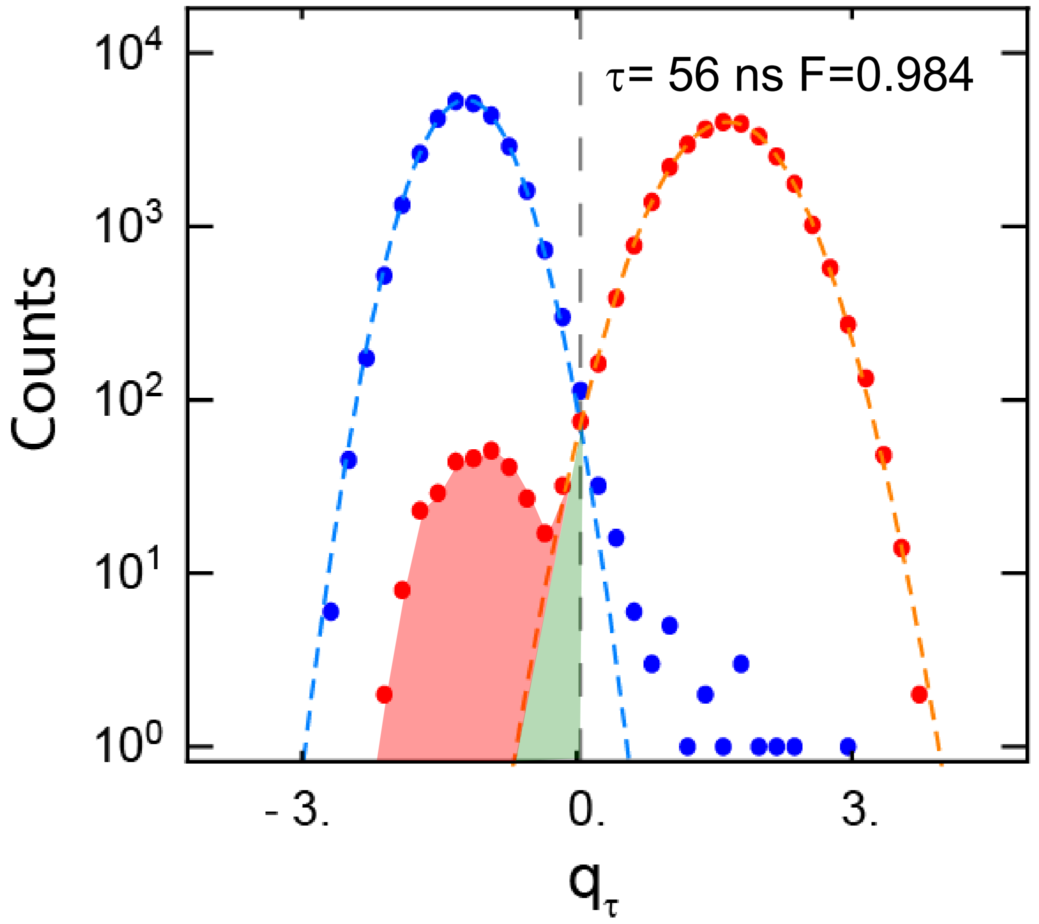

Transmission quadrature integrated with opt. filter in ground/excited state:

- Data of 30k preparations each (*,*)
- Fitted Gaussian distribution (-,-)
- Constant threshold (---)

Definition of errors and fidelities in ground/excited state:

- Overlap error: $\varepsilon_{o,g/e}$
- Transition, preparation (and other) errors: $\tilde{\varepsilon}_{g/e}$
- Total error $\varepsilon_{g/e} = \varepsilon_{o,g/e} + \tilde{\varepsilon}_{g/e}$

For measurement of unknown state:

- Total error $\varepsilon = \varepsilon_g + \varepsilon_e$
- Total fidelity $F = 1 - \varepsilon$

Note:

- Threshold is either kept fixed at midpoint or adjusted for highest fidelity

T. Walter, P. Kurpiers *et al., Phys. Rev. Applied* **7**, 054020 (2017)

Fast, High-Fidelity Readout

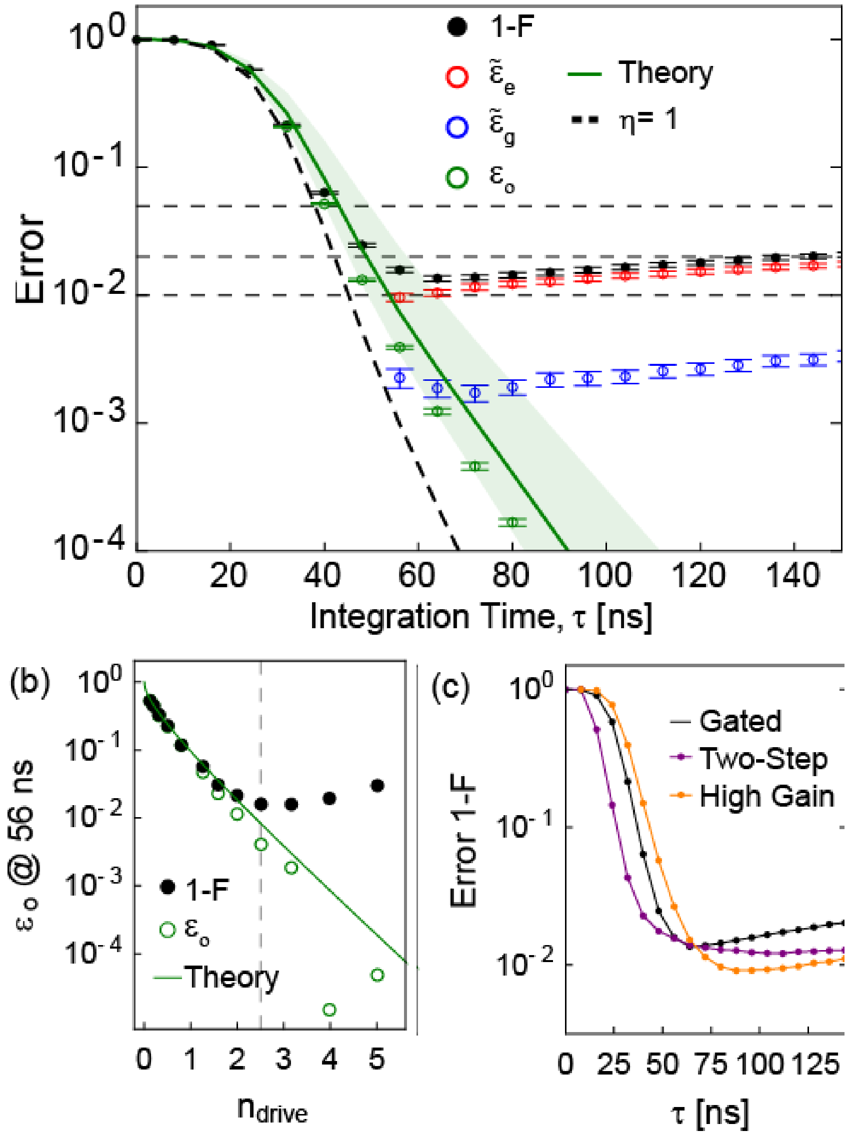

Measurement Error *vs.* Integration Time:

- Fast state discrimination with overlap error dropping to below 1 % in only < 50 ns
- Excited state error < 0.96 %
- Ground state error < 0.23 %
- Max. total fidelity > 98 % limited (in this data) by qubit T_1

Readout power dependence

- Tradeoff between reduction of overlap error and measurement induced mixing errors

Improvements

- Two-step readout pulse
- Higher measurement efficiency at 36 dB paramp gain
- 99.2% total fidelity reached

T. Walter, P. Kurpiers *et al.*, *Phys. Rev. Applied* **7**, 054020 (2017)

A Comparison of Quality Measures of Readout

Reference	[1]	[2]	[3]	[4]	[5]	[6]
Integration time τ [ns]	48	140	300	300	50	750
Total fidelity F [%]	98.4	98.7	97.6	91.1	97.4	97.8
Readout $\kappa/2\pi$ [MHz]	37	4.3	0.6	9	10	1.6
Dispersive shift $2\chi/2\pi$ [MHz]	-16	~	-5.2	7.4	'~60'	'1.3'
Resonator population n,	2.5	~	3300	37.8	-	2.6
Number of qubits on chip	1	4	10	1	1	1
Qubit T_1 [μs]	8	12	25	1.8	3.3	90

[1] T. Walter, P. Kurpiers et al., *Phys. Rev. Applied* **7**, 054020 (2017)
[2] E. Jeffrey et al., *PRL* **112**, 190504 (2014)
[3] C. C. Bultink et al., *Phys. Rev. Applied* **6**, 034008 (2016)
[4] J. E. Johnson et al., *PRL* **109**, 050506 (2012)
[5] R. Dassonneville *et al.*, *Phys. Rev. X* **10**, 011045 (2020)
[6] S. Touzard et al., *PRL* **122**, 080502 (2019)

Lectures, April 22 - 24, 2024

Part 1:
An Introduction to Superconducting Circuits
- Quantum physics of electronic circuits
- Circuit QED

Part 2:
Controlling and Reading Out Qubits
- Single and two-qubit gates
- Qubit readout

Reading Material:
Circuit QED Review:
A. Blais *et al.*,
Rev. Mod. Phys. **93**, 025005 (2021)

SCAN ME

The slides:

Part 3:
Quantum Error Correction
- Quantum error correction, why and how?
- The concept
- The device
- Stabilizer measurements
- Distance-Three surface code

Reading Material:
S. Krinner, N. Lacroix et al., Nature 605, 669 (2022)
C. K. Andersen et al., Nat. Phys. 16, 875 (2020)

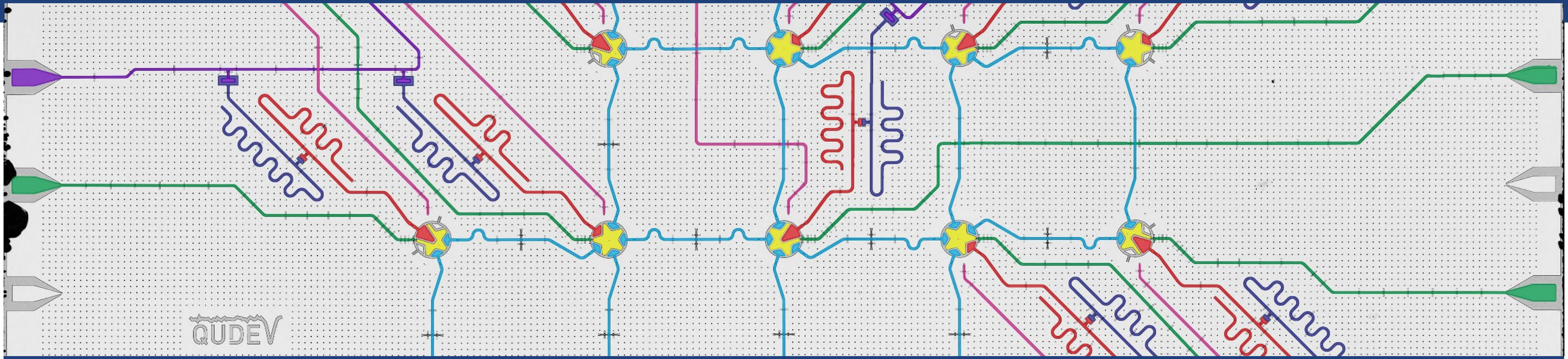

Repeated Quantum Error Correction in a Distance-Three Surface Code Realized with Superconducting Circuits

Sci. Team: J.-C. Besse, D. Colao Zanuz, C. Hellings, J. Herrmann, S. Krinner, N. Lacroix, S. Lazar, G. Norris, A. Remm, K. Reuer, J. Schaer, S. Storz, F. Swiadek, C. Eichler, A. Wallraff *(ETH Zurich)*

A. Di Paolo, E. Genois, C. Leroux, A. Blais *(U. de Sherbrooke)*

M. Müller *(RWTH Aachen)*

Tech. Team: A. Akin, M. Bahrani, A. Flasby, A. Fauquex, T. Havy, N. Kohli, R. Schlatter *(ETH Zurich)*

IARPA
BE THE FUTURE

Schweizerischer Nationalfonds

Innovation project supported by

Schweizerische Eidgenossenschaft
Confédération suisse
Confederazione Svizzera
Confederaziun svizra

Swiss Confederation

Innosuisse – Swiss Innovation Agency

Why is Error Correction Needed?

- Computational basis states are eigenstates of the Pauli Z operator

$$\hat{Z} = \begin{pmatrix} 1 & 0 \\ 0 & -1 \end{pmatrix}$$

$$\hat{Z}|0\rangle = +1\,|0\rangle$$
$$\hat{Z}|1\rangle = -1\,|1\rangle$$

- Every excited quantum system undergoes spontaneous emission

$$|1\rangle \to |0\rangle$$

- **Bit flip errors** also occur due to
  - Thermal excitation
  - Control inaccuracies
- The expectation value of $\hat{Z}$ characterizes the decay of the excited state on average

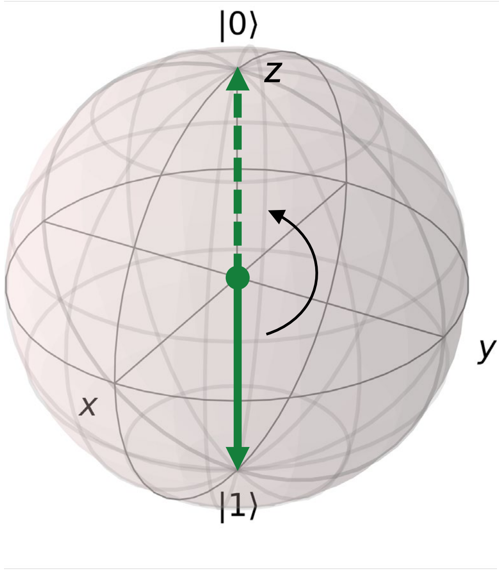

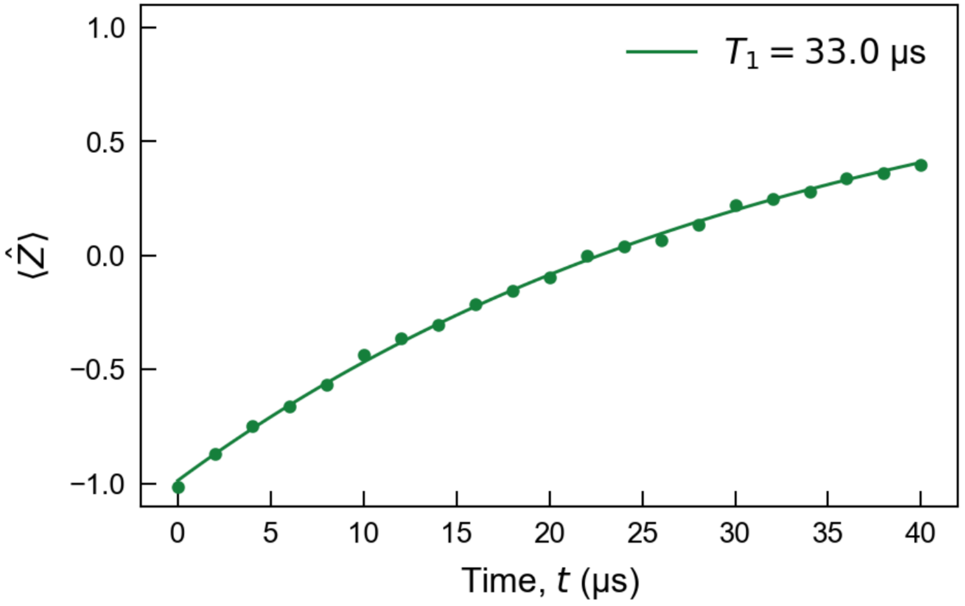

A Second Type of Error: Phase Flips

- Quantum computers make use of superposition states $|\pm\rangle = \frac{1}{\sqrt{2}}(|0\rangle \pm |1\rangle)$
- Eigenstates of

$$\hat{X} = \begin{pmatrix} 0 & 1 \\ 1 & 0 \end{pmatrix}$$

$$\hat{X}|+\rangle = +1\,|+\rangle$$
$$\hat{X}|-\rangle = -1\,|-\rangle$$

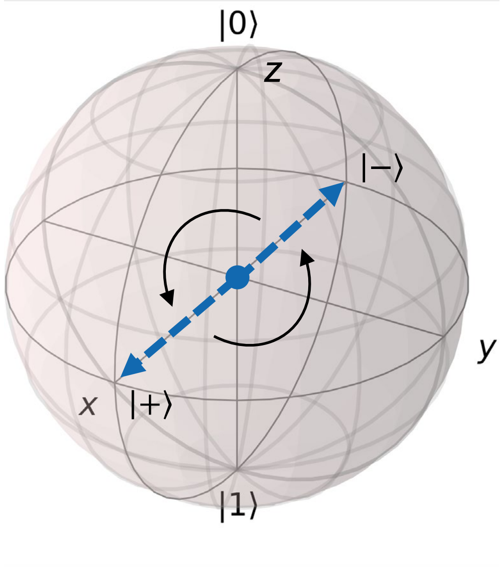

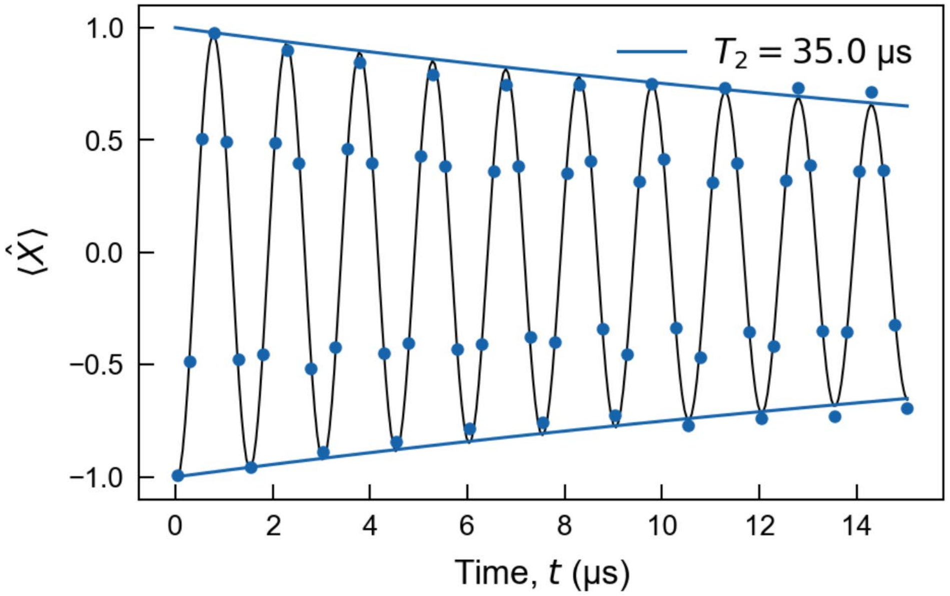

- **Phase flip errors** occur due to
  - Environmental field fluctuations
  - Control inaccuracies
  - Energy relaxation
- Expectation value of $\hat{X}$ characterizes the decay of the quantum phase on average

ETH zürich

Quantum Error Correction with Superconducting Circuits

Approaches:

- Digital, qubit-based encodings: e.g. surface code, color code

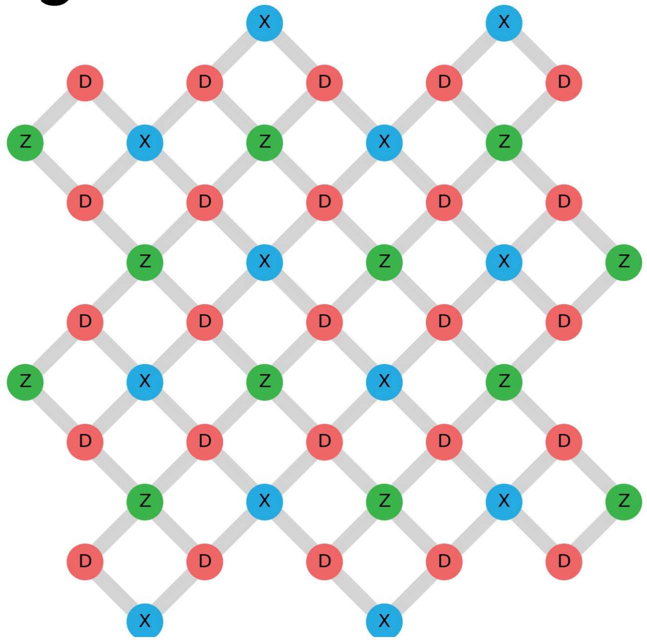

- Continuous variable encodings in harmonic oscillator states: e.g. cat states, GKP states

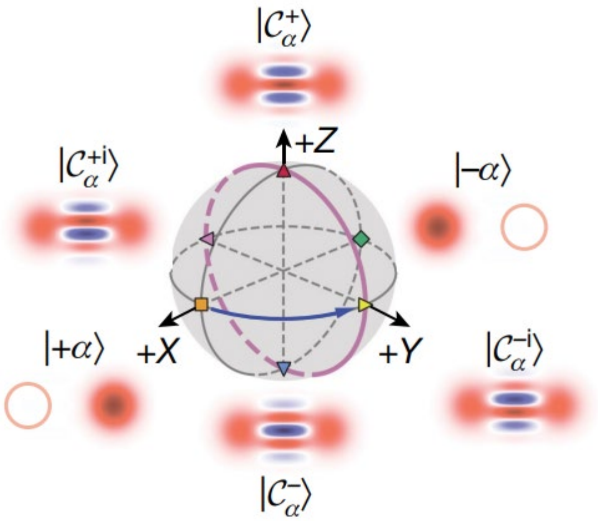

picture from Grimm et al., *Nature* **584**, 205 (2020)

Preskill, *Quantum* **2**, 79 (2020)

Review: Terhal, *Rev. Mod. Phys*. **87**, 307 (2015)

Bosonic Quantum Error Correction Experiments

Continuous QEC

- Dissipative-cat codes
  Leghtas, et. al. Science 347, 853 (2015)
  Lescanne, et. al. Nature Physics 16, 509 (2020)
  Gertler et. al. Nature 590, 243 (2021)
- Kerr-cat codes
  Grimm, et. al. Nature 584, 205 (2020)

Discrete QEC

- Binomial bosonic codes
  Ni, Z. et al., Nature 616, 56 (2023).
  Hu et al., Nature Physics 15, 503 (2019).
- Cat-Codes
  Ofek et. al., Nature 536, 441 (2016)

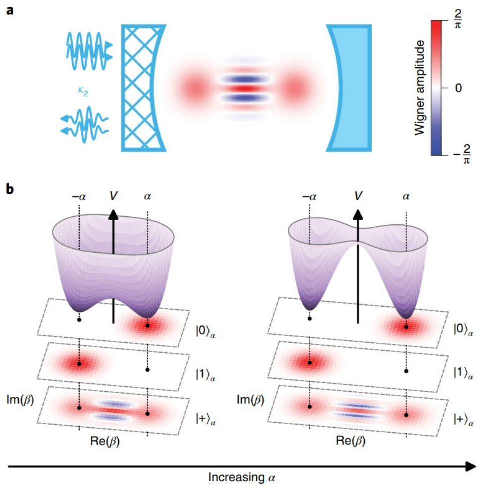

Lescanne et. al. Nat. Phys. 16, 509 (2020)

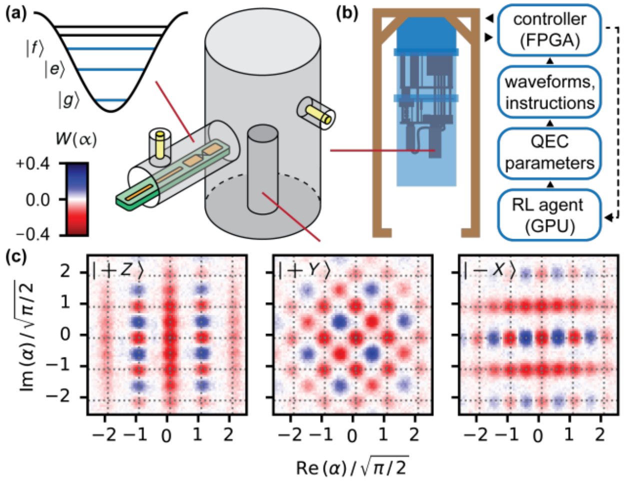

Sivak et. al. arXiv:2211.09116 (2022)

GKP codes

- Trapped ions
  Flühmann et. al., Nature 566, 513 (2019)
  de Neeve et. al., Nature Physics 18, 296 (2022)
- Superconducting circuits
  Campagne-Ibarcq et. al., Nature 584, 368 (2020)
  Sivak et al., Nature 616, 50 (2023).

The Challenge of Quantum Error Correction

Detect and correct two types of errors:

- Bit flips
- Phase flips

Preserve stored quantum states while detecting and correcting errors:

- Measurements collapse quantum (superposition) states

Solution: Use encoding

- Store **logical qubit** state $|\psi\rangle$ in a system of many **physical qubits**
- Make use of **symmetry properties (parity)** of logical qubit states
  - revealing errors ...
  - ... but not the encoded quantum state

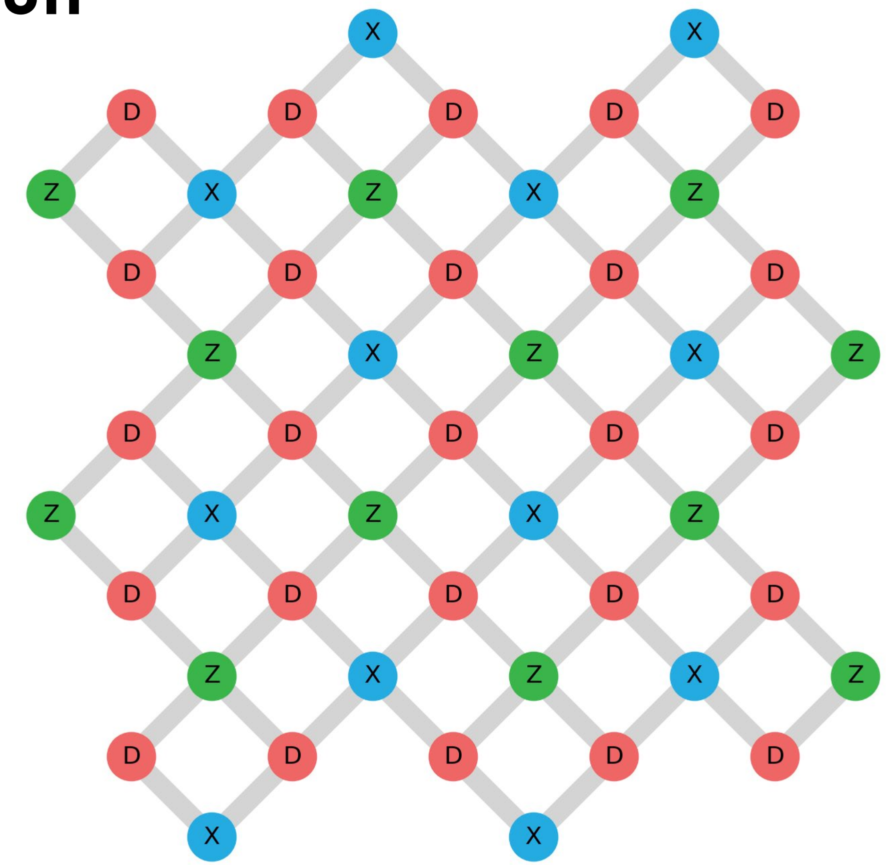

Kitaev, *Annals of Physics* **303**, 2 (2003),

Dennis et al., *Journ. of Math. Physics* **43**, 4452 (2002)

Raussendorff, Harrington, *Phys. Rev. Lett.* **98**, 190504 (2007)

Fowler *et al., Phys. Rev. A* **86**, 032324 (2012)

The Surface Code – Main Features

Two-dimensional architecture

- All operations realizable on a planar qubit lattice
- Topological code: only local operations needed for error correction process

Large error threshold $\epsilon_{\mathrm{th}} \sim 1\ \%$

- Logical error rate $\epsilon_{\mathrm{L}} \propto \left(\epsilon_{\mathrm{phys}}/\epsilon_{\mathrm{th}}\right)^{(d+1)/2}$

  ϵ_{phys}: Physical error rate per step

  ϵ_{th}: Threshold error rate

  d: Distance of the code

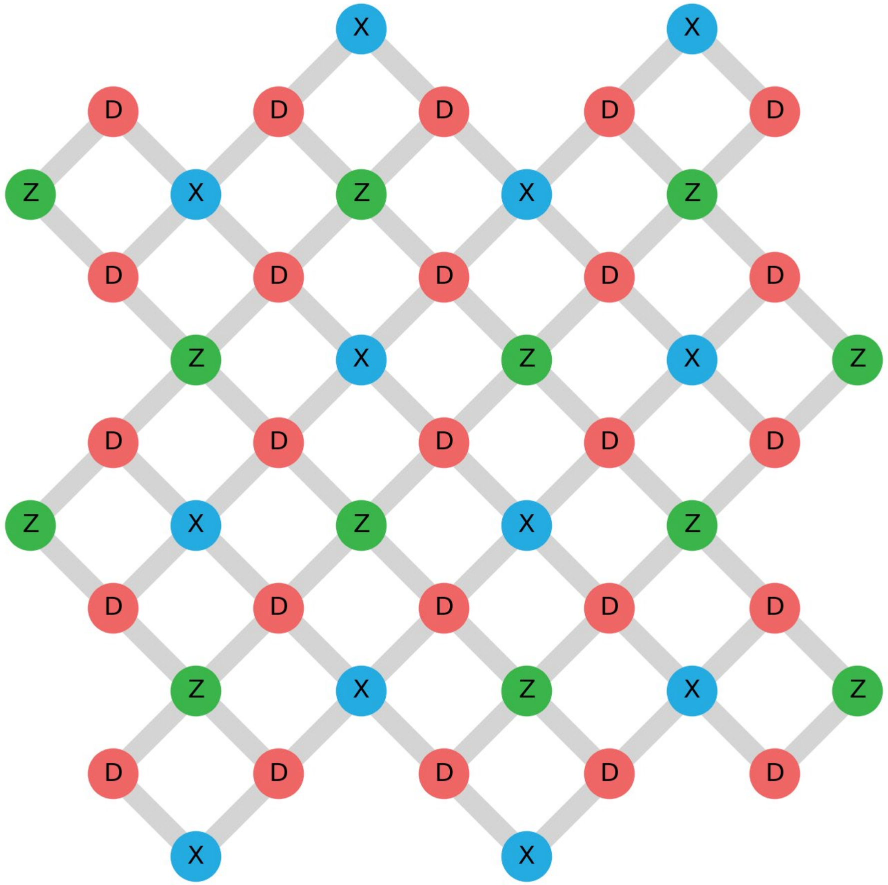

Kitaev, *Annals of Physics* **303**, 2 (2003),
Dennis et al., *Journ. of Math. Physics* **43**, 4452 (2002)
Raussendorff, Harrington, *Phys. Rev. Lett.* **98**, 190504 (2007)
Fowler *et al.*, *Phys. Rev. A* **86**, 032324 (2012)

Elements of the Surface Code

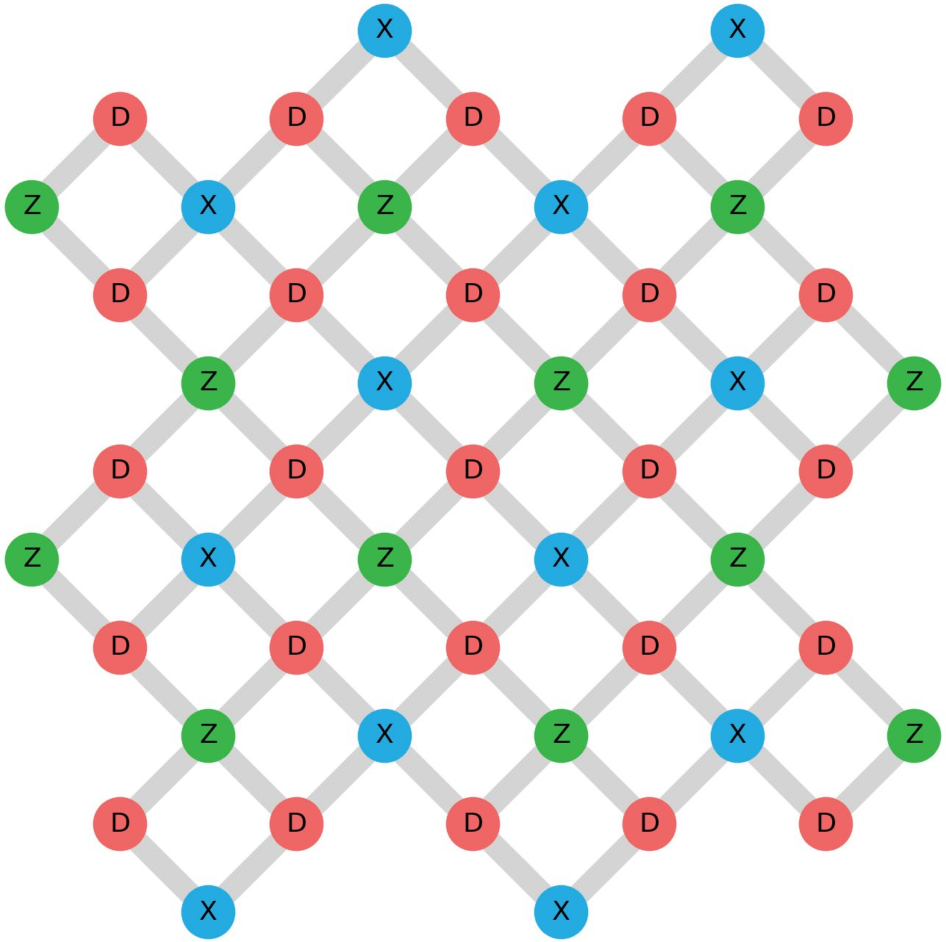

Features:
- Two-dimensional $(d \times d)$ grid of data qubits
- X-type and Z-type auxiliary qubits
- Auxiliary-qubit-assisted stabilizer measurement
  - $Z_1Z_2Z_3Z_4$ (or Z_1Z_2 at the edges)
  - $X_1X_2X_3X_4$ (or X_1X_2 at the edges)

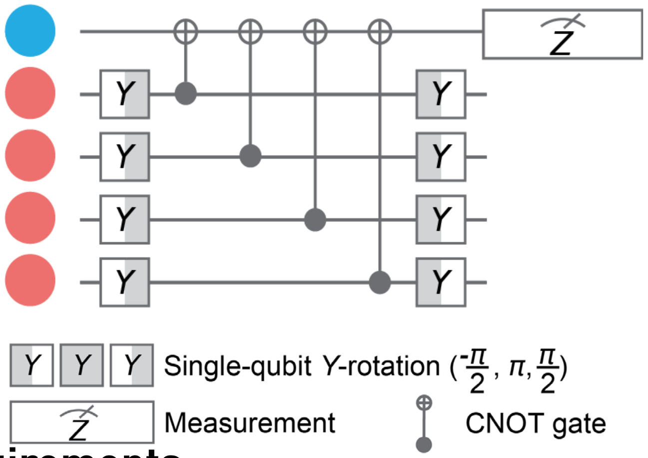

Requirements:
- High-fidelity entangling gates between data and ancilla qubits
- Fast high-fidelity measurements of the ancilla qubits
- Low readout crosstalk between ancilla and data qubits
- Ability to do repeated gates and mid-cycle measurements

Fowler *et al.*, *Phys. Rev. A* **86**, 032324 (2012)
Versluis *et al.*, *Phys. Rev. Applied* **8**, 034021 (2017)

Parity Measurements

Goal: indirect (QND) measurement of two-qubit parity operator (stabiliser) $Z_1 Z_2$

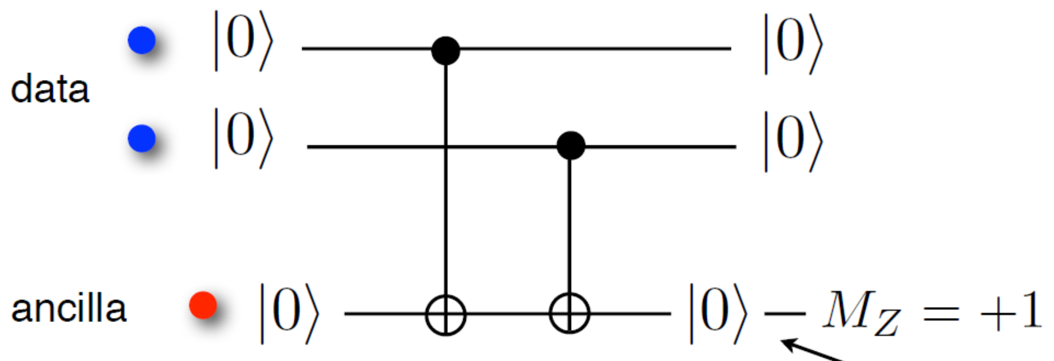

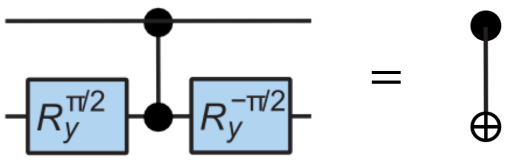

ancilla ends in $|0\rangle$ if the **parity** of the data qubits is **even** (parallel orientation)

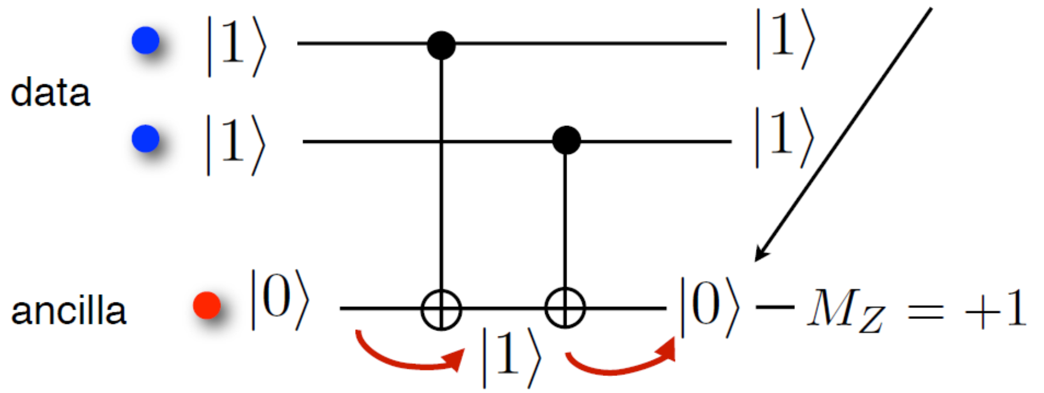

⇨ ancilla outcome

$$M_Z = +1$$

signals correlation

$$Z_1 Z_2 = +1$$

because

$$Z_1 Z_2 |00\rangle = +|00\rangle$$
$$Z_1 Z_2 |11\rangle = +|11\rangle$$

Markus Muller, RWTH Aachen

Distance-Two Surface Code for Error Detection

- Distance-two code: detect 1 error, correct 0 errors
- Stabilizers for parity measurement:

$$\underbrace{\hat{X}_1\hat{X}_2\hat{X}_4\hat{X}_5, \quad \hat{Z}_1\hat{Z}_4, \quad \hat{Z}_2\hat{Z}_5}_{\text{Stabilizers commute, common eigenstates}}$$

- Logical eigenstates and their equal superpositions:

$$|0\rangle_L = \frac{1}{\sqrt{2}}(|0000\rangle + |1111\rangle)$$
$$|1\rangle_L = \frac{1}{\sqrt{2}}(|0101\rangle + |1010\rangle)$$
$$|+\rangle_L = \frac{1}{2}(|0000\rangle + |1111\rangle + |0101\rangle + |1010\rangle)$$
$$|-\rangle_L = \frac{1}{2}(|0000\rangle + |1111\rangle - |0101\rangle - |1010\rangle)$$

- Logical operators:
  - $\hat{X}_L = \hat{X}_1\hat{X}_4$ or $\hat{X}_L = \hat{X}_2\hat{X}_5$
  - $\hat{Z}_L = \hat{Z}_1\hat{Z}_2$ or $\hat{Z}_L = \hat{Z}_4\hat{Z}_5$

Anti-commute with each other and commute with stabilizers (as needed for logical operators in a stabilizer code)

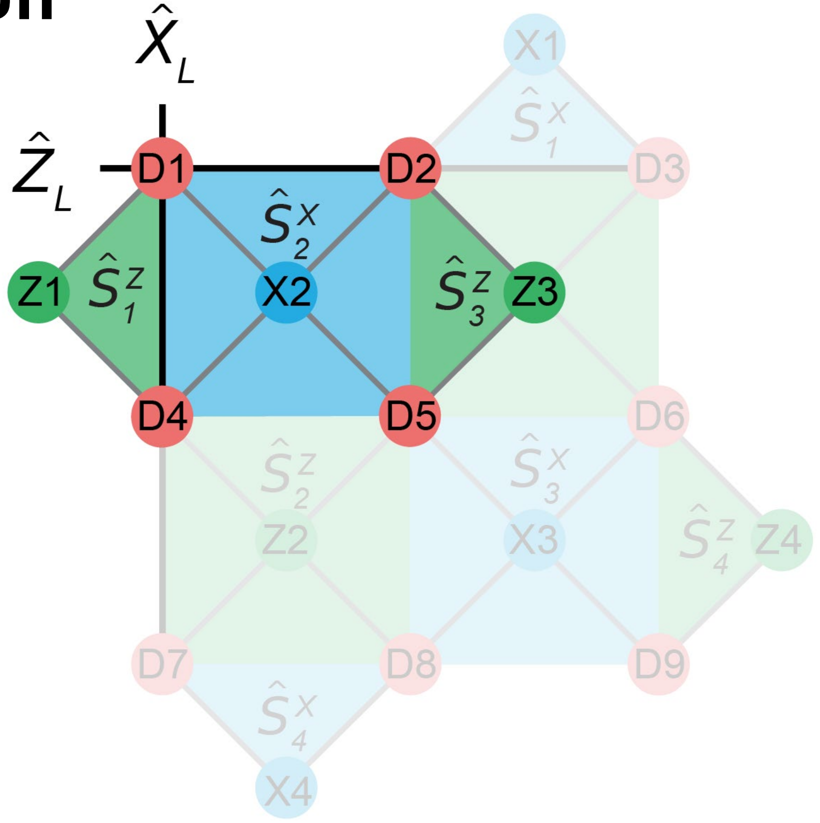

Andersen *et al.*, *Nat. Phys.* **16**, 875 (2020)
Chen *et al.*, *Nature* **595**, 7867 (2021)
Marques *et al.*, *Nat. Phys.* **18**, 80 (2022)

Distance-Three Surface Code for Error Correction

Two-dimensional square lattice of qubits

- $d^2 = 9$ Data qubits: encode single (logical) qubit
  - Logical operators: $\hat{Z}_L = \hat{Z}_1\hat{Z}_2\hat{Z}_3$ $\hat{X}_L = \hat{X}_1\hat{X}_4\hat{X}_7$
  - Distance d: min. number of Pauli operators in $\hat{Z}_L, \hat{X}_L$
  - Number of correctable errors: $\lfloor (d-1)/2 \rfloor = 1$
- $d^2 - 1 = 8$ Auxiliary qubits: for parity measurements

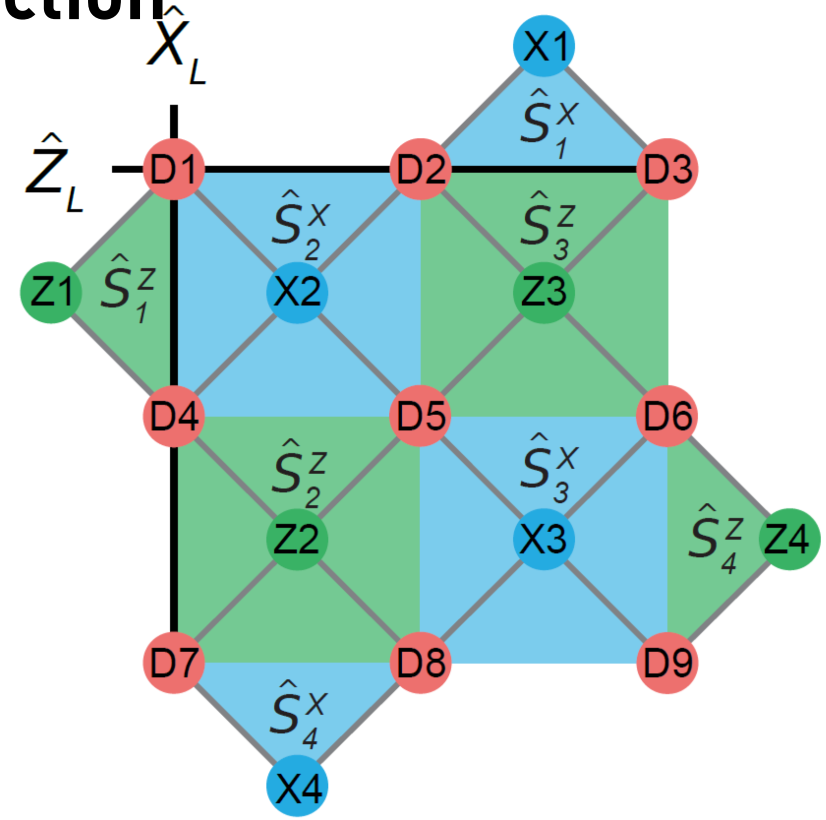

Parity/Stabilizer measurements

- Detect errors without collapsing data-qubit state (Stabilizer operators commute with $\hat{Z}_L, \hat{X}_L$)
- 4 Z-type Stabilizers $\hat{S}^{Zi}$ to detect bit-flip errors
- 4 X-type Stabilizers $\hat{S}^{Xi}$ to detect phase-flip errors

$\hat{S}^{Z1}$	$\hat{Z}_1\hat{Z}_4$
$\hat{S}^{Z2}$	$\hat{Z}_4\hat{Z}_5\hat{Z}_7\hat{Z}_8$
$\hat{S}^{Z3}$	$\hat{Z}_2\hat{Z}_3\hat{Z}_5\hat{Z}_6$
$\hat{S}^{Z4}$	$\hat{Z}_6\hat{Z}_9$

$\hat{S}^{X1}$	$\hat{X}_2\hat{X}_3$
$\hat{S}^{X2}$	$\hat{X}_1\hat{X}_2\hat{X}_4\hat{X}_5$
$\hat{S}^{X3}$	$\hat{X}_5\hat{X}_6\hat{X}_8\hat{X}_9$
$\hat{S}^{X4}$	$\hat{X}_7\hat{X}_8$

Bombin, Delgado, *Phys. Rev. A* **76**, 012305 (2007)
Tomita, Svore, *Phys. Rev. A* **90**, 062320 (2014)

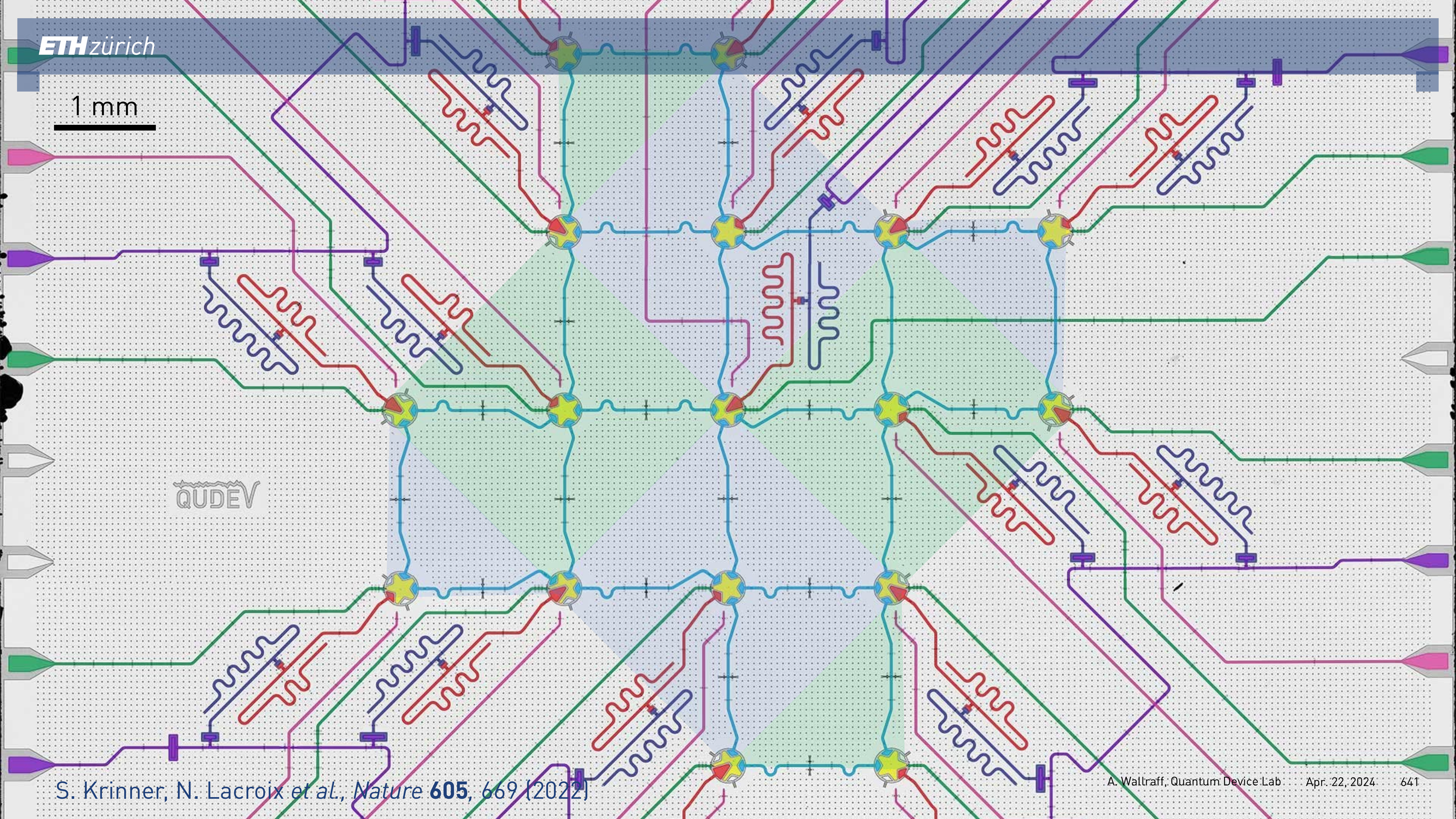

S. Krinner, N. Lacroix *et al.*, *Nature* **605**, 669 (2022)

Device Architecture

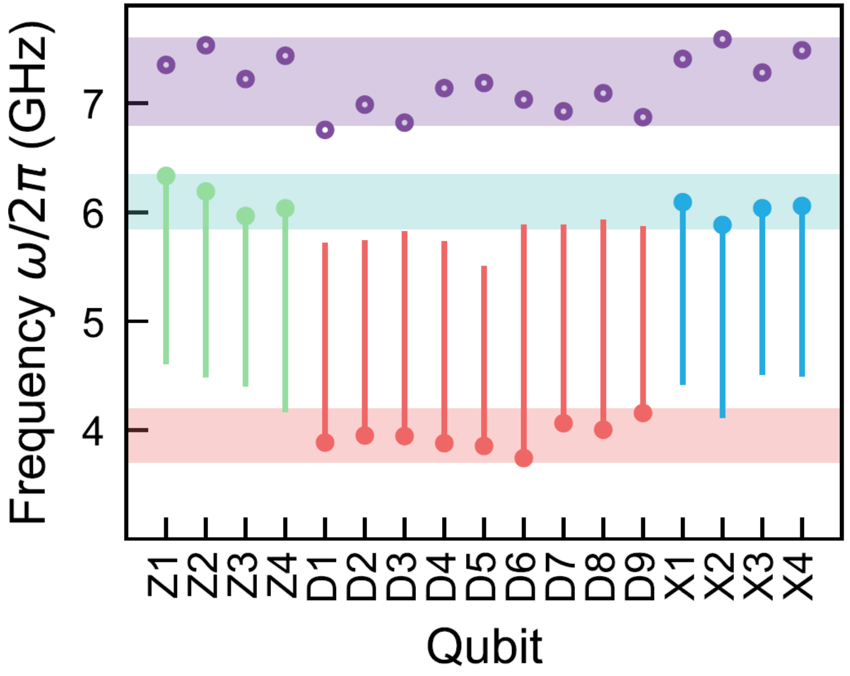

Frequency tunable qubits in two bands

- Data qubits at ~ 4 GHz
- Auxiliary qubits at ~ 6 GHz

Features

- Small residual-ZZ couplings ($\leq$ 8 kHz)
- Improved coherence using asymmetric SQUIDs creating upper and lower-frequency sweet spots
- Two-qubit CZ gates initiated by tuning both qubits
- Tuning range indicated by vertical bars
- Only auxiliary qubits evolve through $|2\rangle$ during a two-qubit gate

Readout resonators

- Single frequency band ~ 7 GHz

S. Krinner, N. Lacroix *et al.*, *Nature* **605**, 669 (2022)

Device Performance

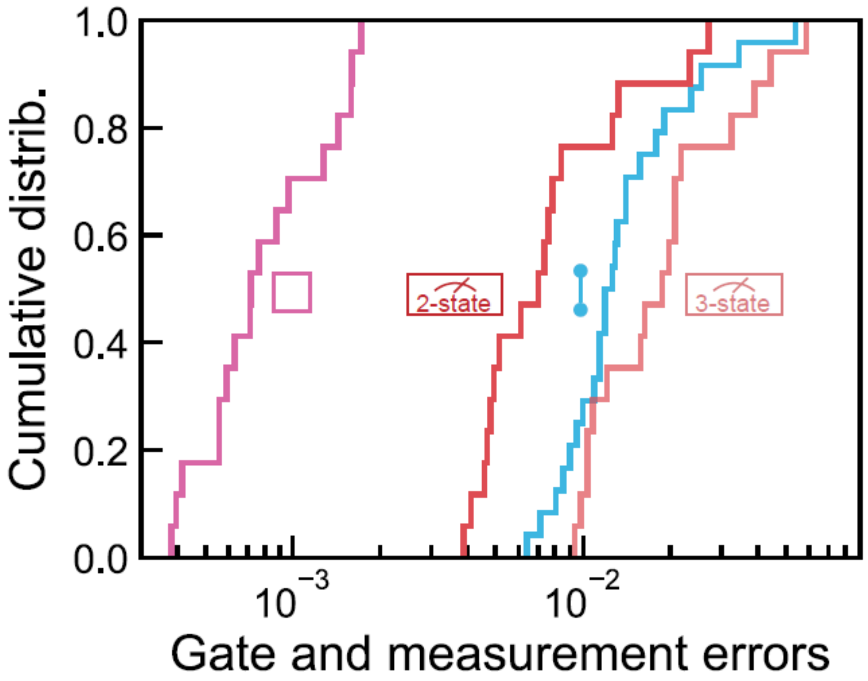

Averaged qubit coherence

- Energy relaxation time $T_1 \sim 33$ μs
- Ramsey decay time $T_2^* \sim 38$ μs

Single-qubit gates

- Mean gate error of 0.9(4) 10^{-3}
- Duration of 40 ns

Two-qubit gates

- Mean gate error of 15(10) 10^{-3}
- Mean duration of 98(7) ns (including buffers)

Readout:

- Mean two-state assignment error: 9(7) 10^{-3} and three-state assignment error: 22(14) 10^{-3}
- Duration: 300 ns (aux.) to 400 ns (data)

S. Krinner, N. Lacroix *et al.*, *Nature* **605**, 669 (2022)

Leakage Detection and Rejection

- Leakage errors are detrimental for quantum error correction
- Device designed to minimize leakage on data qubits: $< 2\ 10^{-3}$ per qubit and per cycle
- Detect residual leakage using three-state readout
  - Auxiliary qubits: in each cycle
  - Data qubits: after final cycle
- Rejected fraction per qubit per cycle
  - Auxiliary qubits: $9.4(4)\ 10^{-3}$
  - Data qubits: $1.7(2)\ 10^{-3}$
- Some contribution from false positives

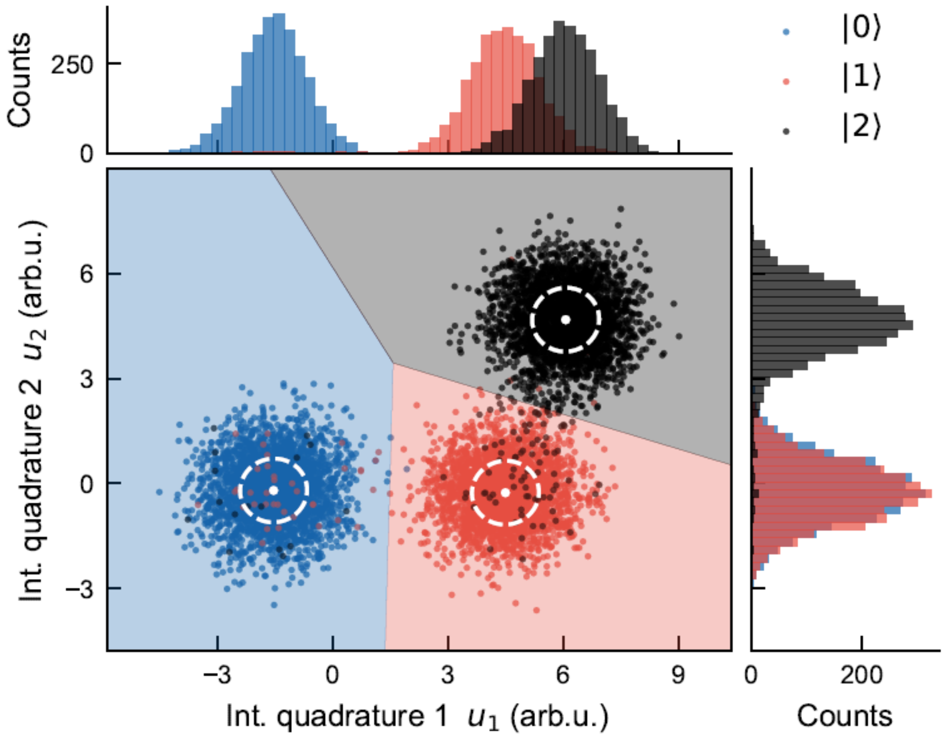

S. Krinner, N. Lacroix *et al.*, *Nature* **605**, 669 (2022)

Alferis, Terhal, *Quant. Info. Comp.* **7**, 139 (2007)
Fowler, *PRA* **88**, 042308 (2013)
Bultink *et al.*, *Science Advances* **6**, eaay3050 (2020)
Varbanov *et al.*, *npj Quantum Information* **15**, 997 (2020)

Distance-Three Surface-Code Device Mounted in Sample Holder

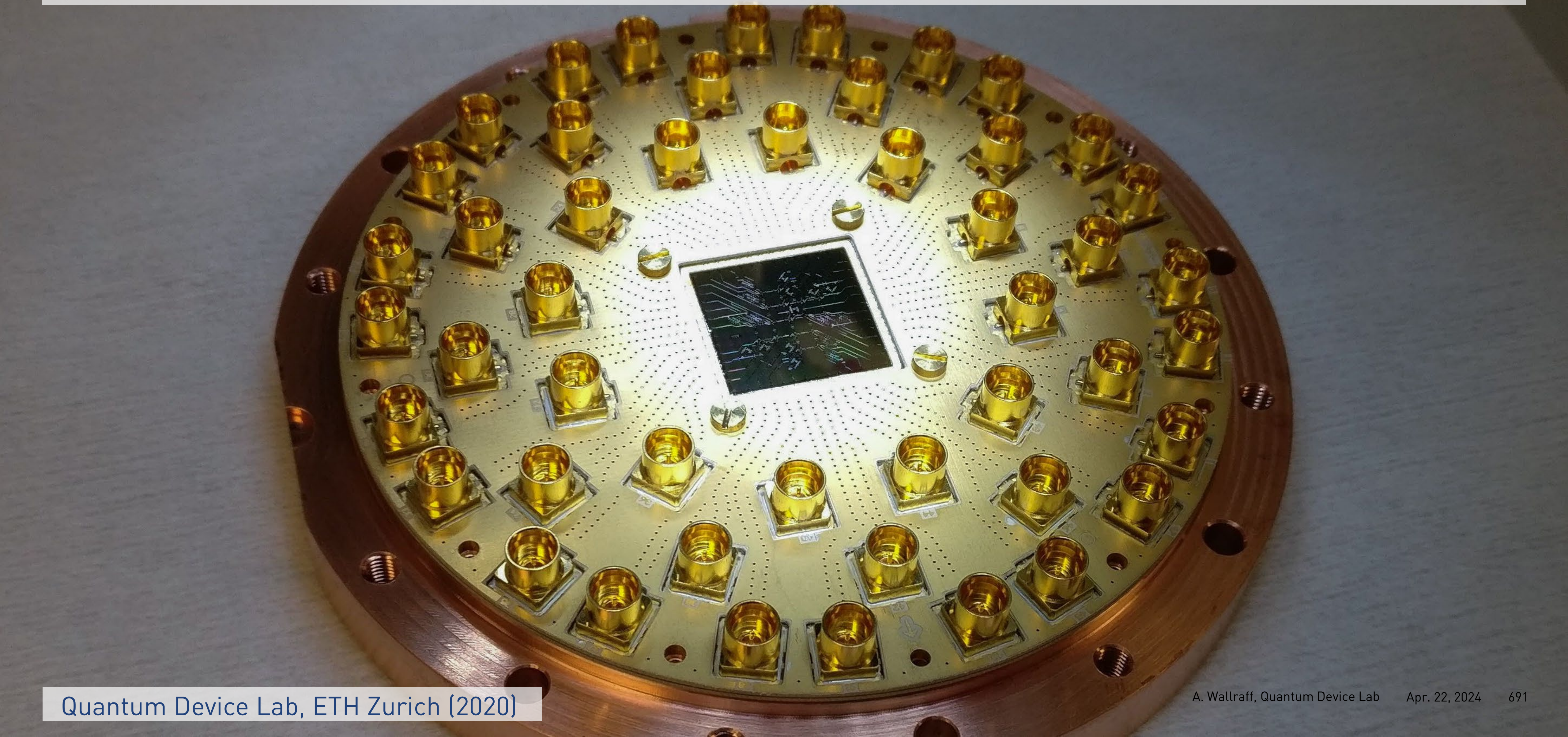

Quantum Device Lab, ETH Zurich (2020)

ETH zürich

48-Port Sample Package (17-Qubit Device)

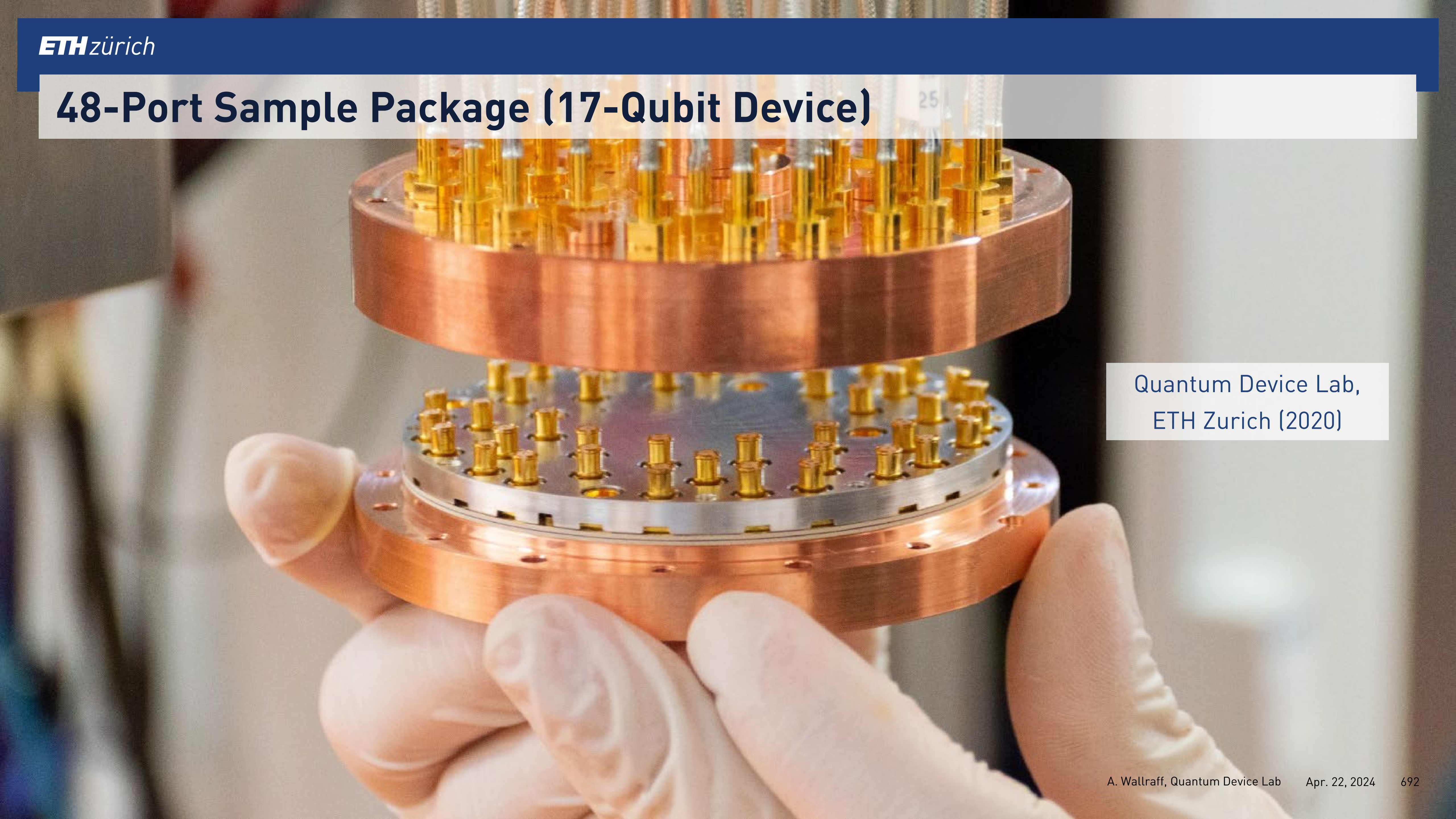

Quantum Device Lab, ETH Zurich (2020)

Quantum Device Lab, ETH Zurich (2021)

Quantum Device Lab, ETH Zurich (2022)

Qubit-Encoded Quantum Error Correction Experiments

Bit or phase-flip codes (only X or Z errors):

- NMR [Cory et al. Phys. Rev. Lett. 81, 2152 (1998)]
- Ions [Chiaverini et al. Nature 432, 602 (2004), Schindler et al. Science 322, 1059 (2011)]
- NV-Centers [Cramer et al. Nature Comm. 7, 11526 (2016)]
- Superconducting qubits [Riste et.al. Nature Comm. 6, 6983 (2015), Kelly et al. Nature 519, 66 (2015), Chen et al., Nature 595, 7867 (2021)]

Quantum codes, single-cycle experiments:

- Five-qubit code [Knill et al., PRL 86, 5811 (2001), Abobeih et al., arXiv:2108.01646 (2021)]
- Bacon-Shor code [Egan et al., Nature 598, 281 (2021)]

Repeated error detection in the surface code

- Andersen et al., Nat. Phys. 16, 875 (2020)
- Chen et al., Nature 595, 7867 (2021)
- Marques et al., Nat. Phys. **18**, 80 (2022)

Trapped ions

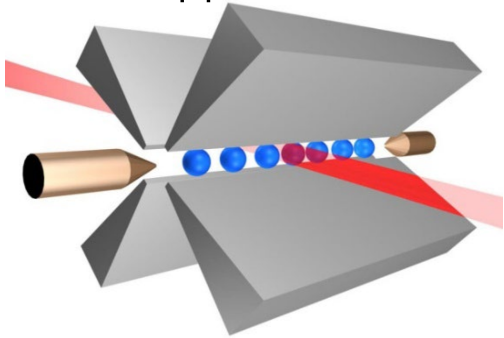

e.g. Blatt & Roos, Nat. Phys. 8, 277 (2012)

Supercond. circuits

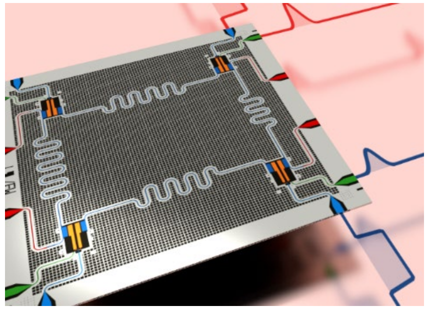

Picture: Y. Salathé
Review: e.g. Krantz et al., Appl. Phys. Rev. 6, 021318 (2019)

Repeated quantum error correction

- Color code (trapped ions) Ryan-Anderson et al., PRX 11, 041058 (2021)
- Distance-3 surface code (s.c.) Krinner, Lacroix *et al.*, *Nature* **605**, 669 (2022) Zhao et al., *PRL* **129**, 030501 (2022)
- Distance-3 heavy-hexagon code (s.c.) Sundaresan et al., *Nat. Commun.* **14**, 2852 (2023)
- Distance-3 to 5 scaling of the surface code (s.c.) Google AI, *Nature* **614**, 676 (2023)

Stabilizer Measurements

Quantum circuit

- Ramsey measurement on auxiliary qubit Ai

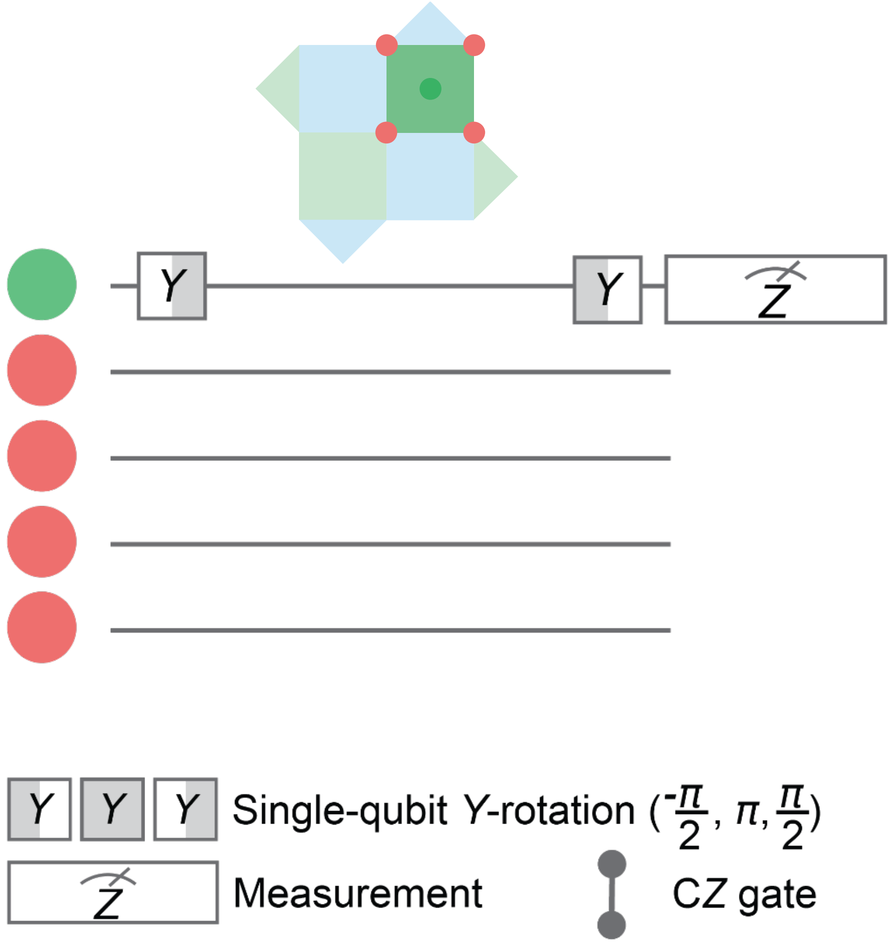

Stabilizer Measurements

Quantum circuit

- Ramsey measurement on auxiliary qubit Ai
- Controlled-phase (CZ) gates between Ai and four data qubits $\mathrm{D}j$
  - If $\mathrm{D}j$ in $|1\rangle$: phase of Ai changes by π
  - ➢ Resulting mapping:

Number of $\mathrm{D}j$ in $\|1\rangle$:	Final phase of Ai	Final state of Ai	Stabilizer value s^{Ai}
Even	0	Unchanged	+1
Odd	π	Changed	-1

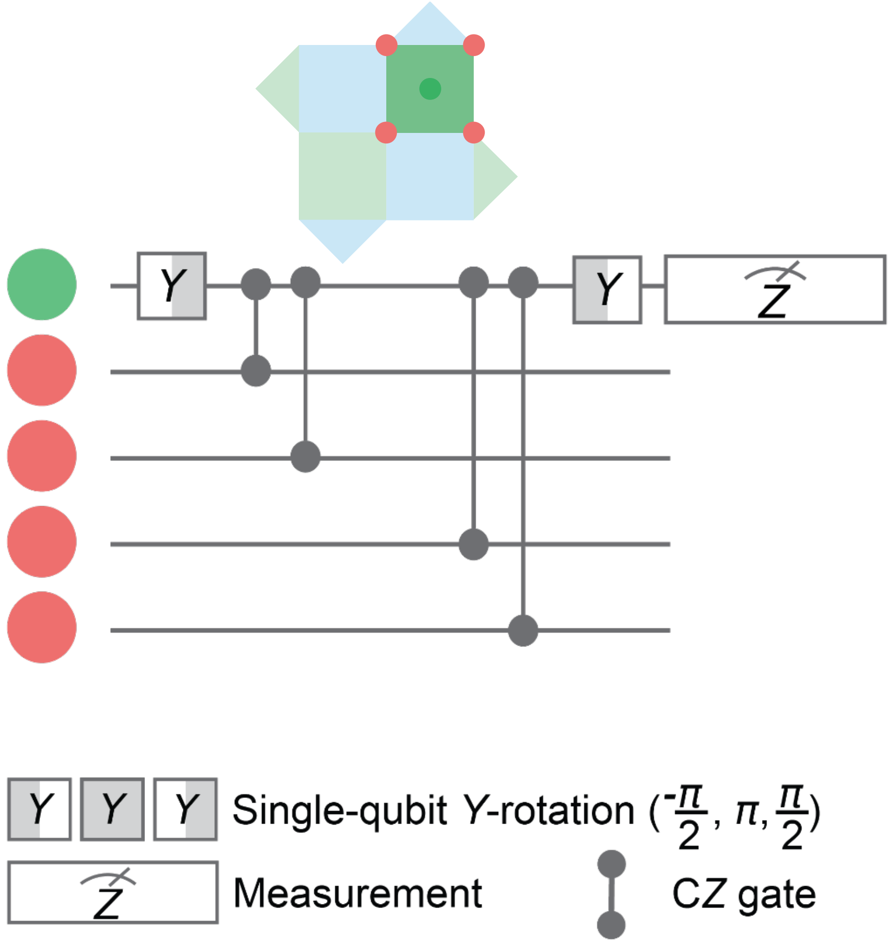

S. Krinner, N. Lacroix *et al.*, *Nature* **605**, 669 (2022)

Stabilizer Measurements

Quantum circuit

- Ramsey measurement on auxiliary qubit Ai
- Controlled-phase (CZ) gates between Ai and four data qubits $\mathrm{D}j$
  - If $\mathrm{D}j$ in $|1\rangle$: phase of Ai changes by π
  - ➢ Resulting mapping:

Number of $\mathrm{D}j$ in $\|1\rangle$:	Final phase of Ai	Final state of Ai	Stabilizer value s^{Ai}
Even	0	Unchanged	+1
Odd	π	Changed	-1

- X-type stabilizer with basis change on data qubits

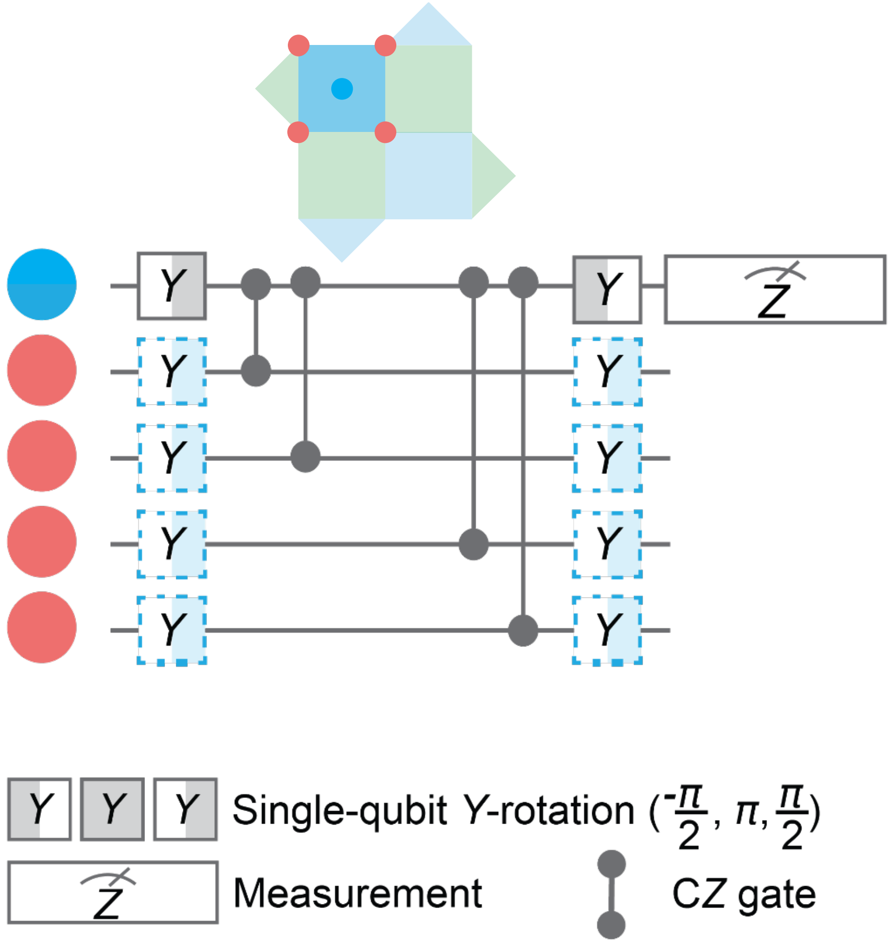

S. Krinner, N. Lacroix *et al.*, *Nature* **605**, 669 (2022)

Stabilizer Measurements

Quantum circuit

- Ramsey measurement on auxiliary qubit Ai
- Controlled-phase (CZ) gates between Ai and four data qubits $\mathrm{D}j$
  - If $\mathrm{D}j$ in $|1\rangle$: phase of Ai changes by π
  - ➢ Resulting mapping:

Number of $\mathrm{D}j$ in $\|1\rangle$:	Final phase of Ai	Final state of Ai	Stabilizer value s^{Ai}
Even	0	Unchanged	+1
Odd	π	Changed	-1

- X-type stabilizer with basis change on data qubits
- Echo pulses on data qubits to reduce both
  - Dephasing
  - Residual coherent coupling to spectator qubits

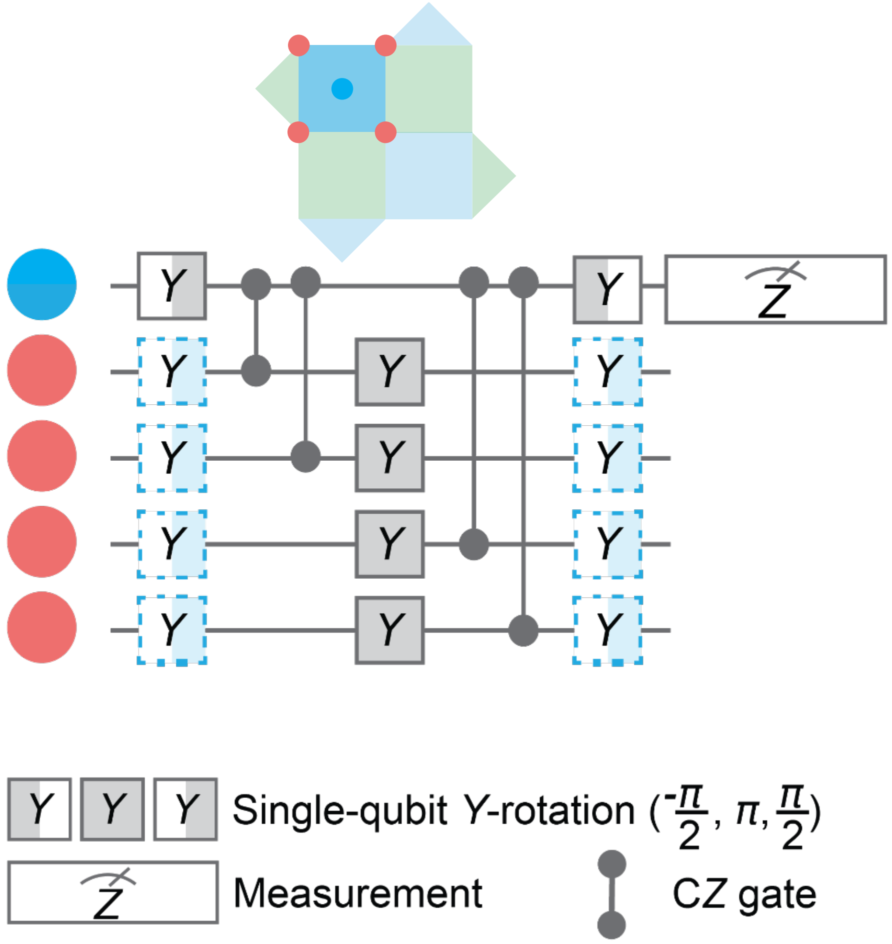

Krinner et al., *Phys. Rev. Applied* **14**, 024042 (2020)

Room-Temperature Electronics

- Close collaboration with Zurich Instruments

Qubit control (7x HDAWG)

- Flux drives (17x)
- Baseband RF drives (17x)

Qubit Readout (4x UHFQA)

- FPGA Baseband signal generation & analysis

Up- and down-conversion electronics for qubit drive and readout

Synchronization using PQSC

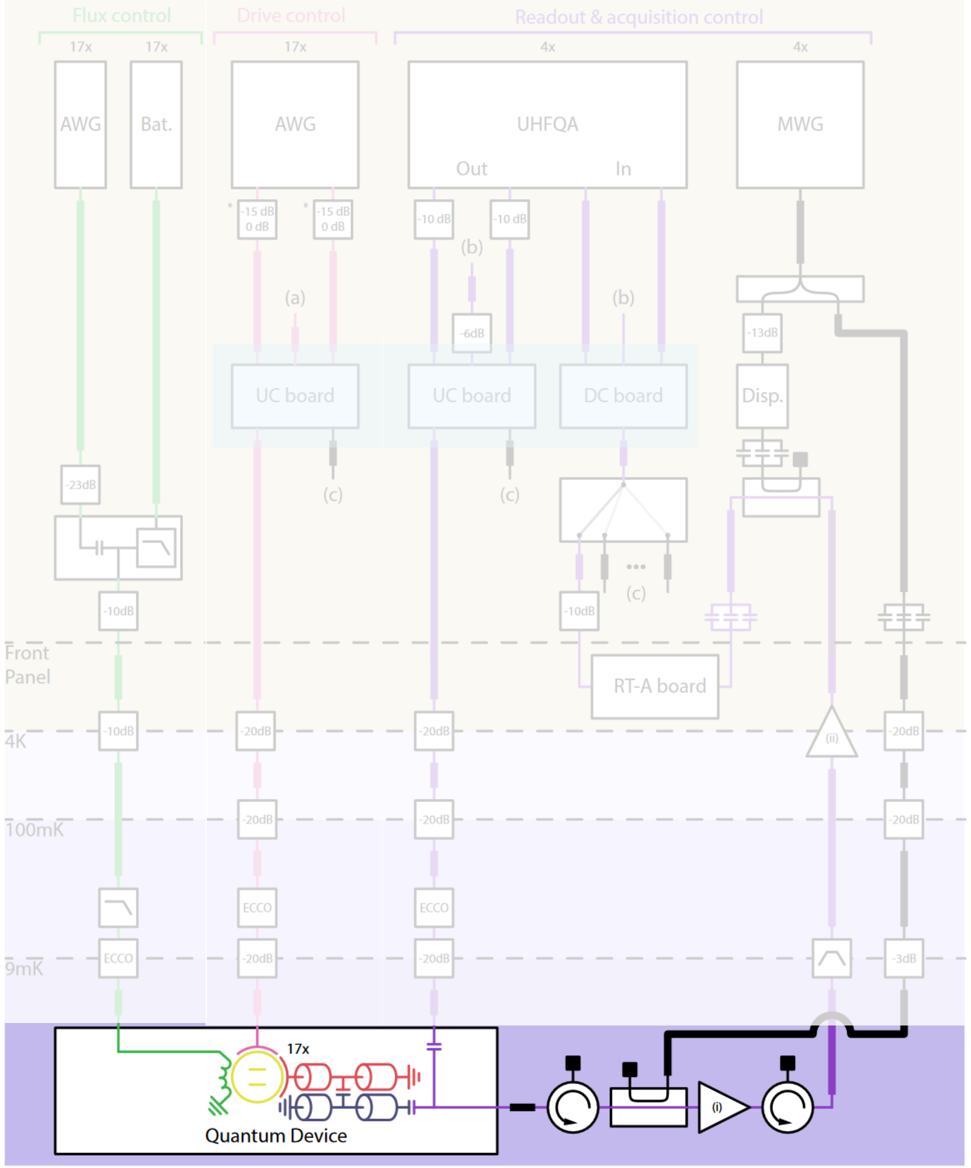

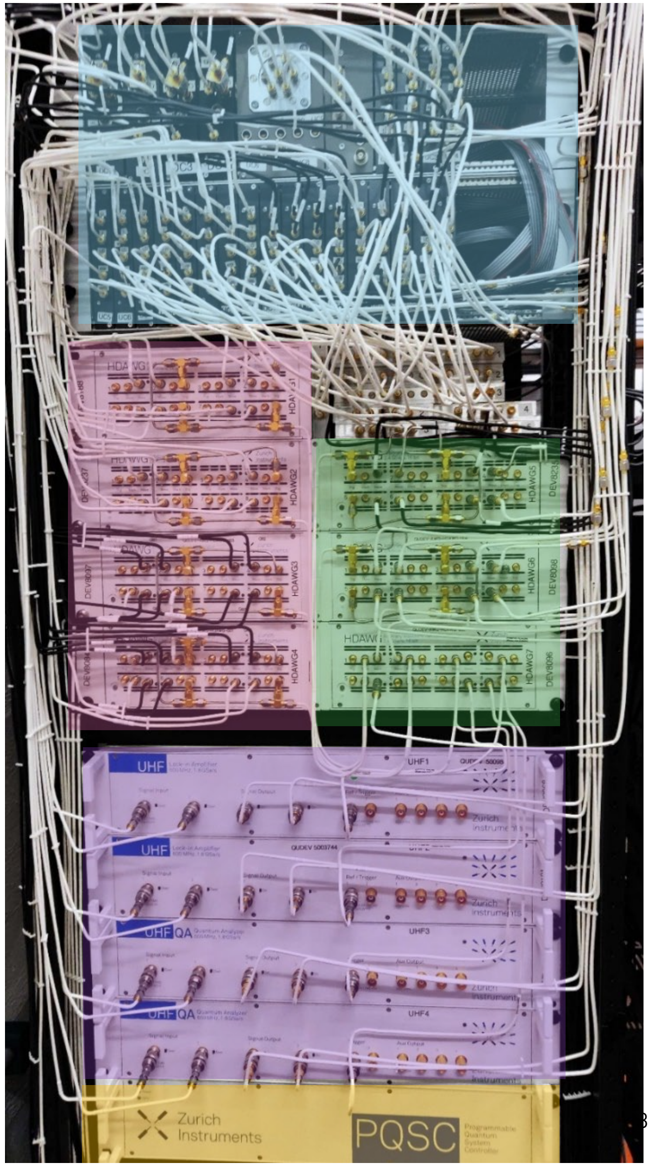

Stabilizer Characterization

Individual characterization

- Prepare data qubits of plaquette in all 4 (weight-2) or 16 (weight-4) basis states
- Stabilizer execution yields $s^{Ai} = \pm 1$
- Average over $\sim 4 \times 10^4$ measurements to obtain $\bar{s}^{Ai}$
- Measured and calculated error

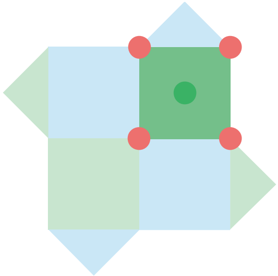

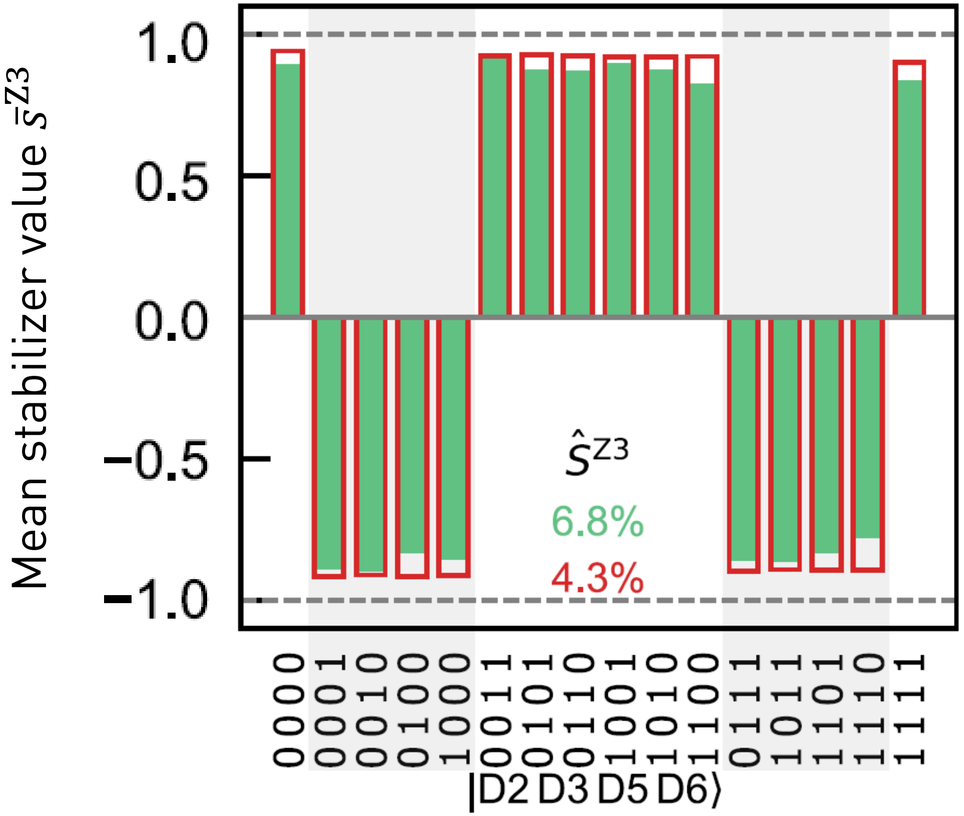

S. Krinner, N. Lacroix *et al.*, *Nature* **605**, 669 (2022)

Stabilizer Characterization

Individual characterization

- Prepare data qubits of plaquette in all 4 (weight-2) or 16 (weight-4) basis states
- Stabilizer execution yields $s^{Ai} = \pm 1$
- Average over $\sim 4 \times 10^4$ measurements to obtain $\bar{s}^{Ai}$
- Measured and calculated error

Average parity error

- Weight-2 stabilizers: 3.9(1.3) %
- Weight-4 stabilizers: 8.2(2.2) %

Qualitative agreement with master-equation simulations

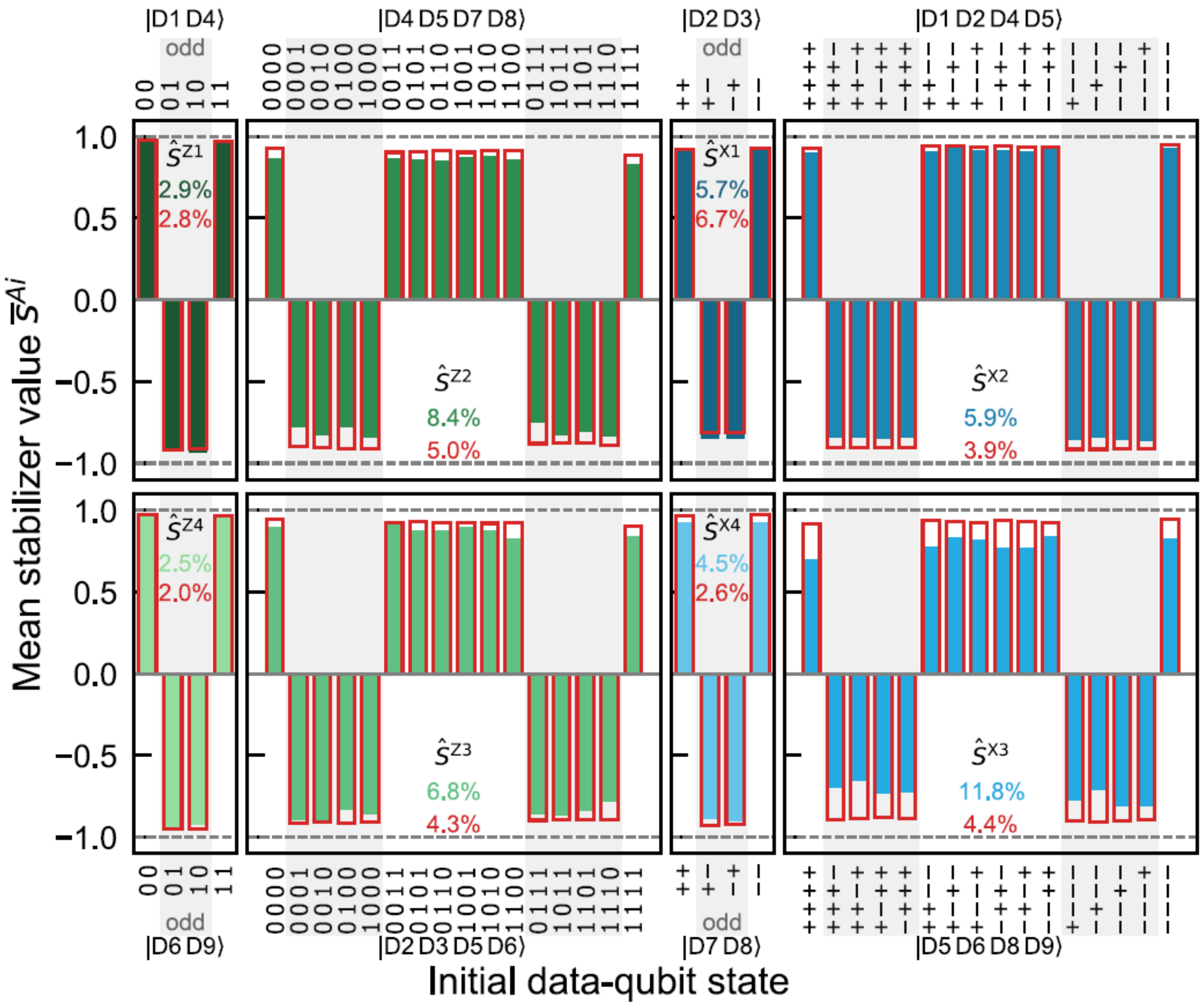

S. Krinner, N. Lacroix *et al.*, *Nature* **605**, 669 (2022)

The Surface Code Cycle

- All four $\hat{S}^{Zi}$ measured in parallel
- All four $\hat{S}^{Xi}$ measured in parallel
- Pipelining: Read out one stabilizer type while running gates of the other.

- Logical state preparation: $|0\rangle_L$, $|1\rangle_L$ and $|\pm\rangle_L = (|0\rangle_L \pm |1\rangle_L)/\sqrt{2}$ in single cycle.

- State preservation over n cycles
  - Cycle duration: 1.1 μs
  - Leakage detection and rejection executed in every cycle
  - circuits with ~ 800 single-qubit gates and ~ 400 two-qubit gates

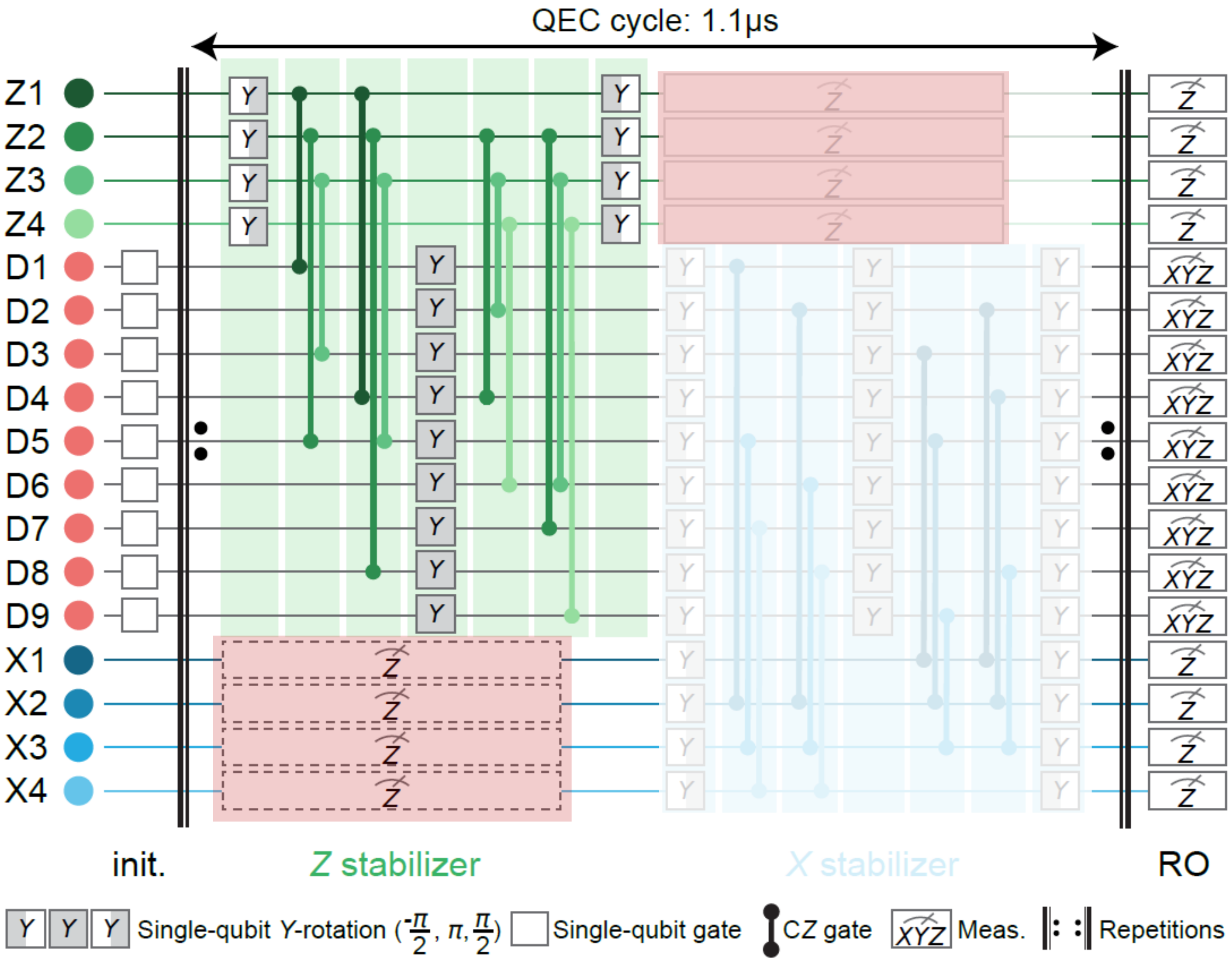

Versluis et al., *PR Applied* **8**, 034021 (2017)

S. Krinner, N. Lacroix *et al.*, *Nature* **605**, 669 (2022)

Error Syndrome: Concept

- Changes in stabilizer values s^{Ai} between subsequent cycles signal errors (no reset)

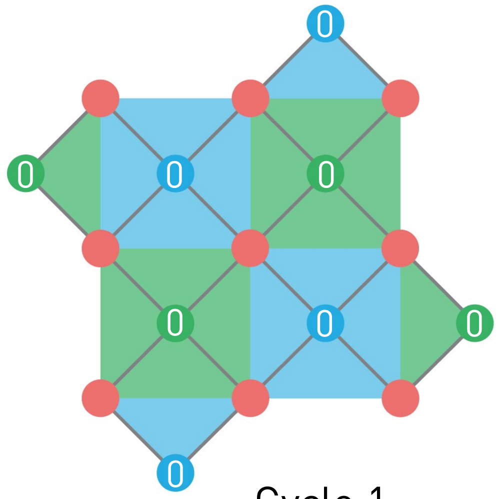

Cycle 1

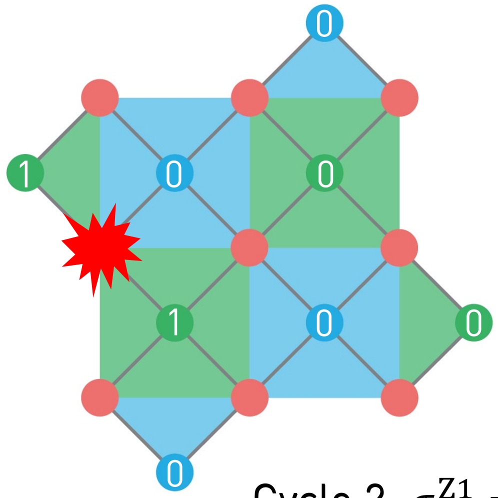

Cycle 2: $\sigma_2^{Z1} = 1$
$\sigma_2^{Z2} = 1$

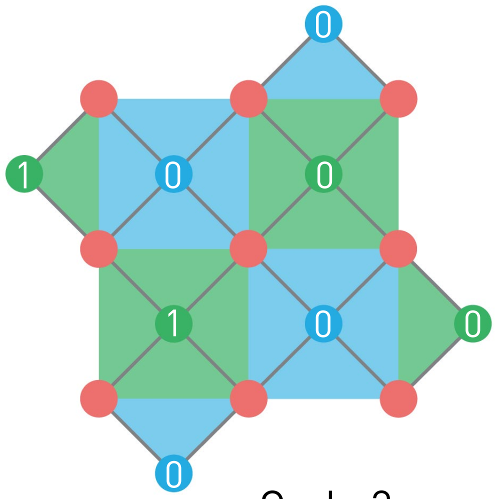

Cycle 3

- For each cycle m construct error syndrome σ_m :
  eight syndrome elements $\sigma_m^{Ai} = (1 - s_m^{Ai} \times s_{m-1}^{Ai})/2$
- $\sigma_m^{Ai} = 1$ (0) signals an error (no error)

S. Krinner, N. Lacroix *et al.*, *Nature* **605**, 669 (2022)

Syndrome Measurements

- Average σ_m^{Ai} over experimental repetitions: $\bar{\sigma}_m^{Ai}$
- Average over Ai and m: $\bar{\sigma} = 0.14 \ll 1$

- For $m \geq 2$: $\bar{\sigma}_m^{Ai}$ approximately constant
- Finite remaining slope due to increasing excited state population of auxiliary qubits

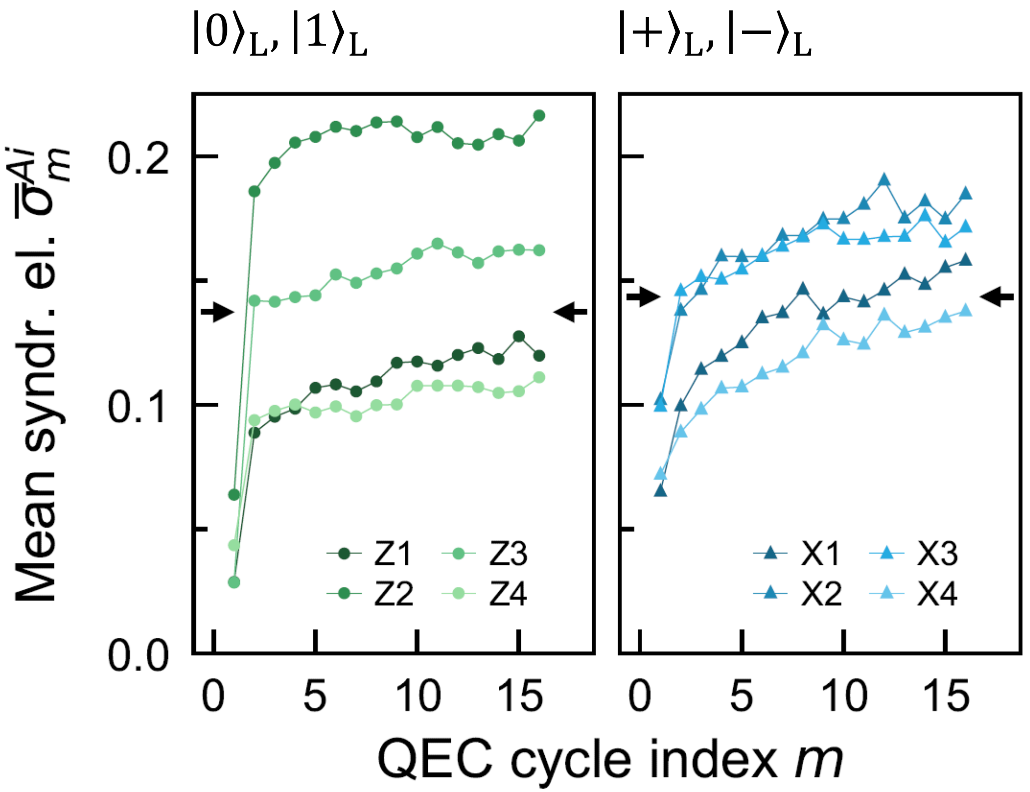

arXiv: 2112.03708 (2021)

Syndrome Measurements

- Average σ_m^{Ai} over experimental repetitions: $\bar{\sigma}_m^{Ai}$
- Average over Ai and m: $\bar{\sigma} = 0.14 \ll 1$

- For $m \geq 2$: $\bar{\sigma}_m^{Ai}$ approximately constant
- Finite remaining slope due to increasing excited state population of auxiliary qubits

- Qualitative agreement with simulations

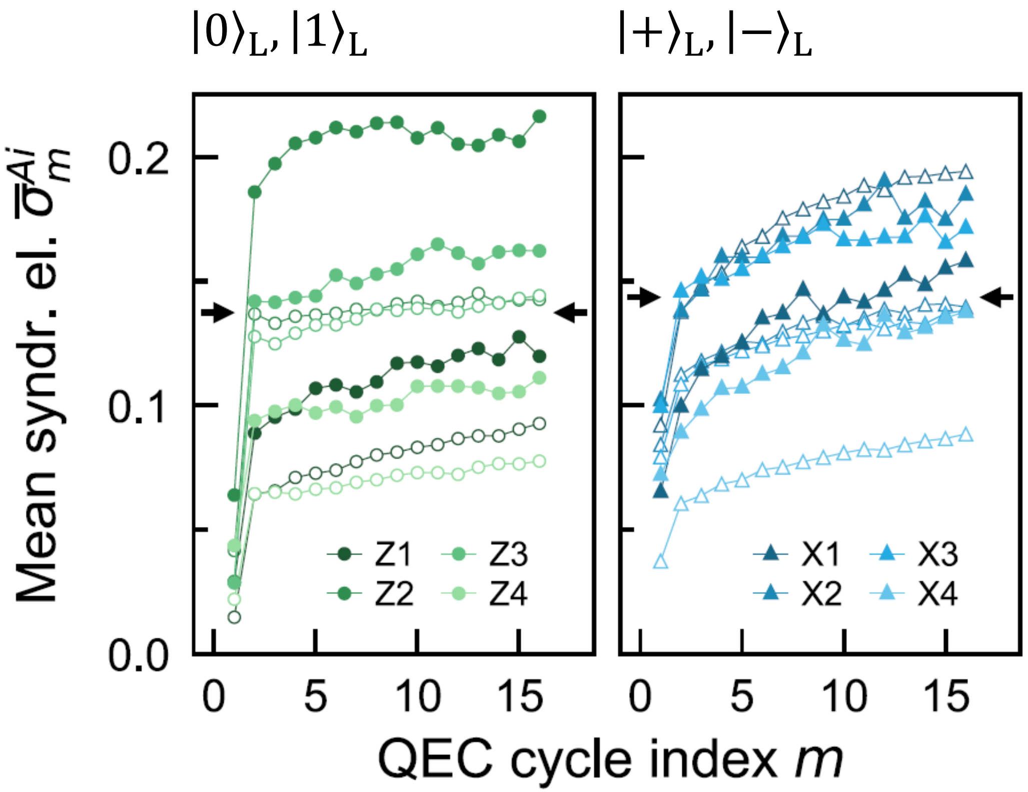

arXiv: 2112.03708 (2021)

S. Krinner, N. Lacroix *et al.*, *Nature* **605**, 669 (2022)

Decoding of Syndromes

Decoder:

- Determine most likely errors given observed sequence of syndromes
- Mapping to minimum-weight-perfect-matching algorithm
  - Syndrome graph
  - Weights determined in error-model-free approach

Spitz et al., *Adv. Quantum Techn.* **1**, 1800012 (2018)
Chen et al., *Nature* **595**, 383 (2021)

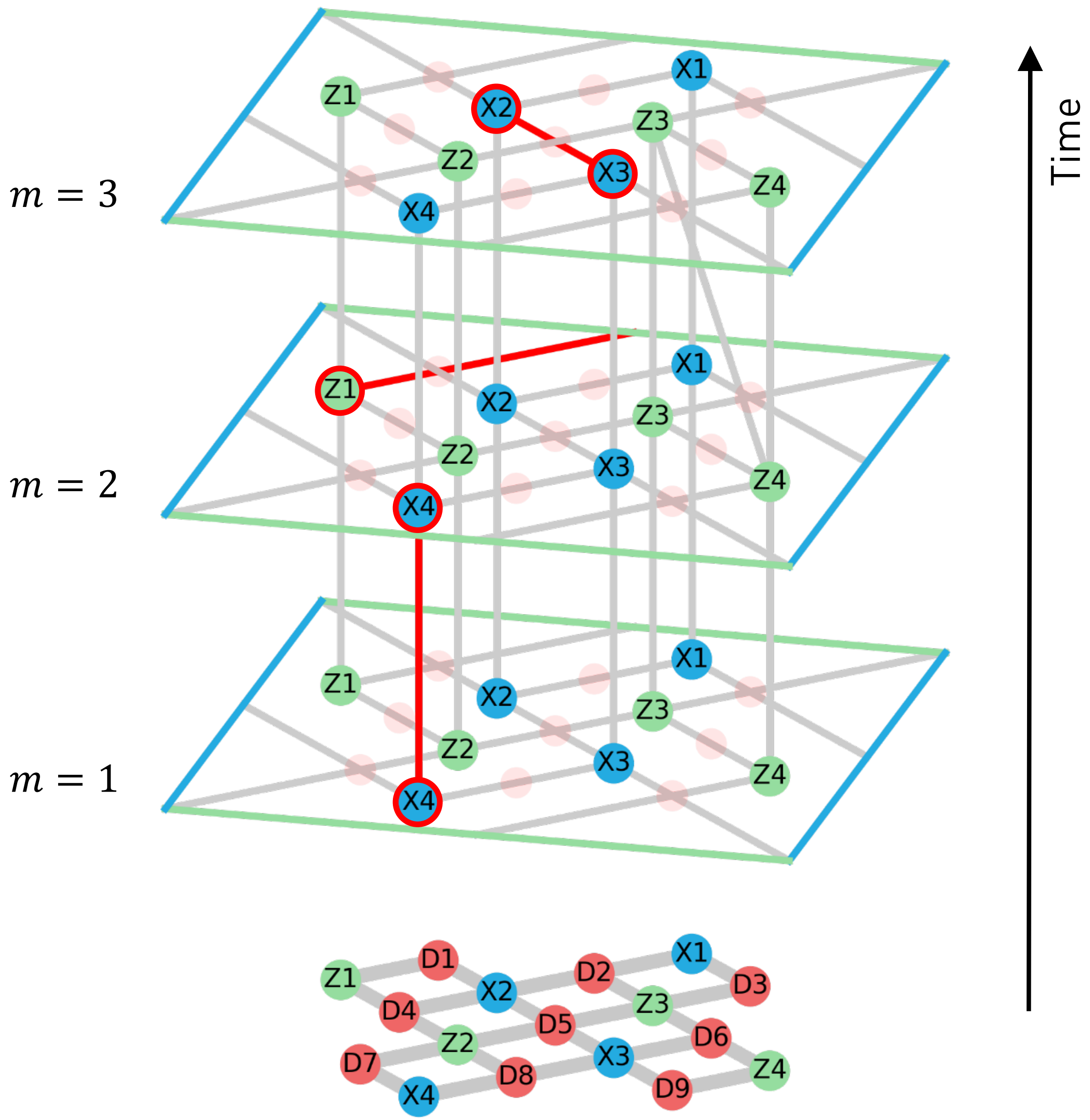

Repeated Quantum Error Correction

Measurement of Logical Z and Logical X Operators

- Initialization
  - $|0\rangle_L$: prepare data qubits in $|0\rangle^{\otimes 9}$
  - $|1\rangle_L$: prepare data qubits in $X_L|0\rangle^{\otimes 9}$
  - $|+\rangle_L$: prepare data qubits in $|+\rangle^{\otimes 9}$
  - $|-\rangle_L$: prepare data qubits in $Z_L|+\rangle^{\otimes 9}$
- Perform n QEC cyles
- Read out all data qubits in Z-basis (X-basis)

Analysis

- Determine logical operator $z_\mathrm{L} = z_1 z_2 z_3 = \pm 1$ ($x_\mathrm{L} = x_1 x_4 x_7 = \pm 1$) for each run with up to n repeated cycles
- Apply correction conditioned on decoded syndromes for each run
- Average over runs with n repeated cycles to compute $\bar{z}_\mathrm{L} = \langle \hat{Z}_\mathrm{L} \rangle$ ($\bar{x}_\mathrm{L} = \langle \hat{X}_\mathrm{L} \rangle$)

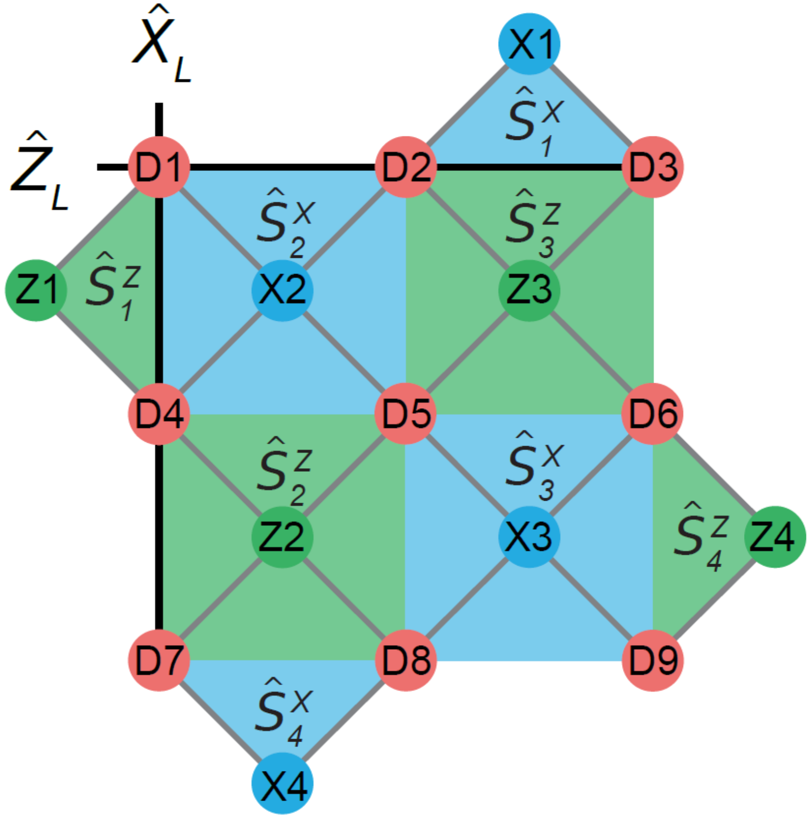

S. Krinner, N. Lacroix *et al.*, *Nature* **605**, 669 (2022)

Repeated Quantum Error Correction

Outcomes Logical Z and Logical X

- Exponential decay of logical expectation values
- Logical lifetime
  $T_{1,\mathrm{L}} = 16.4(8)\ \mu\mathrm{s} \gg t_c = 1.1\ \mu\mathrm{s}$
- Logical coherence time
  $T_{2,\mathrm{L}} = 18.2(5)\ \mu\mathrm{s} \gg t_c = 1.1\ \mu\mathrm{s}$
- Master equation simulation of logical lifetimes of $\sim 26\ \mu\mathrm{s}$ provide upper bound for achievable lifetimes with our device performance

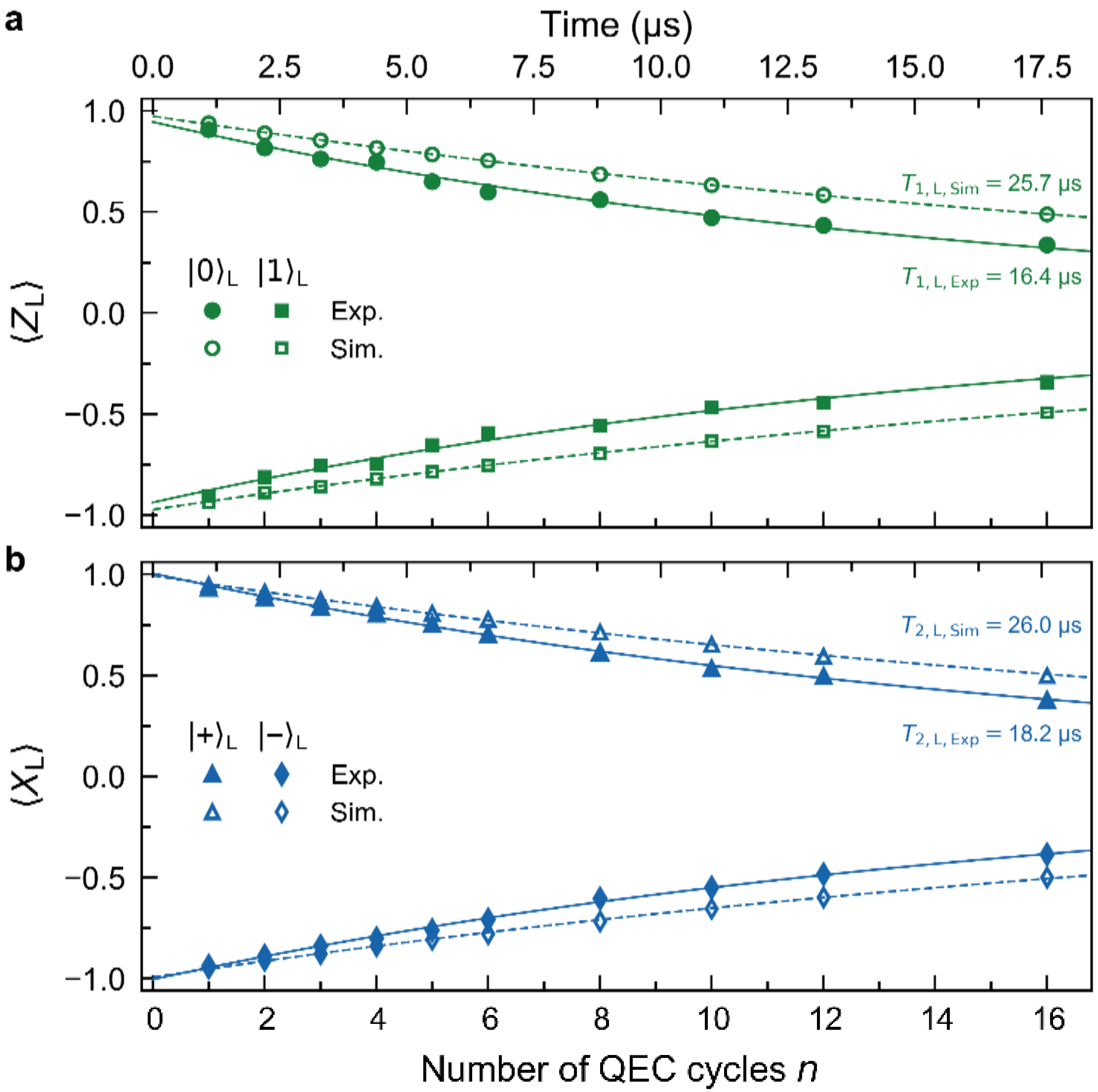

S. Krinner, N. Lacroix *et al.*, *Nature* **605**, 669 (2022)

Logical Error Probability and Logical Error per Cycle

Logical error probability:

- $E_\mathrm{L} = (1 - \langle \hat{Z}_\mathrm{L} \rangle)/2$ for eigenstates of $\hat{Z}_\mathrm{L}$
- $E_\mathrm{L} = (1 - \langle \hat{X}_\mathrm{L} \rangle)/2$ for eigenstates of $\hat{X}_\mathrm{L}$

Logical error per cycle:

- Extracted from fit to $E_\mathrm{L}(n)$ or from $T_{1/2,\mathrm{L}}$:

  $\epsilon_\mathrm{L} = \frac{1}{2}\left[1 - \exp(-t_\mathrm{c}/T_{1/2,\mathrm{L}})\right] \approx t_\mathrm{c}/2T_{1/2,\mathrm{L}}$
- $\epsilon_\mathrm{L} \sim 0.03$

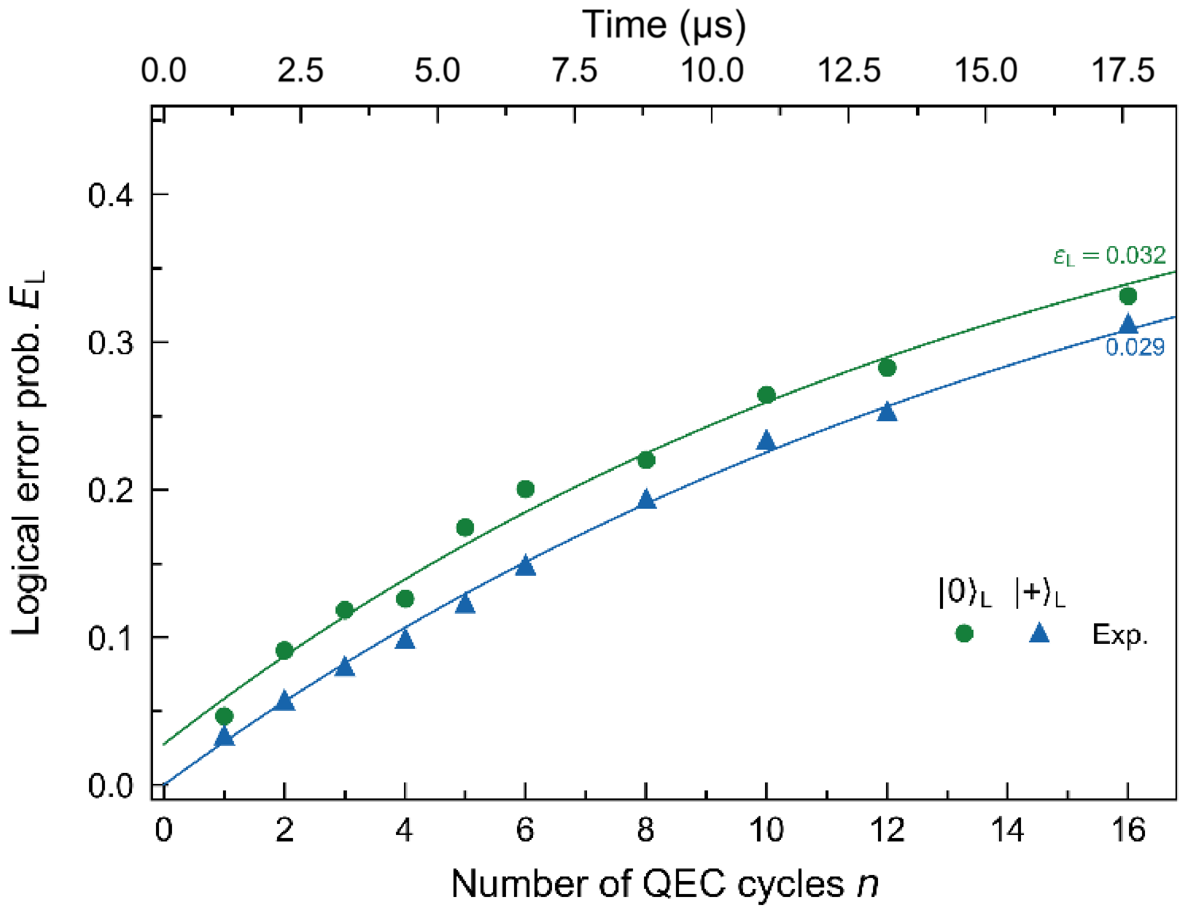

S. Krinner, N. Lacroix *et al.*, *Nature* **605**, 669 (2022)

Comparison of Repeated Distance-Three QEC Experiments

The competition:

- Honeywell: [1] Ryan-Anderson *et al.*, *Phys. Rev. X* **11**, 041058 (2021)
  ETHZ: [2] Krinner, Lacroix *et al. Nature* **605**, 669 (2022)
  USTC: [3] Zhao et al., *PRL* **129**, 030501 (2022)
  IBM: [4] Sundaresan *et al.*, *Nat. Commun.* **14**, 2852 (2023)
  Google: [5] Google AI, *Nature* **614**, 676 (2023)

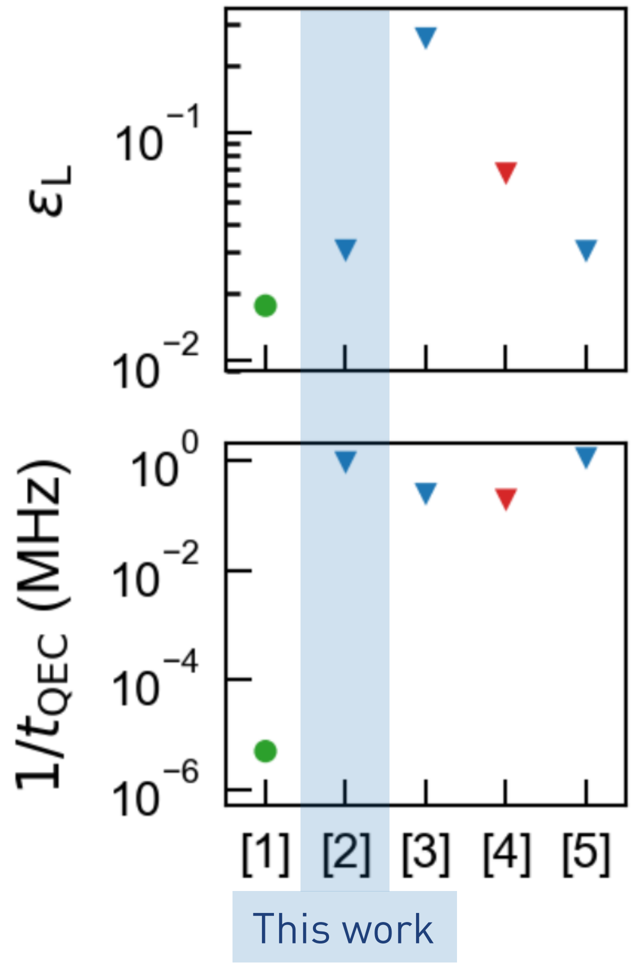

Implementations:

- superconducting-circuits (∇) and trapped-ions (O)
- Color code, surface code and heavy-hexagon code

Performance criteria

- Small logical error per cycle ε_L
  -> critical for fault tolerant quantum computing with high accuracy
- High QEC cycle rate $1/t_{QEC}$
  -> crucial for execution of deep quantum circuits on short time scales

Performance Assessment and Projection

Two-qubit-gate break-even

- Compare $\epsilon_\mathrm{L} = 0.03$ to dominant physical error
  - Two-qubit gate error $\epsilon_\mathrm{2Q} = 0.015$
  - Logical two-qubit gate error is expected to be dominated by ϵ_L
- Used simulations to project performance with physical error rates reduced by factor x
  - $\epsilon_\mathrm{L} \propto 1/x^2$
  - Break-even within reach

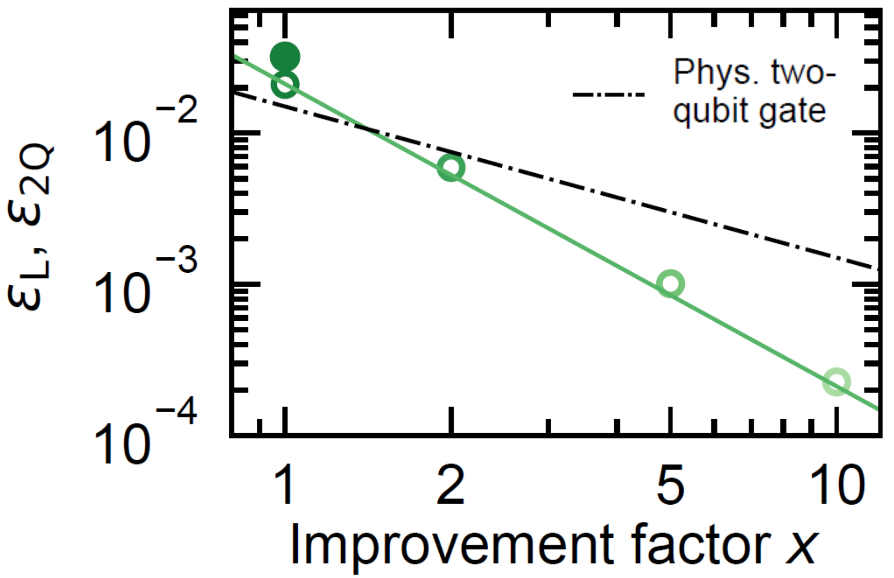

Error threshold

- $\epsilon_\mathrm{L} \sim 0.03$ comparable to predicted logical error per cycle at error threshold
  Fowler *et al.*, *Phys. Rev. A* **86**, 032324 (2012)
  Stephens, *Phys. Rev. A* **89**, 022321 (2014).

S. Krinner, N. Lacroix *et al.*, *Nature* **605**, 669 (2022)

Summary & Outlook

Here:

- Repeated quantum error correction in a distance-3 surface code
  - Fast QEC cycle of 1.1 μs
  - Low logical error per cycle $\epsilon_{\mathrm{L}} \sim 0.03$
  - Break-even within reach, potentially close to threshold

Up next:

- Reduce leakage
- Logical operations on single logical qubit
- Gates between two logical qubits

S. Krinner, N. Lacroix *et al.*, *Nature* **605**, 669 (2022)

SCAN ME

The Paper

ETH zürich

The Quantum Device Lab

with fall term project students

Innovation project supported by

Schweizerische Eidgenossenschaft
Confédération suisse
Confederazione Svizzera
Confederaziun svizra

Swiss Confederation

Innosuisse – Swiss Innovation Agency

ETH
Eidgenössische Technische Hochschule Zürich
Swiss Federal Institute of Technology Zurich

Schweizerischer Nationalfonds

IARPA
BE THE FUTURE

Want to work with us?
Looking for Grad Students, PostDocs and Technical Staff.